

ETD Archive

---

2009

## Development of Quantitative Bioanalytical Methods for the Measurement of Pharmaceutical Compounds via HPLC-UV and HPLC-MS/MS

Melissa A. Mcculloch  
*Cleveland State University*

Follow this and additional works at: <https://engagedscholarship.csuohio.edu/etdarchive>

 Part of the [Chemistry Commons](#)

[How does access to this work benefit you? Let us know!](#)

---

### Recommended Citation

Mcculloch, Melissa A., "Development of Quantitative Bioanalytical Methods for the Measurement of Pharmaceutical Compounds via HPLC-UV and HPLC-MS/MS" (2009). *ETD Archive*. 197.  
<https://engagedscholarship.csuohio.edu/etdarchive/197>

This Dissertation is brought to you for free and open access by EngagedScholarship@CSU. It has been accepted for inclusion in ETD Archive by an authorized administrator of EngagedScholarship@CSU. For more information, please contact [library.es@csuohio.edu](mailto:library.es@csuohio.edu).

DEVELOPMENT OF QUANTITATIVE BIOANALYTICAL METHODS  
FOR THE MEASUREMENT OF PHARMACEUTICAL COMPOUNDS  
VIA HPLC-UV AND HPLC-MS/MS

MELISSA A. McCULLOCH

Bachelor of Science in Chemistry

Cleveland State University

December, 2003

submitted in partial fulfillment of requirement for the degree

DOCTOR OF PHILOSOPHY IN CLINICAL AND BIOANALYTICAL CHEMISTRY

at

CLEVELAND STATE UNIVERSITY

AUGUST, 2009

© COPYRIGHT BY MELISSA A. McCULLOCH 2009

This dissertation has been approved  
for the Department of CHEMISTRY  
and the College of Graduate Studies by

---

Dissertation Chairperson, Dr. Yan Xu

---

Department and Date

---

Dr. Joanne Belovich

---

Department and Date

---

Dr. Baochuan Guo

---

Department and Date

---

Dr. Xue-Long Sun

---

Department and Date

---

Dr. Xiang Zhou

---

Department and Date

DEVELOPMENT OF QUANTITATIVE BIOANALYTICAL METHODS FOR THE  
MEASUREMENT OF PHARMACEUTICAL ANALYTES VIA HPLC-UV AND  
HPLC-MS/MS  
MELISSA A. McCULLOCH

**ABSTRACT**

Research in pharmaceutical treatments for illnesses and disease processes has rapidly grown in the past decade. The field is fueled by advances in our understanding of the molecular mechanics of the human body, coupled with the development of sophisticated scientific instruments which can efficiently generate massive amounts of important data. This has led to an ever-growing need for the development of quantitative bioanalytical methods to measure pharmaceutical compounds.

In this work, the theory behind the analytical processes and instruments that make these investigations possible is discussed. Further, the development of two high performance liquid chromatographic (HPLC) methods with both ultra violet (UV) spectrometry and mass spectrometry (MS) detection of the cannabinoid (CB) antagonists' rimonabant and surinabant is presented. The methods developed for the CB antagonists' are successfully applied to animal studies in clinical and pre-clinical investigations. Thirdly, preliminary work is included which was conducted for the development of two methods to be used in the measurement of anti-cancer agents, quinacrine and triapine. Finally, a discussion is presented for the consideration of the challenges and potential solutions in the development of an HPLC-MS method for triapine.

The theory, experimental designs and results discussed here demonstrates how analytical chemistry and instrumentation are used in bioanalytical method development. This research also illustrates how once developed, these methods serve to advance the progress in biochemical, preclinical and clinical studies.

## TABLE OF CONTENTS

ABSTRACT .....	iv
TABLE OF CONTENTS .....	vi
LIST OF TABLES .....	x
LIST OF FIGURES .....	xi
CHAPTER I INTRODUCTION TO BIOANALYTICAL METHOD DEVELOPMENT: PHARMACEUTICAL ANALYTE EXTRACTION, HIGH PERFORMANCE LIQUID CHROMATOGRAPHY AND MASS SPECTROMETRY .....	1
1. Rationale for Method Development .....	1
2. Extraction of Pharmaceutical Analytes from Biological Matrices .....	3
1. Introduction .....	3
2. Liquid Liquid Extraction .....	4
3. Protein Precipitation .....	7
4. Solid Phase Extraction .....	14
3. High Performance Liquid Chromatography .....	16
1. Introduction .....	16
2. Column Selection .....	19
3. Mobile Phase Selection .....	25
4. Pump .....	29
5. Injector .....	31

6. Detector .....	33
4. Ultraviolet Spectroscopic Detectors .....	35
1. Introduction .....	35
2. Beer-Lambert Law .....	35
3. Types of UV Detectors .....	36
4. Concluding Remarks .....	42
5. Mass Spectrometric Detectors .....	42
1. Introduction .....	42
2. Ion Sources .....	43
3. Mass Analyzers .....	49
4. Detectors .....	58
6. Conclusion .....	63
CHAPTER I REFERENCES .....	64
CHAPTER II THE DEVELOPMENT OF QUANTITATIVE BIOANALYTICAL METHODS FOR THE DETERMINATION OF CANNABINOID ANTAGONISTS RIMONABANT AND SURINABANT .....	67
2.1 Introduction to Cannabinoids .....	67
2.1.1 Cannabinoid Discovery .....	67
2.1.2 Endogenous Cannabinoid System .....	70
2.1.3 Cannabinoid Antagonists .....	80
2.1.4 Rimonabant .....	83
2.1.5 Surinabant .....	86
2.1.6 Conclusion .....	89

2.2 Development of a Quantitative Bioanalytical Method for the	
Determination of Rimonabant .....	90
2.2.1 Introduction .....	90
2.2.2 Materials and Methods .....	91
2.2.3 Results and Discussion .....	97
2.2.4 Conclusion .....	120
2.3 Development of a Quantitative Bioanalytical Method for the Measurement	
of Surinabant .....	120
2.3.1 Introduction .....	120
2.3.2 Materials and Methods .....	121
2.3.3 Results and Discussion .....	127
2.3.4 Conclusion .....	139
CHAPTER II REFERENCES .....	141
CHAPTER III PRELIMINARY WORK CONDUCTED TO DEVELOP	
BIOANALYTICAL METHODS FOR THE MEASUREMENT OF ANTI-CANCER	
AGENTS, QUINACRINE AND TRIAPINE .....	146
3.1 Quinacrine .....	146
3.1.1 Introduction .....	146
3.1.2 Materials and Methods .....	151
3.1.3 Discussion .....	153
3.2 Triapine (3-AP)	
3.2.1 Introduction .....	163
3.2.2 Materials and Methods .....	168

3.2.3 Discussion .....	171
3.2.4 Challenges and Future Direction for The Development of a Quantitative Bioanalytical Method to Measure 3-AP .....	179
CHAPTER III REFERENCES .....	182

## LIST OF TABLES

### CHAPTER I

Table I	Properties of common solvents .....	27
Table II	Characteristics of different types of pumps .....	30
Table III	Detection limits achievable using various detectors .....	34
Table IV	Properties of various mass analyzers .....	51

### CHAPTER II

Table V	Absolute and relative recoveries of rimonabant and AM251 in human plasma .....	59
Table VI	Intra- and inter-assay precision of rimonabant in human plasma .....	102
Table VII	Analytical performance of the HPLC-UV method .....	112
Table VIII	Analytical performance of HPLC-MS method .....	131
Table IX	Analytical performance of HPLC-MS method .....	138

## LIST OF FIGURES

### CHAPTER I

Figure 1.1	Representation of LLE .....	6
Figure 1.2	Electrostatic forces present in protein solutions .....	8
Figure 1.3	Ion distribution in the hydration layer of a protein solution ..	9
Figure 1.4	Hydration layer disruption caused by protein-protein Interactions .....	11
Figure 1.5	Protein precipitation procedure .....	13
Figure 1.6	SPE procedure .....	15
Figure 1.7	Flow diagram of HPLC setup .....	18
Figure 1.8	Figural depiction of longitudinal diffusion .....	20
Figure 1.9	Mass transfer due to (A) resistance in the mobile phase and (B) resistance in the stationary phase .....	22
Figure 1.10	Example of injector port .....	32
Figure 1.11	Fixed wavelength UV detector .....	37
Figure 1.12	Multiple wavelength UV detector .....	39
Figure 1.13	Diode array detector .....	41
Figure 1.14	API ionization .....	46
Figure 1.15	ESI ionization .....	48
Figure 1.16	Quadrapole design .....	53
Figure 1.17	Schematic of a QQQ design .....	54

Figure 1.18	IT-MS .....	56
Figure 1.19	Electron multiplier process .....	61
Figure 1.20	Photomultiplier .....	62

## CHAPTER II

Figure 2.1	Chemical structure of THC .....	69
Figure 2.2	Normal neurotransmission .....	71
Figure 2.3	Retrograde neurotransmission.....	72
Figure 2.4	Chemical structure of AEA and 2-AG .....	74
Figure 2.5	Biosynthesis of AEA and 2-AG .....	75
Figure 2.6	Protein structure of the CB1 receptor .....	77
Figure 2.7	Areas of the brain with CB1 receptor expression .....	78
Figure 2.8	Overview of the affect of the ECS on food intake, energy storage and balance .....	81
Figure 2.9	Chemical structure of rimonabant .....	84
Figure 2.10	Chemical structure of surinabant .....	87
Figure 2.11	Benefit to using DMSO and acetic acid in protein precipitation .....	100
Figure 2.12	Representative mass chromatograms of rimonabant and AM251 .....	105
Figure 2.13	Full scan mass spectra .....	107

Figure 2.14	Proposed fragmentation scheme for rimonabant (SR141716) and AM251 .....	109
Figure 2.15	Mass chromatograms from rats treated with rimonabant .....	115
Figure 2.16	Mass chromatogram of rimonabant extracted from brain tissue .....	117
Figure 2.17	Mass chromatograms from canines treated with rimonabant .....	119
Figure 2.18	UV chromatogram of surinabant and AM251 .....	129
Figure 2.19	Full scan and daughter scans of surinabant and AM251 .....	134
Figure 2.20	Mass chromatograms of surinabant and AM251 .....	135
Figure 2.21	Proposed fragmentation scheme of surinabant .....	137

### CHAPTER III

Figure 3.1	Chemical structure of quinacrine .....	147
Figure 3.2	Block diagram describing the role of quinacrine in cancer treatment .....	149
Figure 3.3	Chemical structure of 10593-V/2 .....	155
Figure 3.4	Full scan spectra of quinacrine .....	156
Figure 3.5	Full scan spectra of quinacrine and 10593-V/2 .....	157
Figure 3.6	Daughter ion spectra of quinacrine and 10593-V/2 .....	159
Figure 3.7	Mass chromatograms of quinacrine and 10593-V/2 .....	160

Figure 3.8	Fluidic profile for on-line sample extraction of quinacrine ...	162
Figure 3.9	Chemical structure of 3-AP .....	164
Figure 3.10	Role of triapine in cellular proliferation .....	165
Figure 3.11	3-AP as it relates to the conversion of NTP's to dNTP's ....	167
Figure 3.12	Ideal ionization versus ion suppression .....	172
Figure 3.13	Full scan and daughter spectra of 3-AP .....	175
Figure 3.14	Extracted ion chromatogram for 3-AP .....	177
Figure 3.15	Mass chromatograms at 3-AP from 1.00 to 100 ng/mL .....	178

## CHAPTER I

### INTRODUCTION TO BIOANALYTICAL METHOD DEVELOPMENT: PHARMACEUTICAL COMPOUND EXTRACTION, HIGH PERFORMANCE LIQUID CHROMATOGRAPHY AND MASS SPECTROMETRY

#### 1.1 Rationale for Method Development

The development of analytical methods to quantitate drug molecules is critical to the progress of toxicological, biochemical and clinical studies. Methods must be established and validated to demonstrate robustness, precision and accuracy of the ability of the method to determine the amount of drug present in the sample of interest. The ability to ascertain the amount of drug present provides the research community with the ability to establish the pharmacokinetics, or how the body processes the drug [1], as well as the pharmacodynamics [1], how the drug affects the body.

Pharmacokinetic parameters are divided into several sections, referred to as a LADME scheme [2]: liberation, absorption, distribution, metabolism and excretion. Liberation refers to the manner which the drug is released from the formulation. Absorption deals with how the drug is introduced to the body. Distribution is the dispersion or dissemination of the drug within the bodily fluids and tissues. Metabolism describes the transformation of the original drug into metabolites. Excretion refers to how the drug is removed from the body.

Pharmacodynamics consists of three principle components [3]: the desired affects of the drug, undesired affects of the drug and the therapeutic window of the drug. Desired affects of a drug can be caused by a variety of biochemical processes, including: chemical reactions, interaction with proteins, interaction with ion channels and ligand binding. There are also many situations which produce undesirable effects of a drug, including: mutagenic or carcinogenic cellular response, as well as, inducing cellular damage which can lead to chronic biological and physical abnormalities. Finally, the therapeutic window can be though of as the effective dosing, or the dosing amount that provides more desirable effects versus undesirable effects.

In order to study the behavior of a drug within an animal body, it is necessary to establish bioanalytical methods. There are several important considerations for the methods being developed: cost, an effort should be made to favor consumables which are the least expensive; time, the total sample preparation and run time should be kept to a minimum to enable high throughput of the

method; simplicity and transferability, the method developed should avoid over complication.

## **1.2 Extraction of Pharmaceutical Compounds from Biological Matrices**

### *1.2.1 Introduction*

Bioanalytical methods allow the detection of small amounts of a drug within a complex biological matrix, commonly plasma, urine, saliva or tissue. The biological materials are composed of a vast array of compounds, with varying chemistries. In order to detect trace amounts of pharmaceutical compounds present in these materials, the compounds must be removed from the remaining compounds in the sample.

The first step in the development of a method is the extraction or removal of the compound from the biological matrix. The matrix of blood will be discussed here. Blood is composed of red blood cells, approximately 45% by volume, which are suspended in plasma fluid (55% by volume). Plasma is approximately 92% water and 8% plasma proteins and other compounds such as minerals, glucose, carbon dioxide, hormones and pharmaceutical compounds [4].

Prior to analytical treatment, whole blood undergoes several pretreatment steps to separate the plasma from the red blood cells. First and anticoagulant is added to whole blood to prevent clotting. Secondly, the red blood cells are separate from the plasma via centrifugation. In addition to the red blood cells,

many plasma proteins will be removed from the plasma during this step. The protein in highest abundance remaining in the plasma is albumin. In addition to albumin, the plasma matrix consists of many compounds, including other proteins, minerals, electrolytes (salts), glucose, carbon dioxide, hormones and pharmaceutical compounds [5].

Although many potentially interfering substances have been removed from the whole blood, the reduction of matrix components remaining in the plasma will improve the sensitivity of developed method for the compound of interest. Further, salts, proteins, and various chemical species remaining can create contamination as well as negatively affect the precision and accuracy of the method ability to detect the pharmaceutical compound. There are many popular suitable chromatographic methods which are a good choice for removing the pharmaceutical compound from the biological matrix. Common types of chromatography used for this purpose include: liquid/liquid extraction, protein precipitation, and solid phase extraction.

### *1.2.2 Liquid Liquid Extraction (LLE)*

LLE is based on partitioning of compound into two separate liquids. LLE works by exploiting the solubility of an compound in two immiscible liquids, generally an aqueous and an organic. Organic solvents with low polarity are generally immiscible with water. For instance, toluene, diethyl ether and hexane not miscible and less dense than water, forming a partition that floats on top of

the aqueous phase. Chloroform and methylene chloride are immiscible and more dense than water, forming a partition underneath the aqueous phase.

The distribution or partitioning of an compound (solute) between the two phases in LLE can be represented by the following equilibrium equation, equation (1) [6]:



Therefore, the equation describing the partition coefficient, the ratio of species in each respective phase can be written as equation (2) [6]:

$$K_p = [S_{\text{organic}}] / [S_{\text{aqueous}}] \quad (2)$$

Evidenced by equations 1 and 2, the amount of analyte in each phase is an equilibrium process and for any  $K_p$  value, there will remain an amount of analyte in the aqueous phase. The equation describing the amount of analyte remaining in the aqueous phase after  $n$  injections is given in equation (3) [6]:

$$q^n = [V_2 / (V_2 + K_p V_1)]^n \quad (3)$$

where  $q$  is the fraction of  $S$  remaining in the aqueous phase,  $V_1$  is the volume of the organic phase,  $V_2$  is the volume of aqueous phase and  $K_p$  is the partition coefficient. In order to achieve quantitation removal of an analyte, several extractions are often required.

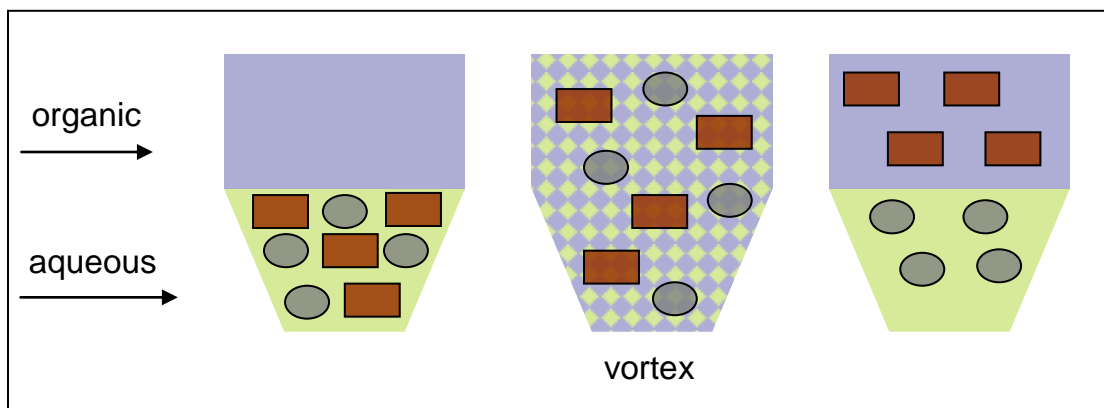


Figure 1.1, Representation of LLE

### *1.2.3 Protein Precipitation*

Protein precipitation bears many similarities to LLE. Consider a plasma sample which contains an analyte to be extracted, in addition to the analyte; there are countless proteins, salts, metals and other compounds present in the plasma sample. Proteins contain both hydrophilic and hydrophobic amino acid residues. When dissolved in water, the hydrophilic amino acids are oriented so as to interact with the polar, aqueous phase. In the case of hydrophobic amino acids, they interact with various ions in the solution to stabilize the proteins solubility in the aqueous phase [7].

There are two types of forces acting upon a protein molecule in an aqueous solution, repulsive electrostatic force and attractive electrostatic force. Repulsive electrostatic forces are demonstrated in figure 1.2. Further detail describing the solvation (or hydration) layer of proteins is contained in figure 1.3.

## Hydration Layer and Repulsive Forces

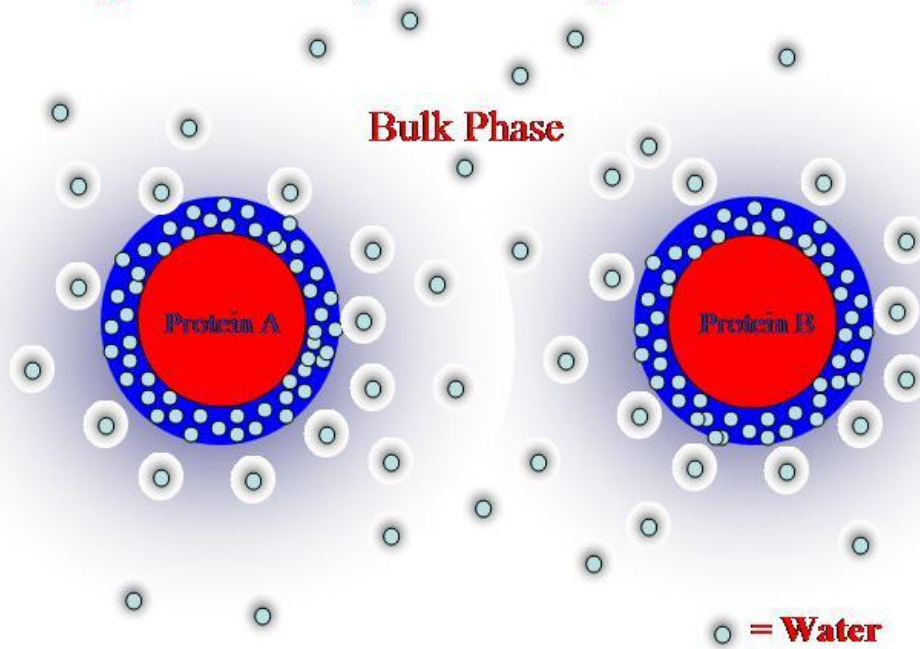


Figure 1.2, Depiction of electrostatic forces present in protein solutions

## Ordering of ions near charged residues on a protein surface

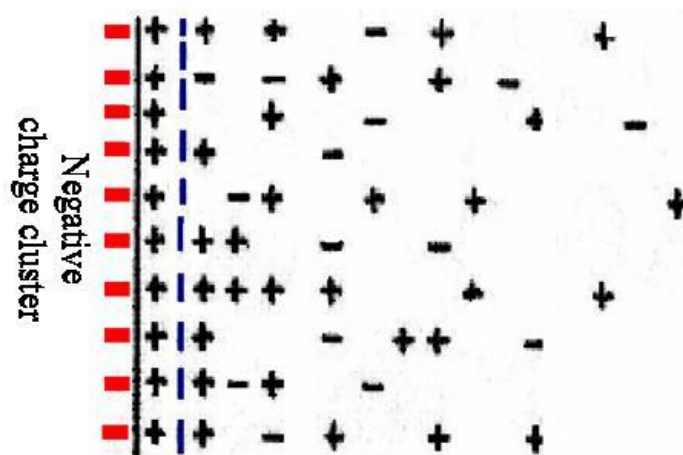


Figure 1.3, Ion distribution in the hydration layer of a protein solution

The repulsive forces between proteins prevent the proteins from interacting with another and promote the dissolution of the proteins in the aqueous solvent. This phenomenon occurs because counter ions migrate to the surface of the protein molecules and form a rigid barrier, effectively neutralizing the surface of a charged molecule. Beyond the rigid counter ion barrier, ions continue to migrate in increasingly lower concentrations. This loose, charged barrier around the proteins, allow the protein molecules to remain dissolved in solution while, at the same time, prevent the aggregation of protein molecules into clusters. Water itself can serve to generate the barrier surrounding the proteins [7].

Attractive electrostatic forces exist due to induced or permanent dipoles of protein molecules. A general illustration of attractive electrostatic forces is contained in figure 1.4. One example of an attractive electrostatic force between proteins would be the interaction of acidic residues on one protein with basic residues of another. The solvation of the proteins by the hydration layer serves to disrupt the attractive forces between proteins [7].

## Protein Interaction Cause by Disruption of Hydration Layer

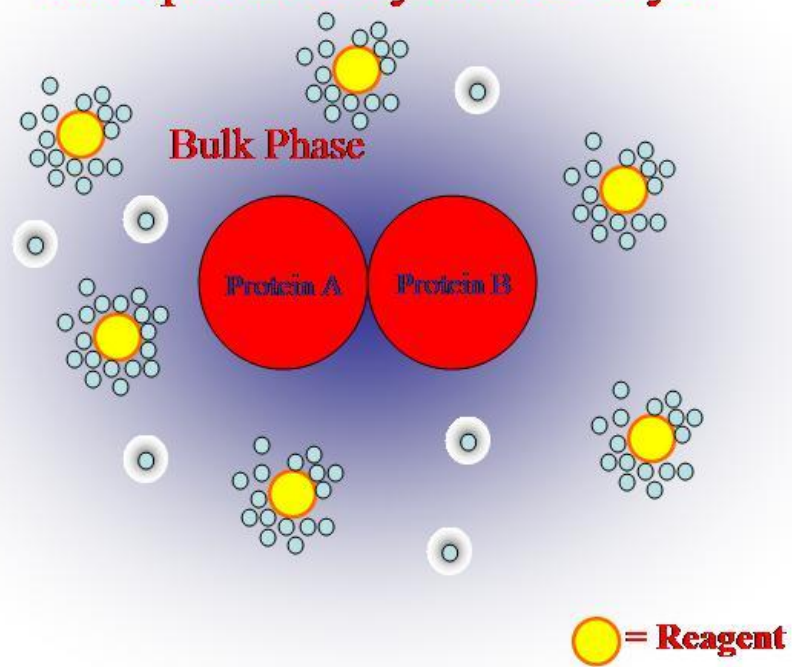


Figure 1.4, Hydration layer disruption caused by protein-protein interactions

Protein precipitation occurs in several steps: addition of precipitating agent, mixing and precipitate formation. Commonly an organic solvent such as acetonitrile or methanol is used as the precipitation agent. Upon the addition of these solvents, the solution loses stability. The unstable solution will cause denaturation of proteins and the mixing will cause the denatured proteins to aggregate and to precipitate from the plasma solution. Based on the size and weight of the precipitated proteins, they begin to fall to the bottom of the extraction vessel. Further, many salts are not soluble in the organic solvents and therefore also precipitate out of the plasma solution. The precipitated proteins can further be separated from the extraction solvent via centrifugation. Once centrifuged, the organic supernatant can be evaporated and thereafter reconstituted in order to control the concentration.

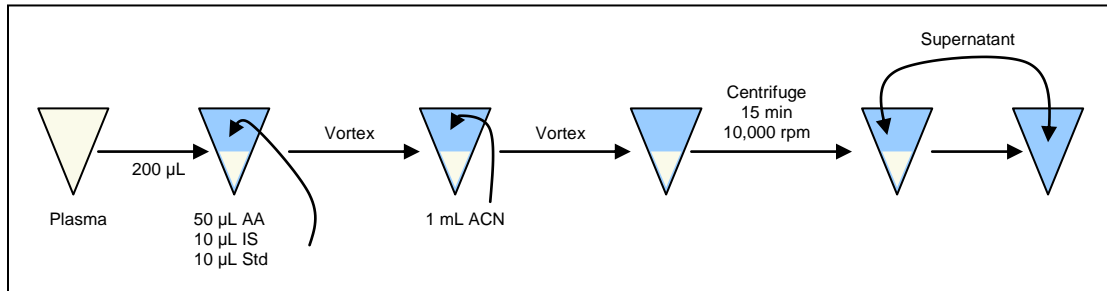


Figure 1.5, Protein precipitation procedure

#### 1.2.4 Solid Phase Extraction (SPE)

SPE is a widely used chromatographic method to separate an analyte from a complex matrix. In SPE, a column is packed with a stationary phase which will retain the analyte of interest. Commonly, the stationary phase, or sorbent is composed of a carbon based packing material as C18 and C8. There are generally four steps in SPE, sorbent conditioning, sample loading, rinsing and sample elution [8]. A block diagram demonstrating a general SPE process is contained in figure 1.6.

Step one is to activate the sorbent by rinsing with an organic solvent in order to wet the stationary phase. The hydrophobic packing is dry initially and the ligands are all collapsed. Organic phase extends the ligands and prepares them for interaction with the analyte [8].

Step two of SPE is the sample loading phase. A solution containing the sample, as well as, any contaminants or interfering substances, is introduced onto the stationary phase. The stationary phase will interact with the analyte molecules, retaining them until step four.

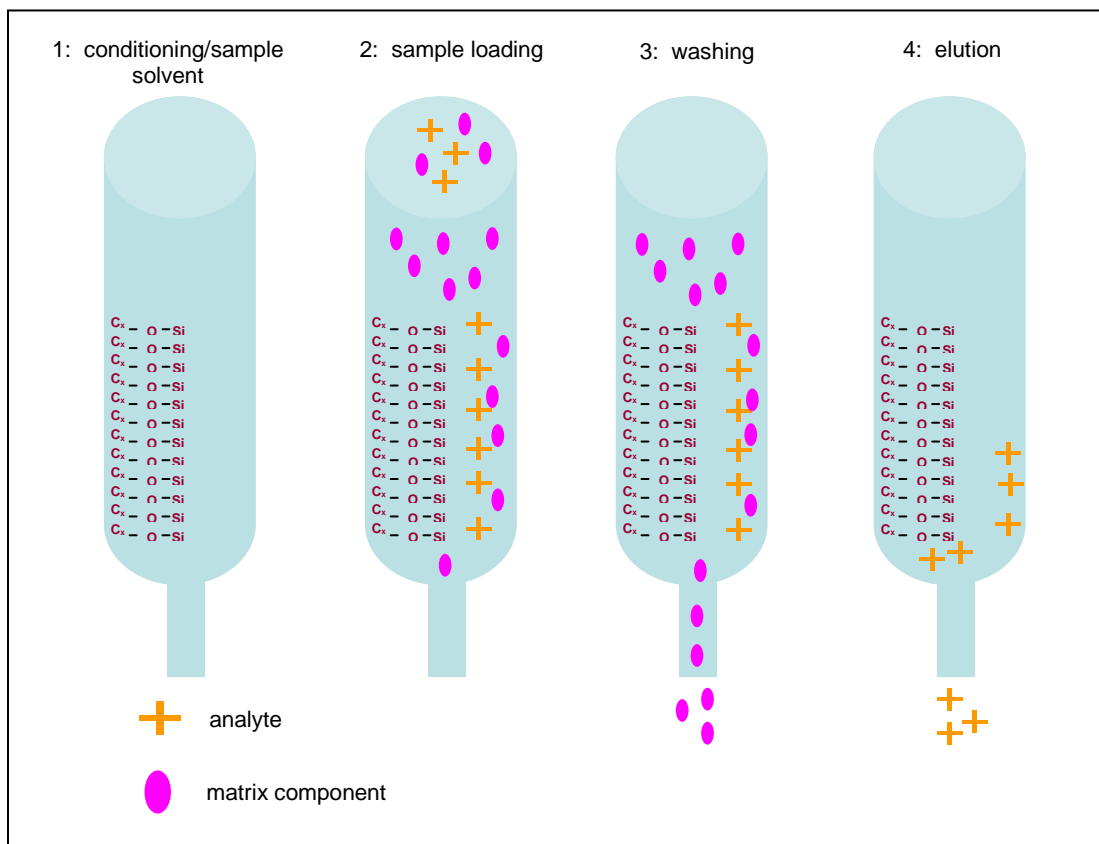


Figure 1.6, SPE procedure

Step three of SPE is a washing step which aids in the removal of contaminants and interfering compounds. This step is conducted again with the solvent composition of the sample matrix. During this step, the analyte will be bound by the stationary phase and will not be released by the column.

Finally, in step four of SPE, an elution solvent is introduced to the column. The elution solvent will have distinctly different properties than the solvent used for the previous three steps. For example, considering a hydrophobic pharmaceutical compound: should the sample be loaded in an aqueous plasma solution, an organic solvent such as acetonitrile may be used to elute the compound. As in LLE, the elution solution collected may be evaporated in order to control the concentration.

### **1.3 High Performance Liquid Chromatography (HPLC)**

#### *1.3.1 Introduction*

HPLC is a cornerstone of bioanalytical chemistry which began development in the 1970's. HPLC can be used to separate, identify and quantitate any compound which can be dissolved in a liquid. HPLC is not bound by sample volatility or thermal stability, is conducted at room temperature, is able to be automated, provides ease of use, and generates powerful data.

Many forms of HPLC exist, including: normal phase, reverse phase, ion exchange, size exclusion and bioaffinity, to name a few. It is important to differentiate between normal and reverse phase chromatography. In the case of normal phase, the compound of interest has a polar, or hydrophilic chemical composition. Chromatographic conditions for normal phase would utilize a polar, hydrophilic analytical column and mobile phase composition. The vast majority of pharmaceutical compounds investigated are either non-polar, hydrophobic or both. Due to the chemical nature of pharmaceutical compounds, reverse phase HPLC is typically used. In reverse phase HPLC, the hydrophobic interactions between the analyte and the column are manipulated and the mobile phase typically has a strong organic component [9].

The work described here deals exclusively with reverse phase HPLC, the most popular type currently used in bioanalytical method development for drug compounds, all references to HPLC will be in respect to reverse phase HPLC. There are five (5) principle components to an HPLC system, the mobile phase, pump, injector, column and detector. A flow diagram of an HPLC system is contained in figure 1.7. A in depth discussion of each component follows.

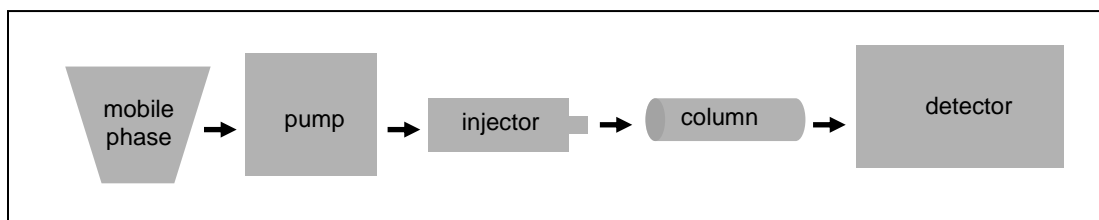


Figure 1.7, Flow diagram of HPLC setup

### 1.3.2 *Column Selection*

In today's entrepreneur driven society, there are countless manufacturers of columns to be used in bioanalytical method development for the detection of pharmaceutical analytes. The discussion that follows will consider only columns suitable for reverse phase chromatographic separations. Within the different manufactures of columns, there exists a broad array of column chemistries. The most widely used columns utilize carbon based chemistry in design, for example C18, C8 and C4. A successful column will allow for suitable resolution of the analytes of interest, low backpressure generation, minimal solvent consumption and short analysis times.

In respect to column choice the most important phenomenon to avoid is band broadening. Band broadening lowers the number of theoretical plates in a column thereby reduces the separation power of a column. There are three factors which contribute to band broadening: longitudinal diffusion, resistance to mass transfer across phases (stationary and mobile), and eddy diffusion which is caused by mobile phase factors.

Longitudinal diffusion is diffusion of the sample in a direction parallel to the sample flow.

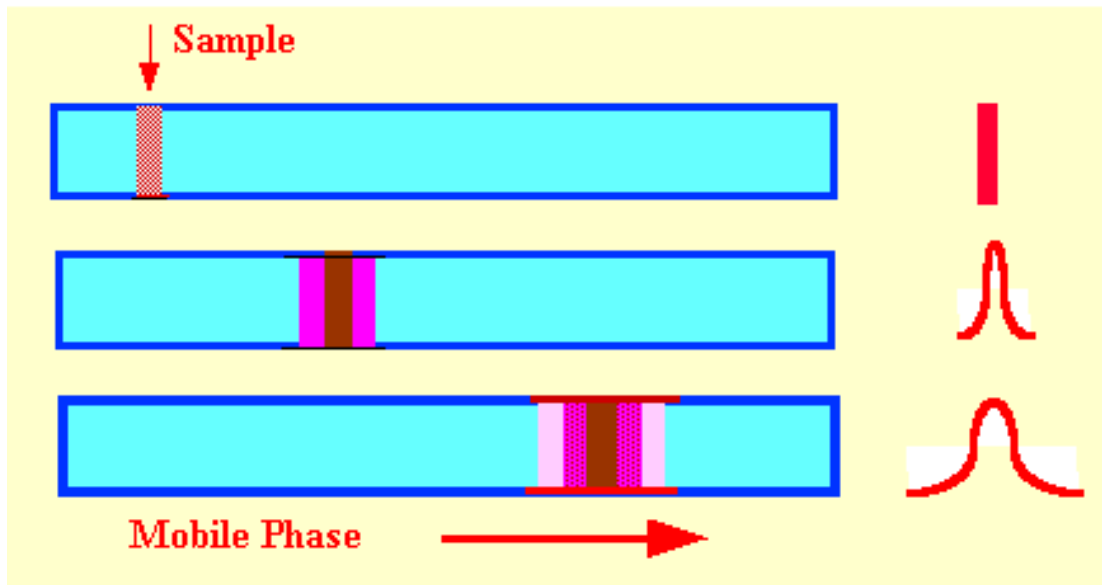


Figure 1.8, Figural depiction of longitudinal diffusion

As evidenced in figure 1.8., the longer a solute remains in a column the more a sample diffuses and the broader the peak shape becomes. The length of time a solute remains in a column has an inverse relationship to the mobile phase flow rate and therefore the longitudinal diffusion is also inversely proportional to the mobile phase flow rate. The equation relating the longitudinal diffusion ( $\sigma_L^2$ ) to the length of the column (L) is given in equation x., where  $D_m$  represents the diffusivity of the solute in the mobile phase  $u$  is the linear velocity of mobile phase and  $\gamma$  is a constant that depends of the column packing material [10].

$$\sigma_L^2 = (2D_m L \gamma) / u \quad (4)$$

As evidenced in equation 4, band broadening due to linear diffusion can be reduced by manipulating the mobile phase flow rate and the column length.

A second factor affecting band broadening is the resistance to mass transfer across the boundaries of both the stationary and mobile phase [11]. Figure x is a simple graphical depiction of how mass transfer can cause band broadening.

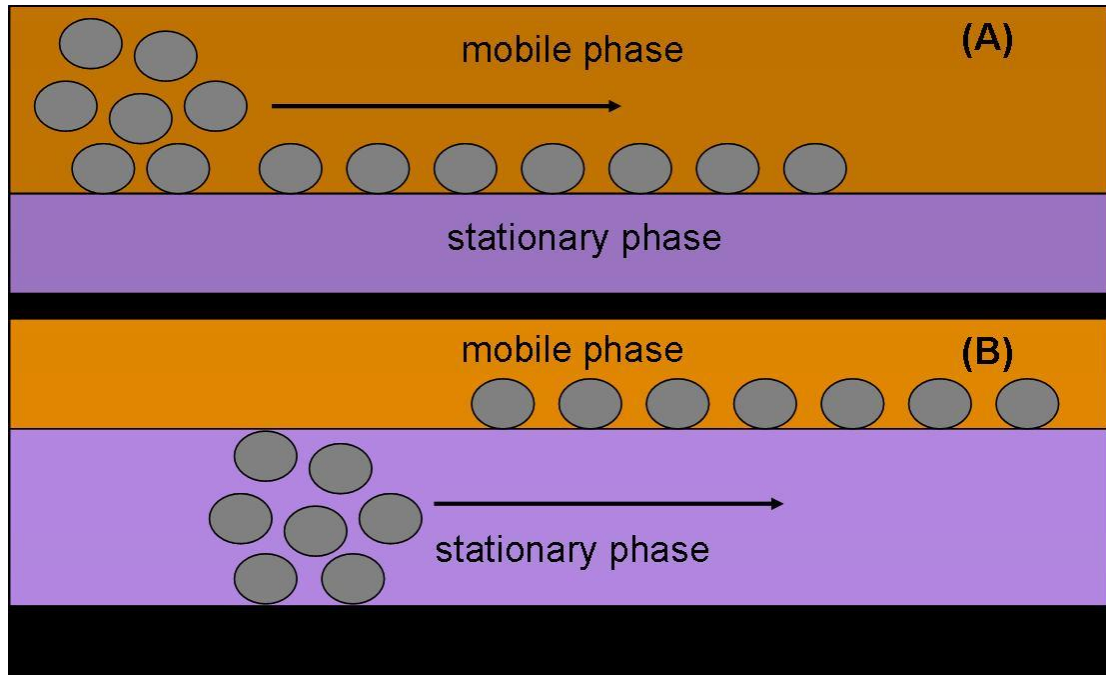


Figure 1.9, Mass transfer due to (A) resistance in the mobile phase and (B) resistance in the stationary phase

In figure 1.9(A) it is evident that in the beginning, all analyte molecules occupy a small horizontal space. During this time, some of the analyte molecules are transferred from the mobile phase to the stationary phase, this process is dictated by the spatial proximity of the molecules to the stationary phase. It will take longer for molecules that are further a longer time to interact with the stationary phase. This time results in band broadening. The same scenario can be considered for the molecule bound to the stationary phase as depicted in figure 1.9(B). While the molecules initially are confined to a narrow horizontal space, it will require time for the molecules a greater vertical distance from the boundary of the phase to migrate to that surface and interact. Again, the resistance to mass transfer causes band broadening.

The last phenomenon that causes band broadening is eddy diffusion [11]. Eddy diffusion is the uneven flow distribution of a mobile phase through a stationary phase. This form of diffusion is not well described using a mathematical equation.

Besides the considerations discussed regarding band broadening and the various diffusions that cause it, there are other factors to consider in column choice. Overall the parameters are column length, particle size, column diameter (internal diameter), and pore size [12, 13].

In respect to column length, the longer a column, the higher the resolution power. However, as column length increases, the backpressure increases which can be unpractical for many HPLC systems. Generally for reverse phase HPLC

analysis of pharmaceutical analytes, columns under 5cm will provide suitable resolving power with limited backpressures.

The smallest particle size practical should be chosen for column material. Currently, standard sizes are 5 $\mu$ m with the smallest size available being 2 $\mu$ m. The smaller the particle size, the more theoretical plates per unit length of column, which is a desirable feature. Additionally, small particle sizes allow for faster column equilibration with mobile phase as well as, faster analysis times.

Common column internal diameters are 4.0-4.6 mm. In this range of internal diameters, the columns can withstand flow rates in the range of 1.0-1.25 mL/min. Narrow bore columns are available with internal diameters in the range of 2.0 to 3.0 mm. These columns can withstand flow rates in the range of 0.2 to 0.6 mL/min. The narrow bore columns are advantageous because their use reduces solvent consumption as well as, improves sensitivity.

In respect to pore size, the smaller the pore size, the larger the surface area and therefore the greater carbon loading of the column. In the case of pharmaceutical analytes, the optimum pore size is in the range of 80-150 Å.

In general, for reverse phase HPLC analysis of pharmaceutical analytes, a carbon based column will be a good choice. A carbon based column is composed of silica molecules which are bonded to a carbon chain. The length of the carbon chain typically ranges from C4 to C18. As the carbon chain length increases, the hydrophobicity of the stationary phase also increases. A common defect of carbon columns is related to unreacted silanol groups in the stationary phase. This defect is remedied via a process called endcapping where the

unreacted silanol groups are reacted through various chemical processes. Each manufacture has unique, proprietary endcapping techniques. The process of endcapping reduces the possibility of undesired, secondary reactions between analytes and the stationary phase. Finally, carbon based columns allow for the use of a wide range of mobile phases; including water, acetonitrile and methanol; as well as a wide pH range.

### 1.3.3. *Mobile Phase Selection*

The selection of a mobile phase is multifaceted: the solvent must be able to elute the analyte with sufficient resolution, the resolution time of the analyte should be low enough to allow for highthroughput, the use of additives such as buffers and acids should be kept to a minimum and the organic component should be chosen with cost in mind. There are endless possibilities for mobile phase compositions; it is helpful to consider two (2) primary features affected by formulation of mobile phase: solvent polarity and solvent selectivity [11, 12]. The equation describing the relationship between solvent polarity and solvent selectivity is contained in equation 5.

$$R_s = \sqrt{N/4} (\alpha - 1/\alpha) (k'/1+k') \quad (5)$$

In equation 5, the term  $(\alpha-1/\alpha)$  represents the solvent selectivity factor and the  $(k'/1+k')$  is the solvent polarity term,  $\sqrt{N}/4$  is the column factor, and  $R_s$  is the resolution value. Table I. lists the properties of several common solvents. The relationship between the polarity index of a solvent and the polarity term given in equation 4 for a reverse phase system is given by equation 6.

$$k'_2/k'_1 = 10^{[(P'_2 - P'_1)/2]} \quad (6)$$

The values of  $k'$  are initial and final values and are related to the retention time  $t_r$  of an analyte and the retention time of the unretained solvent (solvent front)  $t_0$  given by equation 7.

$$k' = (t_r - t_0)/t_0 \quad (7)$$

Table I Properties of common solvents

<b>Solvent</b>	<b>Refractive Index (25°C)</b>	<b>Viscosity, cP</b>	<b>Boiling Point, °C</b>	<b>Polarity, P</b>	<b>Eluent Strength, <math>\epsilon^0</math></b>
water	1.333	0.89	100	10.2	Large
acetonitrile	1.341	0.34	82	5.8	0.65
methanol	1.326	0.54	65	5.1	0.95
n-Hexane	1.372	0.30	69	0.1	0.01
toluene	1.494	0.55	110	2.4	0.29
ethyl acetate	1.370	0.43	77	4.4	0.58
chloroform	1.443	0.53	61	4.1	0.40

A successful mobile phase composition should aim for a  $k'$  value between 2 and 5 for a two component system and for a  $k'$  between 0.5 and 20 for a multiple component system [14]. After the solvent composition of mobile phase is optimized for  $k'$ , generally the analytes will be suitably resolved. In the case that the retention times of the analytes continue to overlap,  $\alpha$ , the selectivity factor can be manipulated. The typical approach to optimizing the selectivity factor is to change the chemical composition of the mobile phase while holding the  $k'$  constant. Equation 8 [14] demonstrates the approach to changing the selectivity of a mobile phase without having an effect on the  $k'$  for a reverse phase system.

$$\Phi_c = [\Phi_b (P_w - P_b)] / (P_w - P_c) \quad (8)$$

In equation 7, there are three solvents to consider: W, water; B, the organic component that is being changed and; C, the organic component that is replacing B. In this equation,  $\Phi_c$  represent the %volume of solvent C;  $\Phi_b$  is the volume of the organic component B; and  $P_w$ ,  $P_b$ , and  $P_c$  represent the polarity indexes of water, solvent B and solvent C, respectively.

As evidenced by the preceding discussion, through the use of a handful of simple equations, it is possible to both predict and adjust the chromatography results based upon mobile phase composition.

#### *1.3.4 Pump*

The goal of a pump is to provide the most constant flow possible of mobile phase to the column. Due to the small particle sizes of column packing material, there is a great resistance to the flow being delivered to the system. The “HP” of HPLC originally represented “high pressure” because of the high pressure which is generated during this process. There are several types of high pressure pumps which can be coupled to HPLC systems. Due to the vast number of pump types available, a summary list of pump types and their characteristics is contained in Table II. [14].

Table II., Performance characteristics of different types of pumps

Pump characteristic	Reciprocating pumps				Positive displacement				Pneumatic		
	Simple single head	Single-head pulse comp.	Simple Duathhead	Duathhead compress corand pulse comp	Duathhead closed loop flow control	Triplethead, low volume	Syringe type	Hydraulic amplifier	Simple	Amplifier	Amplifier with flow control
Resetability	+	+	++	++	++	++	++	++	-	-	+
Drift	+	+	+	++	++	++	++	+	-	+	+
Short term precision (noise)	-	+	+	++	++	++	++	++	+	+	++
Accuracy	+	+	+	+	++	++	+	+	-	-	+
Versatility and convenience	-	+	++	++	++	++	-	+	-	++	+
Serviceability	+	+	+	+	+	+	-	+	++	+	-
Durability	+	+	+	+	+	+	+	-	++	++	++
Cost	low	mod	mod	high	very high	very high	mod-high	mod	low	mod	high
"Constant flow	yes	yes	yes	yes	yes	yes	yes	yes	no	no	no
Constant pressure	no	no	no	yes	no	no	no	no	yes	yes	yes

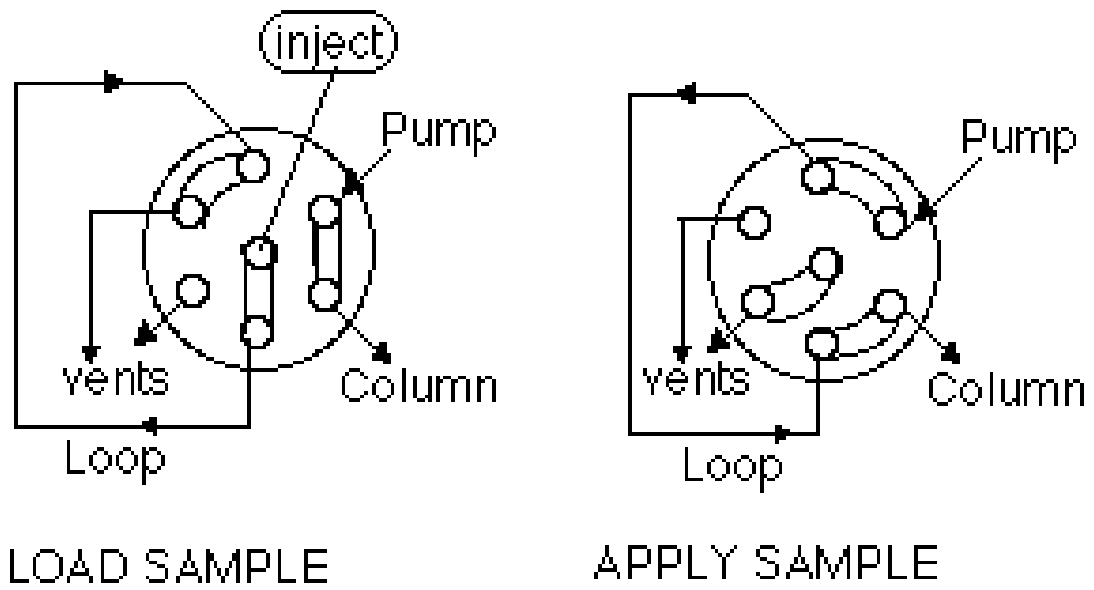
Notation: ++ = optimum, + = satisfactory, - = some deficiencies

### *1.3.5 Injector*

With respect to injectors, there are four primary considerations: the sample should be introduced to the column via a narrow plug; the injector should be easy to use; the results should be reproducible from injection to injection and; the injector should be able to operate at a high back pressure.

Typical sample loop sizes range from 5 to 50  $\mu\text{L}$ . In order to avoid problems related to dilution, the sample loop should be overfilled by at least three loop volumes.

Most modern HPLC instruments are coupled with automatic sample injectors, or autosamplers. The injections are controlled by a computer and robotic instrumental components which diminishes most error introduced during the injection process.



LOAD SAMPLE

APPLY SAMPLE

Figure 1.10, Example of injector port

### *1.3.6 Detector*

A vast array of detectors can be coupled to HPLC systems. A summary of popular detectors and their detection limits is contained in Table III. [14]. The research presented here focuses on two types of detectors, the ultraviolet detector and mass spectrometer, both of which are described in great detail in future sections.

Table III. Detection limits achievable using various detectors

<b><u>Detector</u></b>	<b><u>~ Limit of detection (ng)</u></b>
Ultraviolet	0.1-1
Refractive index	100-1000
Evaporative light scattering	0.1-1
Electrochemical	0.01-1
Fluorescence	0.001-0.01
Conductivity	0.3
Mass spectrometry	0.1-1
Fourier transform infrared	1000

## 1.4 Ultraviolet (UV) Spectroscopic Detectors

### 1.4.1 *Introduction*

UV spectroscopic detectors are one of the most widely used detectors coupled to HPLC systems. These detectors offer ease of use, are available for relatively low cost, allow for excellent linearity and provide sensitivity at a level suitable for a wide range of applications. The principle limitation of the UV detector is the requirement that the analyte absorb light in the range of 200 – 350 Å. This range includes all substances that have at least one double bond as well as any substance possessing non-bonded electrons, this group consists of all aromatic compounds, and substances containing CO, CS, N=O groups. As can be imagined, most pharmaceutical analytes belong to the group of compounds which will absorb light in the range required to use the UV detector.

### 1.4.2 *Beer-Lambert Law*

The Lambert law states that the absorption of light is directly proportional to the path length traveled. Beer's law states the relationship between the absorption of light and the concentration of analyte. Together, the Beer-Lambert law dictates the results afforded in UV spectroscopy. The equation for the Beer-Lambert law is given in equation 10.

$$A = \xi \ell C \quad (10)$$

Where A represents absorption,  $\xi$  is the molar absorptivity, a constant,  $\ell$  is the path length that the light travels, and C is the concentration of analyte.

### *1.4.3 Types of UV Detectors*

There are two types of UV detectors, fixed wavelength and multiple wavelength detectors [15, 16]. Fixed wavelength detectors operate on a single wavelength of light that is generated from a specific type of lamp. These lamps can be mercury (254 nm), cadmium (225 nm), and zinc (214 nm). It is important to note that while these lamps generate the majority of light at the wavelengths listed, there is a range of wavelengths emitted, in order to achieve true monochromatic light, a filter would be required.

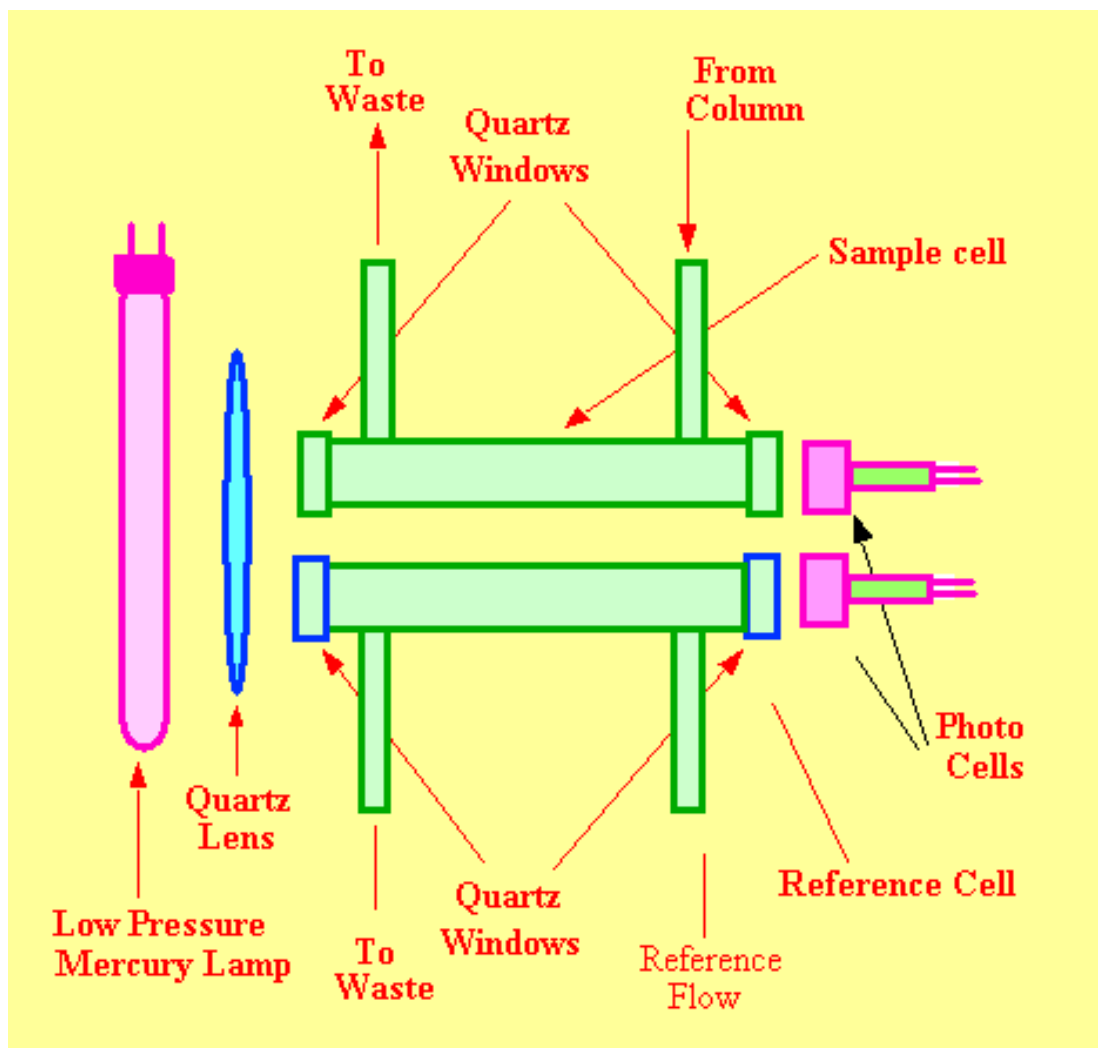


Figure 1.11, Fixed wavelength UV detector

A multi wavelength detector emits light over a broad range of wavelengths. Within the category of multi wavelength detectors, there are two types: the dispersive detector and the diode array detector. The dispersive detector monitors the eluent at a single wavelength while the diode array examines the eluent over a wide range of wavelengths.

Figure 1.12 illustrates a dispersive detector. In this detector light is generated from either a deuterium or xenon lamp and is focused by a curved mirror onto a diffraction grating. The light is dispersed and refocused onto a plane mirror, the angle of tilt of the mirror is able to control the wavelength of light emitted which then travels through the sample cell and column eluent. Commonly a wavelength is chosen based on a range of wavelengths that a particular analyte is known to absorb.

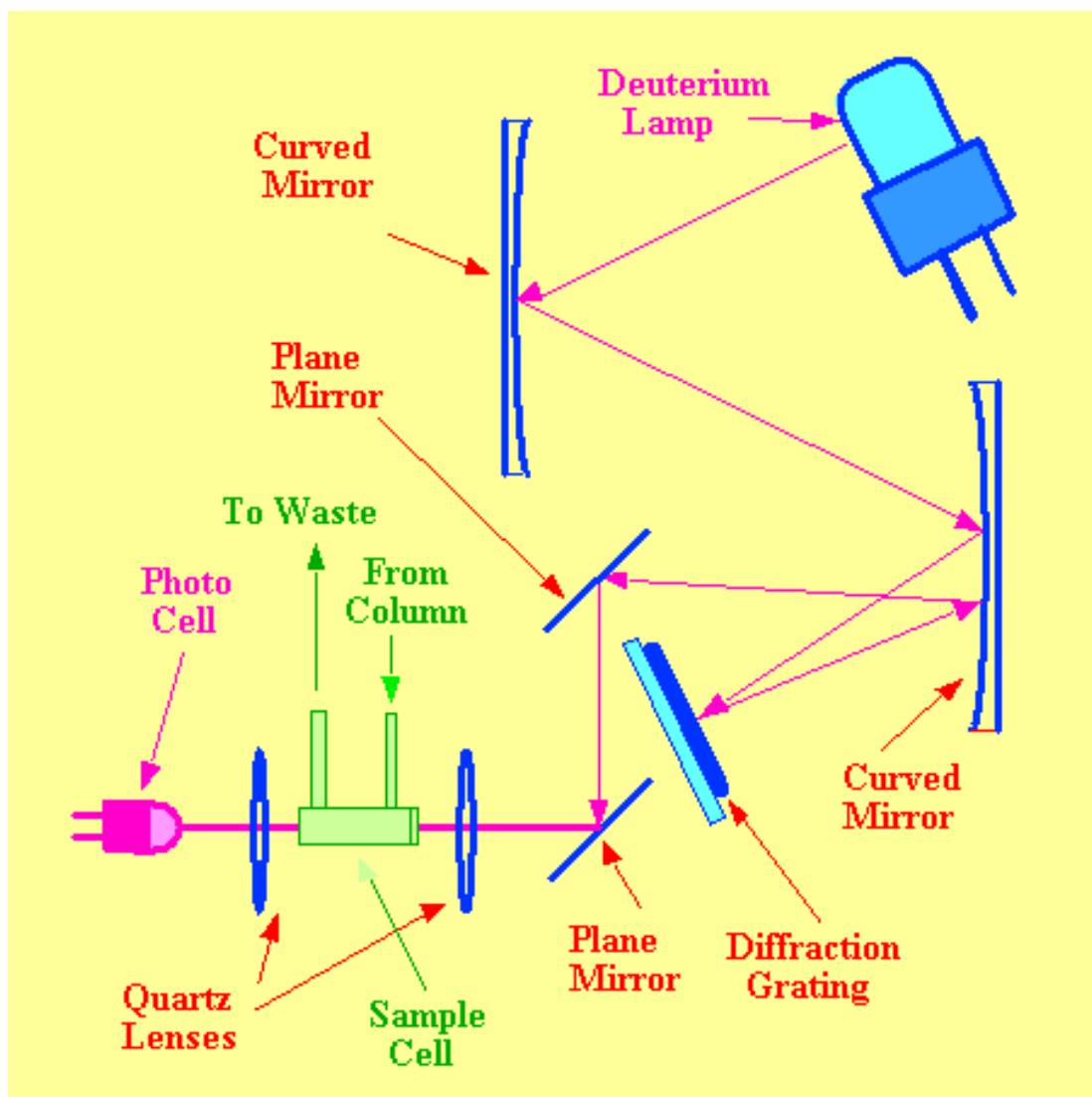


Figure 1.12, Multiple wavelength UV detector

Diode array detectors also use deuterium or xenon lamps, however, the path that light takes differs greatly from the dispersive detector. The light generated by the lamp passes through a lens system and is then directed through the flow cell, permitting light of all wavelengths to pass through the column eluent and onto a holographic grating. Light then travels to a photo diode array which can contain a large amount of diodes. Each diode is regularly sampled and a computer reports the output. Once the spectra is finished being recorded, it is possible to go back and review the data generated from any particular diode, depending on the wavelength(s) of interest.

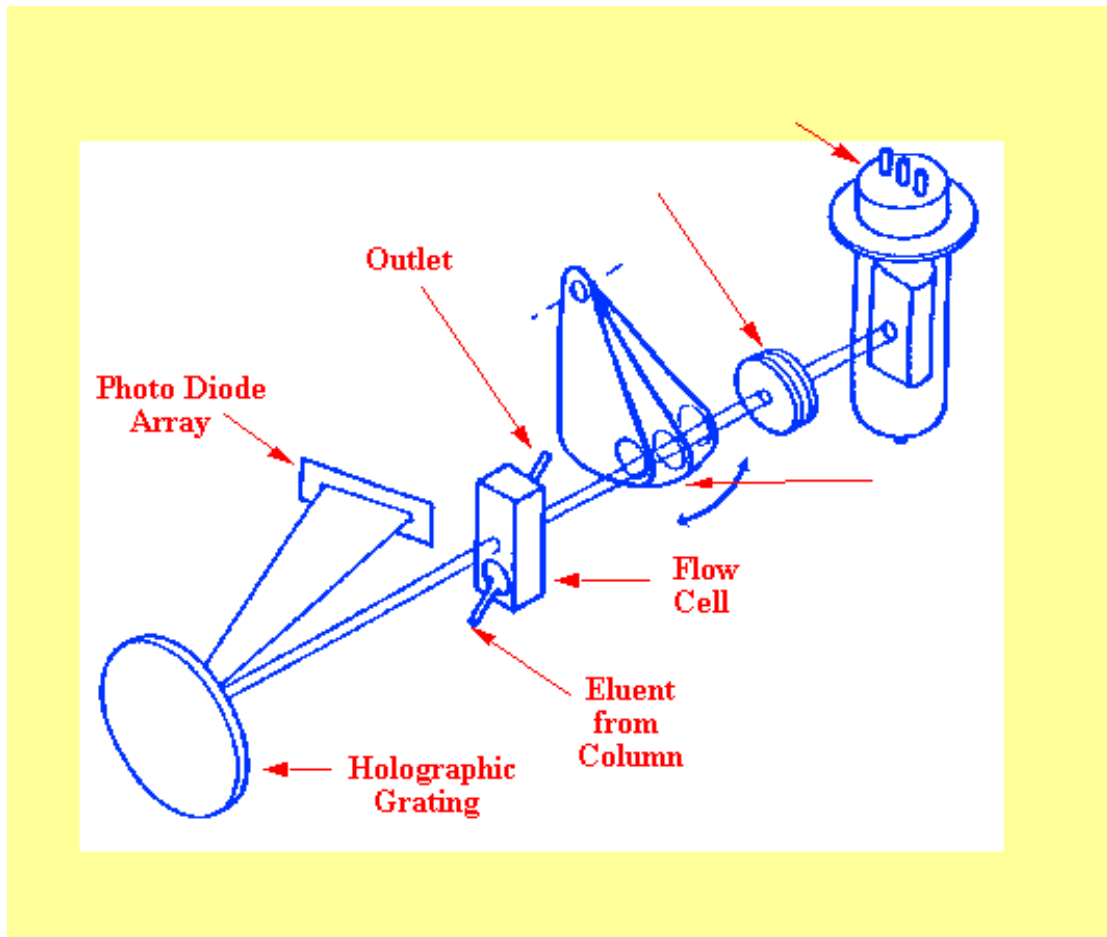


Figure 1.13, Diode array detector

#### 1.4.4 Concluding Remarks

As discussed, UV detectors are suitable for a wide range of applications. The instrumental setup provides an ease of use that is remarkable when the power of data generated is to be considered. The linear range afforded by either the fixed or multi wavelength detector is in the range of  $5 \times 10^{-8}$  to  $5 \times 10^{-4}$  g/mL. Further, an average HPLC with UV detector can be purchased for under \$100,000, which puts these instruments within the financial grasp of many researchers.

### 1.5 **Mass Spectrometric (MS) Detectors**

#### 1.5.1 Introduction

Mass spectrometers are arguably the most powerful instruments available to the analytical chemist today. The data generated via these instruments is able to both qualitate and quantitate chemical species, provide structural elucidation, as well as elemental analysis for compounds. There are many types of mass spectrometers including: triple quadrupole (QQQ), ion trap (IT) and time of flight (TOF).

Mass spectrometers work by detecting a signal based on a mass to charge ( $m/z$ ) ratio for ionized compounds. A mass spectrum is a graph of the intensity of ions versus the mass to charge ratio.

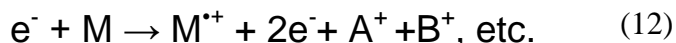
There are four principle steps carried out by the components of a mass spectrometer: ionization, acceleration, deflection and detection [17]. An ion source causes the analyte compounds to enter the gas phase. A mass analyzer is equipped with sophisticated electronics which accelerate and deflect or focus the ions. Finally, a detector measures the ion signal produced from the preceding components.

### 1.5.2 *Ion sources*

Ion sources vary widely and are dependant upon the type of material which needs to be ionized. The ion source can be viewed as the most important of the mass spectrometers components, without successful ionization there will be no analyte to be focused in the mass analyzer and thereafter detected. Some of the many types of sources include: electron ionization (EI), chemical ionization (CI), atmospheric pressure ionization (API), and electrospray ionization (ESI). A brief discussion of the theory involved in each of the four ionization methods mentioned follows, however, this work described here focuses primarily on ESI, which will be considered in more detail.

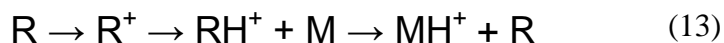
In electron ionization (EI) a beam of electrons passes through an electric field and gains energy. The accelerated electrons interact with the analyte molecules causing the analytes to form ions and ion fragments. Representative reactions are contained in equations 11 and 12. In equation 11, a neutral analyte forms a radical cation. In some situations the interaction with accelerated electrons

causes the ion formed to possess such an amount of energy that it is further fragmented, which is depicted in equation 12 [17].



In these equations  $x$  and  $x$ ,  $e^{-}$  represents an electron,  $M$  represents the analyte and  $A^{+}$  and  $B^{+}$  are the fragments produced from  $M^{*+}$ .

Chemical ionization (CI) is quite similar to EI, the first ionization step being the same. However, the steps following the initial ionization are different. Chemical ionization uses a flow of reactive gas, often methane ( $\text{CH}_4$ ) to react with an electron beam. In CI, the analyte ( $M$ ) is present in relatively small amounts in the collision gas, therefore the electrons interact more strongly with the gas molecules ( $R$ ) which are in higher concentration. The electron interaction creates a high concentration of gas ions ( $R^{*+}$ ), it is the gas ions that then interact with the analytes ( $M$ ). A representative equation demonstrating the ionization process in CI is contained in equation 13 [17].



CI can be thought of as a more soft ionization process compared with EI and is often favored because often EI generates all fragments, resulting in the absence of analyte ions.

Atmospheric pressure ionization (API) differs primarily from CI and EI in that with both CI and EI, the ionization process occurred in the gas phase, therefore any compound to be analyzed must first be vaporized. Contrary to CI and EI, API is a method of ionizing nonvolatile species. Although API differs from CI, there are many similarities and API is sometimes referred to APCI, or CI conducted under atmospheric pressure. A diagram which illustrates API is contained in figure 1.14 [19].

In API the analyte and solvent flow from a discharge needle and are exposed to a nebulizing gas at atmospheric pressure. Heat is applied to the liquid flow via a drying gas and further aids in the vaporization of the solvent and analyte molecules. Within the heated source is a corona discharge needle which applies a voltage, ionizing the solvent molecules. The ionized solvent molecules then act similar to the process of CI, where collisions and charge transfers generate ionized analytes. API or APCI, is often favored in high molecular weight, biological molecules such as proteins, oligosaccharides, and oligonucleotides.

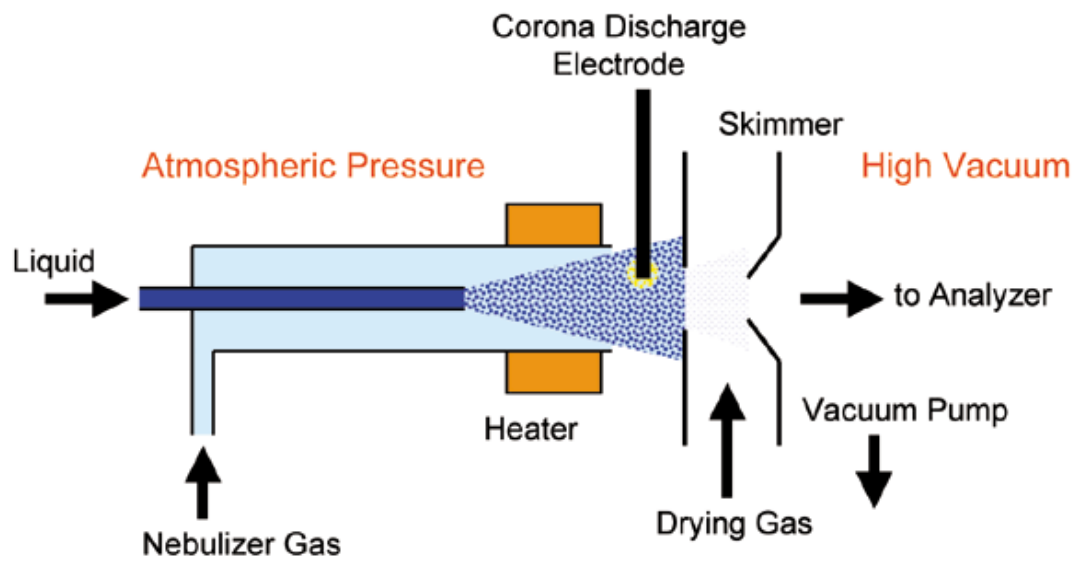


Figure 1.14, API ionization

The final ionization method to be discussed is by far the most commonly used and the most widely applicable. Electrospray ionization (ESI) is similar to API in that a liquid is subjected ionization at atmospheric pressures, however in ESI, the actual ionization is not a chemical ionization procedure [18].

In ESI, a solution is pumped through a capillary at a low flow rate, the optimal flow rate is a design feature of each instrument, in the work presented here it is should be less than 100  $\mu\text{L}/\text{min}$ . The capillary is subjected to a high voltage, and can be positive or negative, depending on the analyte of interest. The voltage applied to this capillary facilitates the formation of an electrical gradient and promotes charge separation; the result is the droplets emerge from the tip of the capillary in a formation known as a Taylor cone. The charged droplets emerge from the Taylor cone formation and travel towards the entrance to the mass spectrometer.

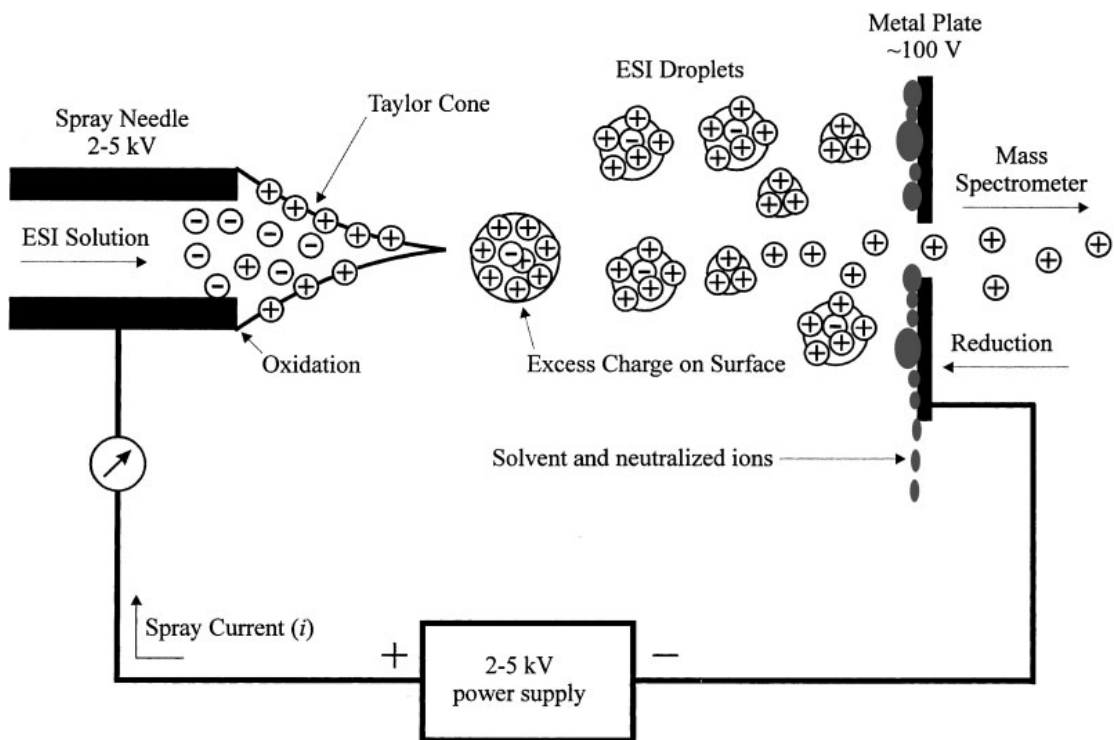


Figure 1.15, ESI ionization

Once droplets have emerged from the tip of the capillary, they are ionized through a process which has been described with various theories. The coulomb fission mechanism asserts that as the solvent evaporates, there is an increase in charge density around the droplets which causes large droplets to break into smaller droplets, eventually resulting in singly charged ions. A second mechanism of ionization, ion evaporation, states that the increased charge density caused by solvent evaporation causes an electric repulsion that provides the force to overcome the surface tension of the droplet and ions are released.

ESI is a suitable ionization technique for the analysis of a wide range of compounds. The relatively “soft” ionization process deems it a method of choice for high molecular weight biological compounds as well as, small drug molecules. As mentioned, the majority of pharmaceutical compounds tend to be non polar and ESI is generally more successful with non-polar compounds versus polar species.

In conclusion, it is important to note that during ESI-MS instrumental development, the pursuit of lower detection limits and increased sensitivity focuses on the design of the ESI source to improve ion transmission. Further, instrumental parameter which is critical to successful ion transmission is the flow rate of liquid entering the ion source.

### 1.5.3 *Mass Analyzers*

The mass analysis component of a mass spectrometer serves to sort

through the ions produced in the ion source so that only the ions of a specific mass or mass range are detected. There are several types of mass analyzers available including: single quadrupole, triple quadrupole, quadrupole ion trap, time of flight and magnetic sector. A table highlighting the characteristics of several types of mass analyzers is contained in table IV. [20]. The work presented here focuses on two types of analyzer, the triple quadrupole (QQQ) and the quadrupole ion trap (IT), the discussion presented will be limited to these types of analyzer.

Both the QQQ and the IT possess a quadrupole design. The quadrupole consists of four metal rods, aligned parallel to one another. Each pair of opposing metal rods is connected electronically and a radio frequency (RF) voltage is applied between them. A direct current voltage is then applied, superimposed upon the RF voltage. The currents applied to the metal rods generate an electric which focuses the ions based on their mass to charge ( $m/z$ ) ratio. As evidenced in figure x. only ions of a specific  $m/z$  ratio will be resonant and permitted to pass through the quadrupole. The remaining ions are deflected out of the quadrupole and therefore, not detected [17].

Table IV., Properties of various mass analyzers

	Quadrupole	Ion Trap	Timeof flight	Time-of-Flight Reflector	Magnetic Sector	F TMS	Quadrupole TOF
Accuracy	0.01% (100 ppm)	0.01% (10ppm)	0.02 to 0.2% (200ppm)	0.001% (1ppm)	≤0.0005% (<5 ppm)	≤0.0005% (<5ppm)	0.001% (10 ppm)
Resolution	4,000	4,000	8,000	15,000	30,000	100,000	10,000
m/zRange	4,000	4,000	>300,000	10,000	10,000	10,000	10,000
Scan Speed	~a second	~a second	milliseconds	milliseconds	~a second	~a second	~a second
Tandem MS	MS <sup>n</sup> (triple quad)	MS <sup>n</sup>	MS	MS <sup>n</sup>	MS <sup>n</sup>	MS <sup>n</sup>	MS <sup>n</sup>
Tandem MS Comments	Good accuracy Good resolution Lowenergy collisions	Good accuracy Good resolution Lowenergy collisions	Not generally applicable	Precursor ion selection is limited to a high mass range, growing number of application	Limited resolution Highenergy collisions	Excellent accuracy and resolution of products	Excellent accuracy Good resolution Lowenergy collisions
General Comments	Lowcost Ease of switching postregions	Lowcost Ease of switching postregions WellsuitedMS	Lowcost	Good accuracy Good resolution	Instrument is massive Capable of high resolution	High resolution, MSHigh vacuum,	Known for high sensitivity and accuracy when used for MS

In the case of a QQQ mass analyzer, three quadrapole are arranged in sequence. As depicted in figure 1.17, the QQQ design is composed of three quadrapoles arranged in series. The first (Q1) and third (Q3) quadrapoles serve as mass filters, with the second (Q2) acting as a collision cell. In Q1, voltages are applied to select for the  $m/z$  ratio or range of  $m/z$  ratio of the analyte of interest, the remaining  $m/z$  ratios are deflected and do not pass to the Q2. The ions which pass from Q1 to Q2 are commonly referred to as parent ions.

In the Q2, or collision cell, a collision gas is introduced to the analytes that have entered from Q1. The collision cell does not have mass filtering capacity; an RF only voltage is applied here to essentially “hold” the ions of a selected  $m/z$  ratio so that they can undergo fragmentation. Fragmentation is carried out using Ar, N<sub>2</sub> or He gas being introduced causing the ions to undergo collision induced dissociation. The pressure of collision gas can be controlled to provide optimal fragmentation.

Once the ions have been fragmented, they travel to Q3 which operates as a second mass filter. The Q3 then scans a range of  $m/z$  ratios so as to allow a range of the fragments produced in Q2 to pass to the detector. This process is considered MS<sub>2</sub> and is referred to as tandem mass spectrometry or MS/MS. The ions which are selected for in Q3 and subsequently detected are typically referred to as daughter ions [17].

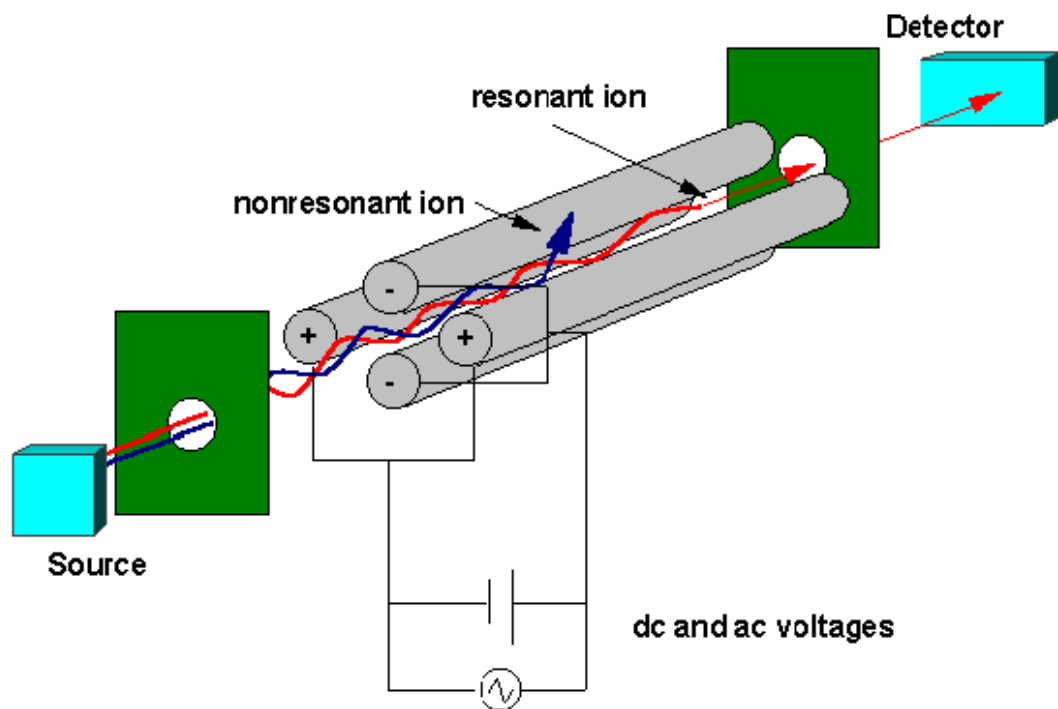


Figure 1.16, Quadrupole design

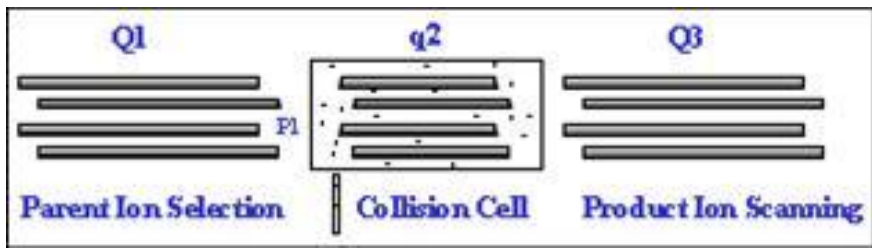


Figure 1.17, Schematic of a QQQ design

QQQ-MS/MS is currently the most popular instrument used in the development of quantitative bioanalytical methods for pharmaceutical analytes. However, the usefulness and power of this instrument is not limited to the development of such methods. The strength of this instrument rests in the generation of daughter ions. The data provided through the  $m/z$  ratio of daughter ions has several applications. First, the  $m/z$  ratios can be used to offer an added degree of specificity to a bioanalytical method. Secondly, the fragmentation pattern can be looked at like puzzle pieces, put together; they can provide structural information regarding an unknown compound. Third, the fragmentation pattern generated can be treated as a fingerprint for identification of complex biological molecules.

The second mass analyzed to be discussed is a linear ion trap (IT). The design of the IT is quite similar to the QQQ, in fact the IT also employs a quadrupole in its design. However, the electronics applied to the quadrupole in an IT differ from the QQQ.

In an IT mass analyzer, ions generated at the source are accelerated into the analyzer by a difference in voltage applied across a glass capillary with metal endcaps. The ions exiting the capillary are focused by a skimmer which has an electrical charge applied that does not permit ions that fall outside  $m/z$  range of interest to pass to the octapoles, mass filters. The octapoles are designed much the same as quadrupoles discussed previously, and they act to guide the ions along the path of the instrument to the ion trap.

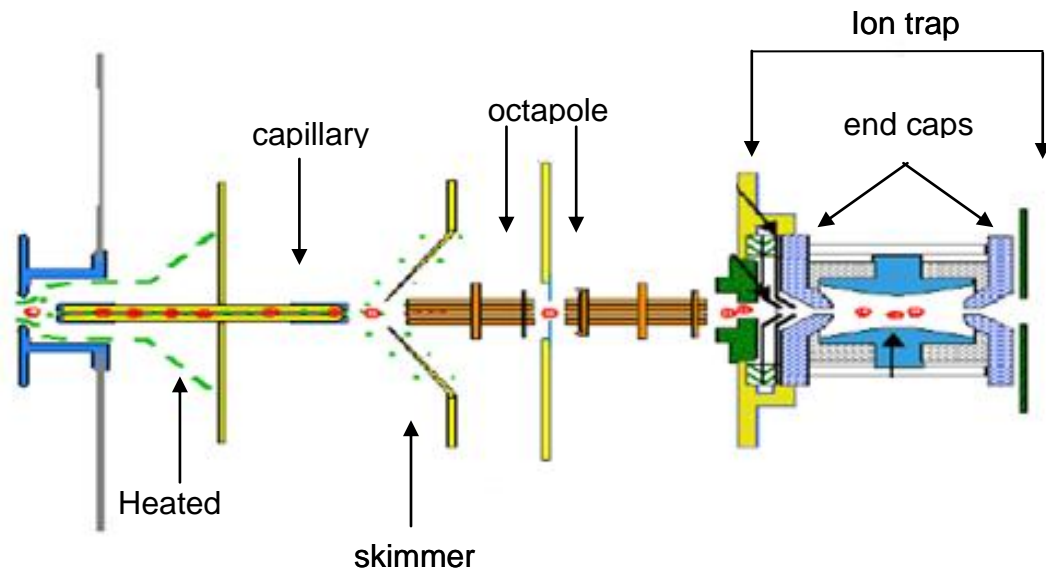


Figure 1.18, IT-MS

The ion trap component of the linear IT mass analyzer is a quadrupole equipped with electrode end caps on both sides. This component is able to hold ions within its boundaries due to an RF frequency being applied to the rods of the quadrupole by the endcapping electrodes. The voltages applied act as gate doors: opening on one side to allow the entrance and accumulation of ions for some time; closing and trapping the ions; then re-opening to allow the ions (or ion fragments) to exit the trap and travel to the detector.

The primary strength of IT mass analyzers is the ability of the trap to hold a single ion species within the trap, apply a collision gas, and for the ions to undergo collision induced dissociation. This isolation - collision process, or tandem MS, can be repeated many times, very rapidly without the need for multiple analyzers. The fragments, or daughters generated from  $MS^n$  steps is extremely valuable for structure elucidation. Another popular analysis made possible by the data generated in  $MS^n$  is the identification of proteins using the fingerprint afforded by the daughter fragments [20].

It is useful to compare the features, or lack of between the QQQ and IT mass analyzer to summarize their operation and application. Arguably the most powerful feature of the IT is the ability to conduct multiple isolations and fragmentations ( $MS^n$ ), whereas, the QQQ is limited to a single fragmentation ( $MS^2$ ). Further, the ability of the quadrupole of an IT to allow the accumulation of a specific ion, affords this mass analyzer some advantages in sensitivity. It should be mentioned that the IT is able to operate under extremely high scan

speeds which allow it to detect a wider mass range of ions, however, when operating under such modes, there is a great loss in resolution.

Whereas, the IT has many advantages for providing structural information, the IT lacks the dynamic or linear range present with QQQ analyzers. While the trap can hold a large volume of ions, as the number of ions increases, space to charge dynamics hinder the performance of the analyzer. The excellent dynamic range afforded by the QQQ, makes it the premier choice for the development of quantitative bioanalytical methods.

#### *1.5.4 Detectors*

The final component of a mass spectrometer is the detector(s). The detector records either the charge or the current produced when an ion comes into contact with its surface. There are many types of detectors available, table V. [20] summarizes the advantages and disadvantages of each type. For this discussion, the electron multiplier and photomultiplier will be discussed.

Table V., Characteristics of MS detectors

Detector	Advantages	Disadvantages
Faraday Cup	<ul style="list-style-type: none"> <li>• Good for checking ion transmission and low sensitivity measurements</li> </ul>	<ul style="list-style-type: none"> <li>• Low amplification (<math>\approx 10</math>)</li> </ul>
Photomultiplier Conversion Dynode (Scintillation Counting)	<ul style="list-style-type: none"> <li>• Robust</li> <li>• Long lifetime (<math>&gt;5</math> years)</li> <li>• Sensitive (<math>\approx</math> gains of <math>10^6</math>)</li> </ul>	<ul style="list-style-type: none"> <li>• Cannot be exposed to light while in operation</li> </ul>
Electron Multiplier	<ul style="list-style-type: none"> <li>• Robust</li> <li>• Fast response</li> <li>• Sensitive (<math>\approx</math> gains of <math>10^6</math>)</li> </ul>	<ul style="list-style-type: none"> <li>• Shorter lifetime than scintillation counting (<math>\sim 3</math> years)</li> </ul>
High Energy Dynodes with electron multiplier	<ul style="list-style-type: none"> <li>• Increases high mass sensitivity</li> </ul>	<ul style="list-style-type: none"> <li>• May shorten lifetime of electron multiplier</li> </ul>
Array	<ul style="list-style-type: none"> <li>• Fast and sensitive</li> </ul>	<ul style="list-style-type: none"> <li>• Reduces resolution</li> <li>• Expensive</li> </ul>
Charge Detection	<ul style="list-style-type: none"> <li>• Detects ions independent of mass and velocity</li> </ul>	<ul style="list-style-type: none"> <li>• Limited compatibility with most existing instruments</li> </ul>

Electron multipliers are comprised of a series of  $\text{AlO}_3$  dynodes held at increasing potentials. When an ion strikes the surface, an electron is released. The release of the first electron causes a chain reaction whereby a great number of electrons are released at each dynode. This is sometimes referred to as an avalanche effect. The large volumes of electrodes are collected by an anode, and thus a signal is recorded. A simple diagram depiction of an electron multipliers is contained in figure 19.

Photomultipliers are similar in design to electron multipliers in that electrons bombard a phosphorous screen, as opposed to a dynode. Photos are released from the phosphorous screen. The photons then encounter a photocathode screen which results in the release of electrons. The electrons then travel through the photomultiplier tube which operates as an electron multiplier, generating a cascade of electrons as discussed previously. There is one main advantage of a photomultiplier over electron multiplier as the photomultiplier tube is sealed in a vacuum. The vacuum prevents the detector from sources of contamination thus increasing the detector lifetime.

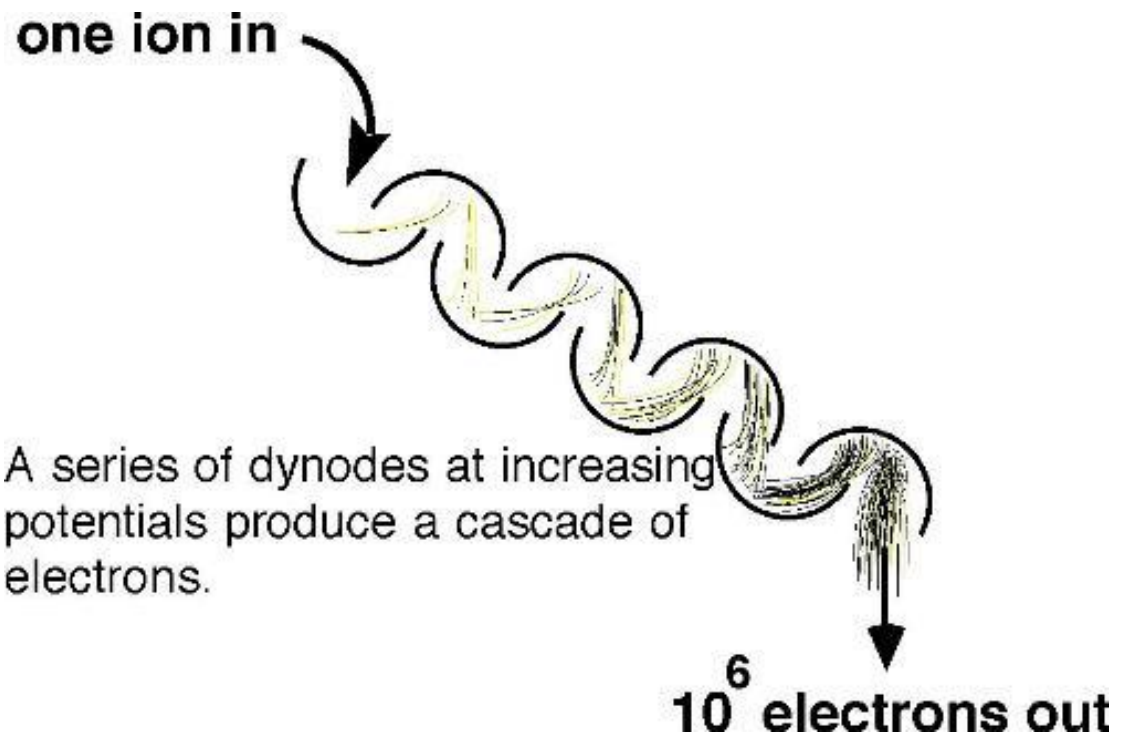


Figure 1.19, Electron multiplier process

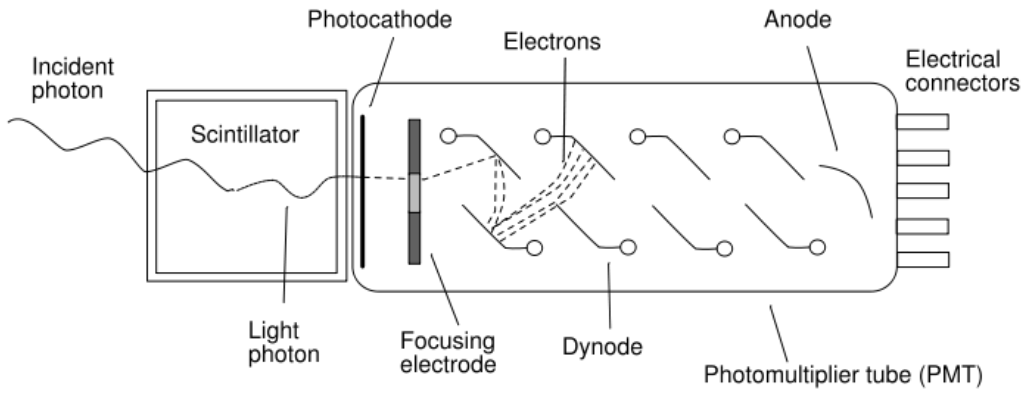


Figure 1.20, Photomultiplier

## **1.6 Conclusion**

This chapter has provided an overview of why it is necessary to develop quantitative bioanalytical methods, the determination of pharmacokinetics and pharmacodynamics. Further, theory has been introduced regarding the all components of methods development. A discussion of the extraction of pharmaceutical analytes from biological matrices has been presented, highlighting the common procedures used and the theory that dictates their success. Thereafter, a detailed explanation of the instrumental setup and design of HPLC was presented. A subsequent discussion of UV detectors followed, highlighting the usefulness of the detection methods. Finally, the instrumentation and theory of mass spectrometers was presented. Overall, this chapter should exhibit the profound understanding of many sophisticated components required to successfully develop a quantitative analytical method for the determination of pharmaceutical compounds.

## Chapter I References

- [1] The Merck Manuals Online Medical Library, available at <http://www.merck.com/mmpe/sec20/ch303/ch303a.html>, retrieved July 16, 2009
- [2] Guttendorf, R.J., Network Science Corporation, available at <http://www.netsci.org/Science/Special/feature06.html>, **retrieved July 16, 2009**
- [3] Tozer, T.N., Rowland, M., Introduction to Pharmacokinetics and Pharmacodynamics**, Lippincott Williams & Wilkins, (2006)
- [4] Nelson, D.R., Cox, M.M., Lehninger Principles of Biochemistry, W.H. Freeman, 4<sup>th</sup> Ed. (2004)
- [5] Guide to the Preparation, Use and Quality Assurance of Blood Components, Council of European Publishing, 12<sup>th</sup> Ed. (2006)
- [6] Harris, D.C., Quantitative Chemical Analysis, W.H. Freeman, 7<sup>th</sup> Ed. (2006)
- [7] Harrison, R.G., Bioseparations Science and Engineering, Oxford University Press (2002)

[8] Guide to Solid Phase Extraction, Bulletin 910, Sigma Aldrich, available at <http://www.sigmaaldrich.com/Graphics/Supelco/objects/4600/4538.pdf>, retrieved

July 16, 2009

[9] Kazakevich, Y., HPLC for Pharmaceutical Scientists, Wiley-Interscience, (2007)

[10] Crombeen, J.P., Chromatographia, 1986, 22, 319-328

[11] Scott, R.P.W., Principles and Practice in Chromatography, Library4Science on line, available at <http://www.chromatography-online.org/Principles>, retrieved

July 16, 2009

[12] Synder, L.R., et al., Practical Guide to HPLC Method Development, Wiley-Interscience, 2<sup>nd</sup> Ed., (1997)

[13] Scott, R.P.W., Plate Theory and Extensions, Library4Science on line, available at <http://www.chromatography-online.org/6/contents.html>, retrieved July

16, 2009

[14] Synder, L.R., Introduction to Modern Liquid Chromatography, Wiley-Interscience, 2<sup>nd</sup> Ed., (1979)

[15] Scott, R.P.W., Liquid Chromatography Detectors, Library4Science on line, available at <http://www.chromatography-online.org/5/contents.html>, retrieved July 16, 2009

[16] Cazes, J., Encyclopedia of Chromatography, CRC, 3<sup>rd</sup> Ed., (2009)

[17] Herbert, C.G., Mass Spectrometry Basics, CRC, (2002)

[18] Dass, C., Fundamentals of Contemporary Mass Spectrometry, Wiley-Intersciences, (2007)

[19] Harrison, A., Chemical Ionization in Mass Spectrometry, CRC, 2<sup>nd</sup> Ed., (1992)

[20] Busch, K.L., et al., Mass Spectrometry/Techniques and Applications of Tandem Mass Spectrometry, Wiley-VCH, (1989)

## CHAPTER II

### THE DEVELOPMENT OF QUANTITATIVE BIOANALYTICAL METHODS FOR THE DETERMINATION OF CANNABINOID ANTAGONISTS RIMONABANT AND SURINABANT

#### 2.1 Introduction to Cannabinoids

##### 2.1.1 *Cannabinoid Discovery*

Cannabinoids are a class of compounds which are found in the cannabis plant. Cannabinoids also refer to a broad class of compounds which include: those structurally related to tetrahydrocannabinol (THC); compounds which bind

to the cannabinoid (CB) receptors; and eicosanoids, which are related to endocannabinoids.

The discovery of cannabinoids began with the isolation of THC, the primary psychoactive component of the cannabis plant in 1964 [1]. THC is a compound which can induce feelings of euphoria, stimulate appetite, and reduce pain [2].

In the body THC is metabolized to 11-hydroxy-THC which continues to possess psychoactive properties. The metabolite is further oxidized to 11-Nor-9-carboxy-THC. Over 100 metabolites of THC have been identified in humans and animals, but 11-hydroxy-THC and 11-Nor-9-carboxy-THC are the most prevalent. THC is metabolized in the liver via p450 enzymes and predominantly excreted in feces (55%) with 20% being excreted in urine [3].

The interesting psychoactive properties of THC have led to its use as a therapeutic agent in the treatment of both cancer and AIDS due to its analgesic, appetite stimulating properties. Its success in these treatments has opened the door to widespread research aiming to elucidate the mechanisms of action of this exciting class of compounds.

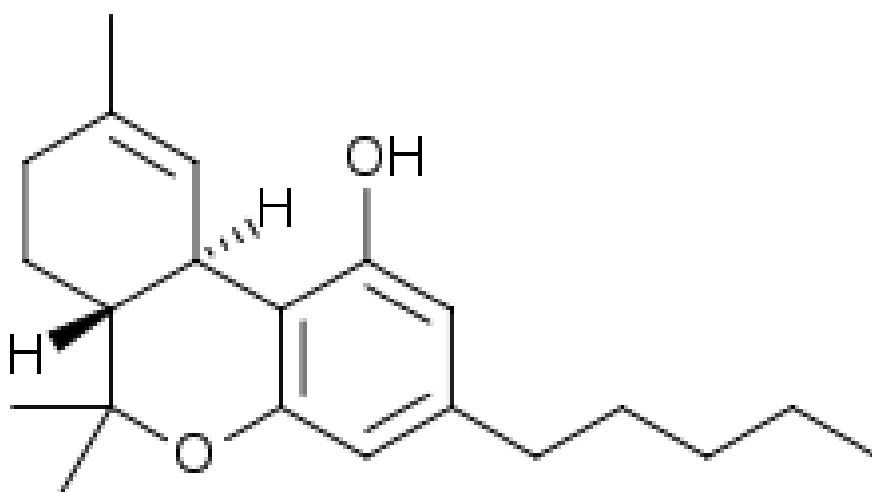


Figure 2.1, Chemical structure of THC

### *2.1.2 Endogenous Cannabinoid System (ECS)*

The discovery of THC and the physiological processes it affects has led to the study of a complex signaling system, termed the endocannabinoid system (ECS). The endocannabinoid system consists of: cannabinoids, both endogenous and exogenous; proteins which are involved with the synthesis and inactivation of cannabinoids; cannabinoid (CB) receptors; and biochemical pathways which are affected by cannabinoids.

Prior to discussing the ECS, it is necessary to explain normal and retrograde neurotransmission. In normal neurotransmission, neurotransmitter are released from the presynaptic neuron, travel across the synaptic cleft, and bind to their receptor on the postsynaptic neuron.

Cannabinoids, both endogenous and exogenous, participate in retrograde neurotransmission. In retrograde neurotransmission (Figure 2.3), the neurotransmitter (cannabinoid) is released from the postsynaptic neuron and binds with a receptor on the presynaptic neuron [4].

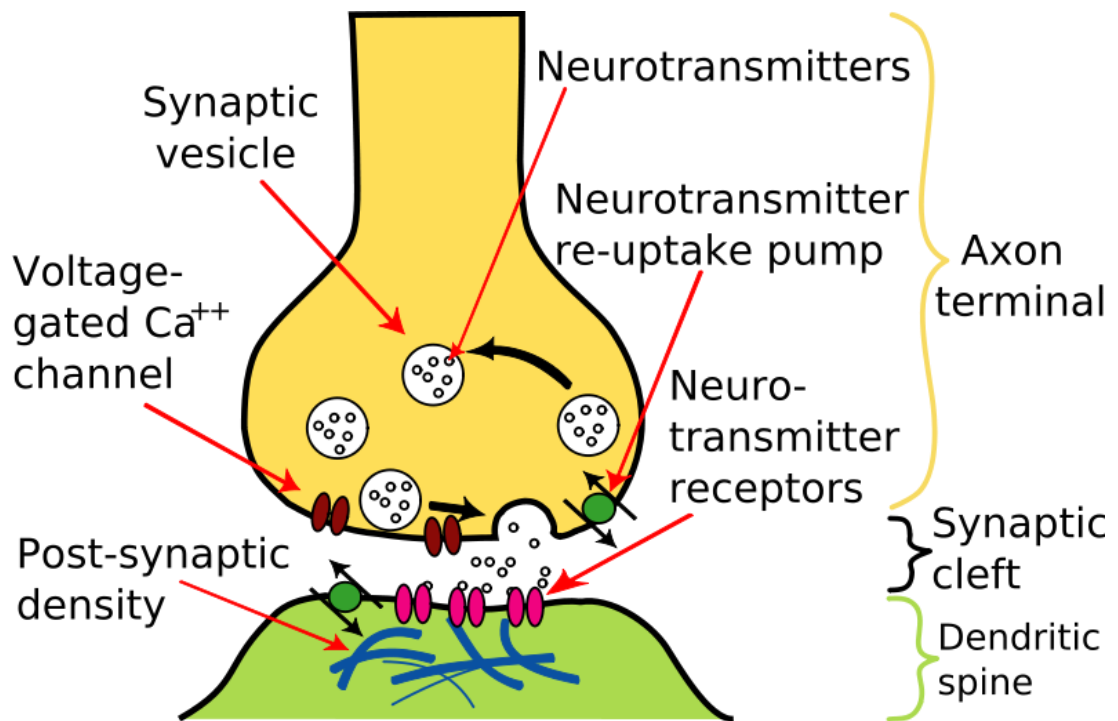


Figure 2.2, Normal neurotransmission

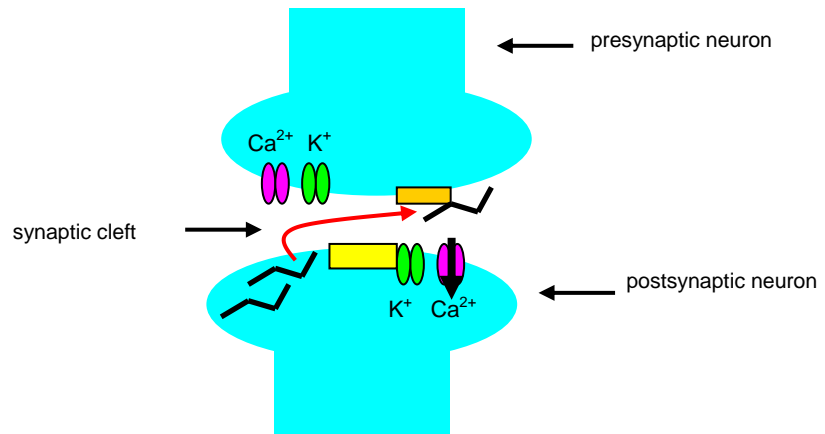


Figure 2.3, Retrograde neurotransmission

The exogenous cannabinoid, THC has been discussed. There are also endogenously produced cannabinoid or endocannabinoids (EC's). Two EC's have been identified, anandamide (AEA) and 2-arachidonyl glycerol (2-AG). Both compounds are metabolites of arachidonic acid [5].

When the ECS is functioning normally, the synthesis of EC's is initiated by membrane depolarization on the postsynaptic neuron which causes an influx of  $Ca^{2+}$  into the neuron.  $Ca^{2+}$  activates the enzyme transacylase which catalyzes the first step of synthesis by converting the membrane phospholipid [phosphatidylethanolamine](#) to N-[phosphatidylethanolamine](#) (NAPE). In one proposed mechanism, NAPE is further cleaved to yield the EC, AEA [6].

The EC's are highly lipophilic, and are able to cross the cellular membrane of neurons freely, as opposed to being stored in vesicles, as required for most neurotransmitters. The synthesis of the EC's happens rapidly, when required, and they are quickly degraded by [fatty acid amide hydrolase](#) (FAAH) back to arachidonic acid plus ethanolamine (AEA) or glycerol (2-AG) [7]. The reaction scheme for the biosynthesis of EC's is presented in figure 2.5.

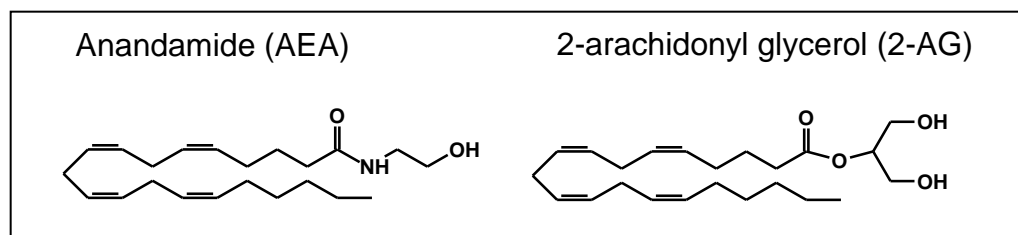


Figure 2.4, Chemical structure of AEA and 2-AG

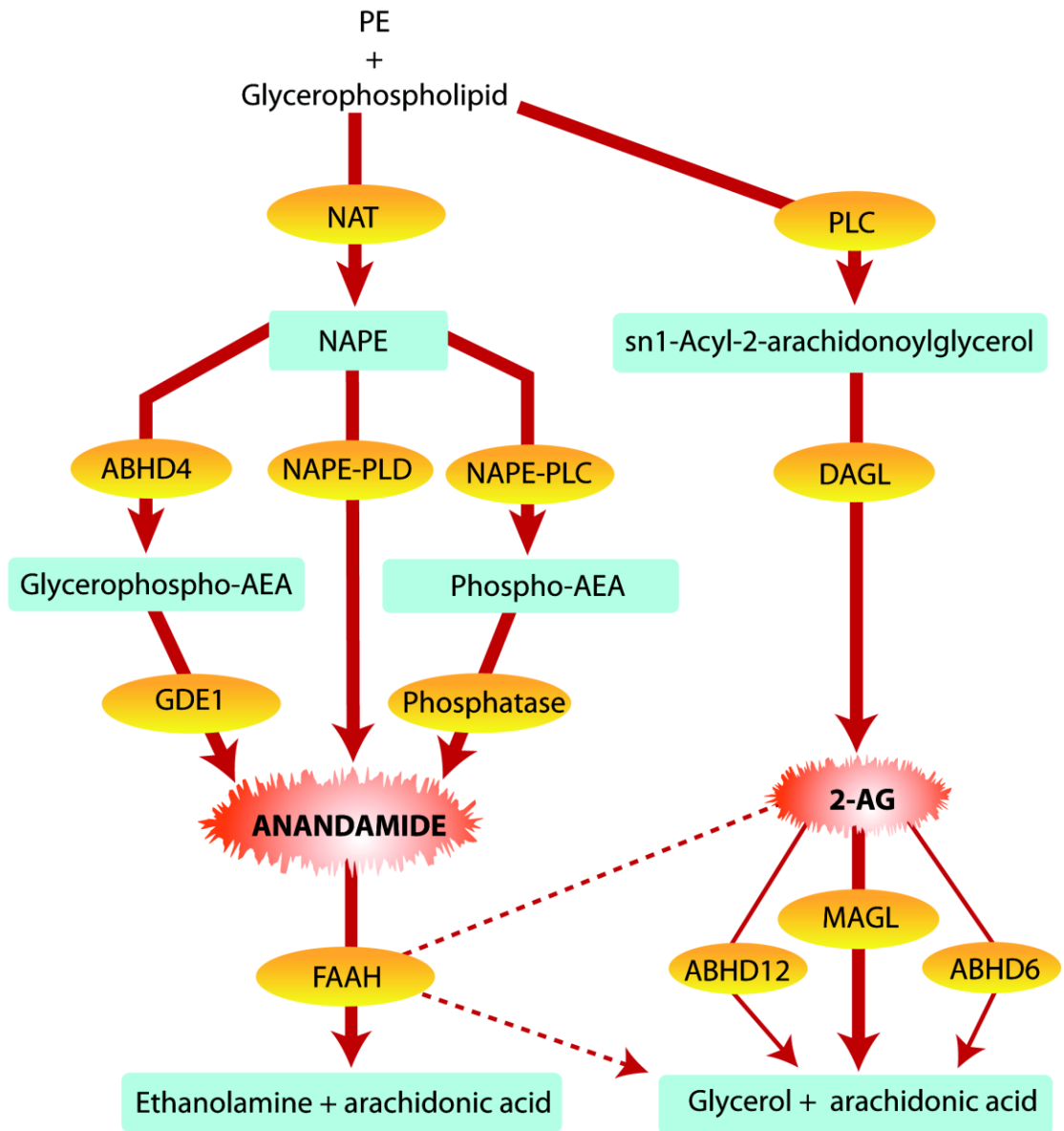


Figure 2.5, Biosynthesis of AEA and 2-AG

Both exogenous cannabinoids and EC act on the CB receptors. CB receptors are a class of G-protein coupled receptors. G-protein coupled receptors are seven domain, transmembrane proteins. Transmembrane proteins are affected by compounds outside of the cell and cause a biochemical response within the cell.

There are two classes of CB receptors, CB1 and CB2. CB1 receptors are primarily concentrated in the brain and nervous system. CB2 receptors are located expressed in the immune system and Hematopoietic stem cells (HSCs). There is also evidence for CB receptors which do not belong to the CB1 or CB2 subtypes [8], however, there is little understood about these receptors.

It has been reported that the CB1 receptor is the most widely expressed receptor in the brain [9]. A diagram which depicts the areas of the brain where the CB1 receptor is expressed is contained in figure 2.7 [9]. When the CB1 receptor is activated by cannabinoids, it is thought to cause neuronal membrane depolarization which causes a reduction in GABA neurotransmission. The CB1 receptor is also expressed in other tissues, notably the liver, where its activation stimulates lipogenesis [10].

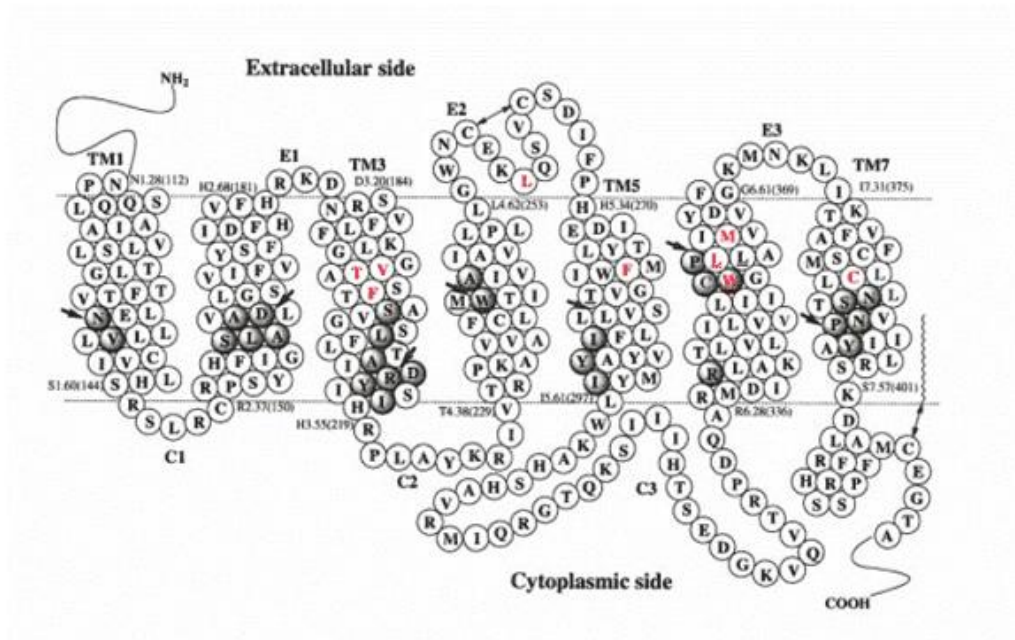


Figure 2.6, Protein structure of the CB1 receptor [8]

**Red = abundant CB<sub>1</sub> receptor expression**    **Black = moderately abundant CB<sub>1</sub> receptor**

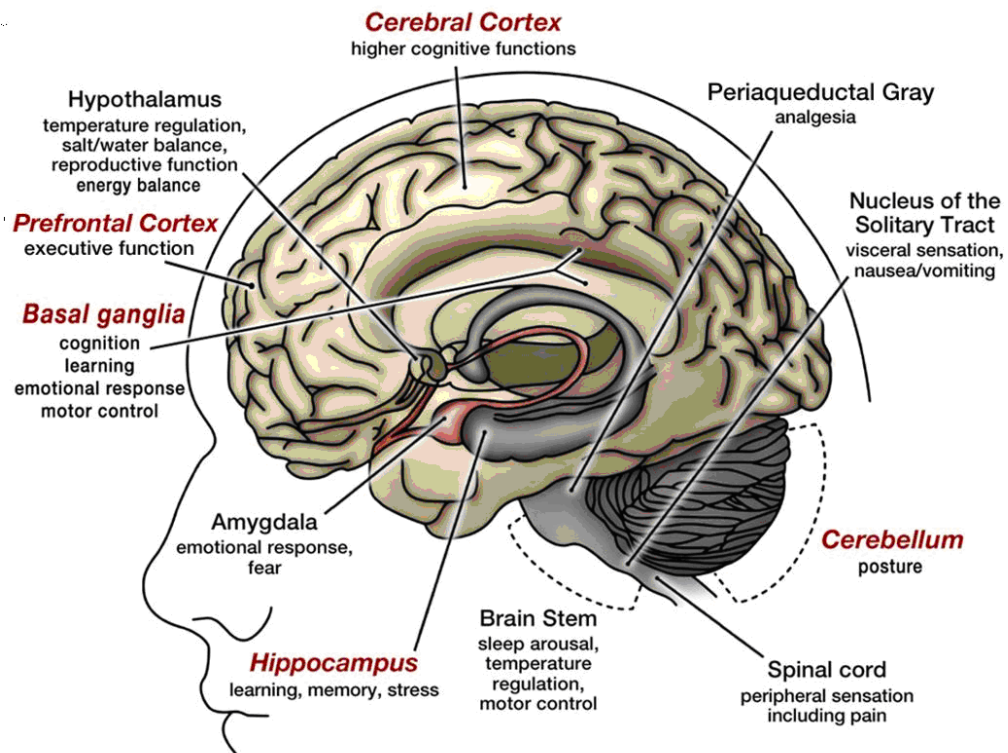


Figure 2.7, Areas of the brain with CB<sub>1</sub> receptor expression

As previously mentioned, the CB2 receptor is expressed predominantly in immune cells, suggest a role in the function of the immune system. Research on the CB2 receptor has shown that it may affect macrophage-mediated helper T cell activation [11]. Although some CB2 receptors have been isolated from brain tissue, the role of this receptor in the nervous system is not well studied.

Cannabinoid binding to the CB receptor causes a wide range of biochemical responses. The activation of CB1 receptors causes the inhibition of [cyclic adenosine monophosphate](#) (cAMP), a secondary messenger involved in transferring the signal of many extracellular molecules [12]. Further CB1 activation causes an inhibition of voltage activated  $\text{Ca}^{2+}$  channels and activates inwardly rectifying  $\text{K}^+$  channels. The inhibition of  $\text{Ca}^{2+}$  combined with the activation of  $\text{K}^+$  together inhibits the release of neurotransmitters [13]. Finally CB activation has to increase the activity of mitogen activated protein kinase (MAPK) which affects several gene transcription factors including [c-Fos](#) and [Krox-24](#) [14].

In addition to the biochemical processes which cannabinoids affect, there are several behavioral or physiological consequences to CB receptor activation. These processes include, but are not limited to: feeding response; energy balance and metabolism; pain perception; and memory, learning and emotion [5]. As evidenced in figure 2.7, CB1 receptors are highly expressed in the hypothalamus and dopamine reward regions of the brain. These brain regions are known to affect food intake, energy balance and reward systems. Therefore, cannabinoids and the modulation of the ECS is the subject of strong investigation for its potential role in the treatment of obesity and drug addiction.

### *2.1.3 Cannabinoid Antagonists*

As discussed in the previous section, cannabinoids, particularly EC's are fervently being investigated to understand how their modulation can be used to treat several conditions. One facet of this investigation revolves around compounds which act to inhibit the biochemical and physiological response to EC's.

The rationale of blocking the cannabinoids from binding to the CB receptor has shown to have two principle therapeutic outlooks; the treatment of obesity and metabolic disorders, and as a treatment for addiction to drugs of abuse. Studies show that by blocking EC's, there is a reduction in food intake. Further, when the CB1 receptor is not activated, there is effect on metabolism, causing the body to use energy more efficiently. Finally, lipogenesis, the generation of fat cells is slowed by the inhibition of CB receptors.

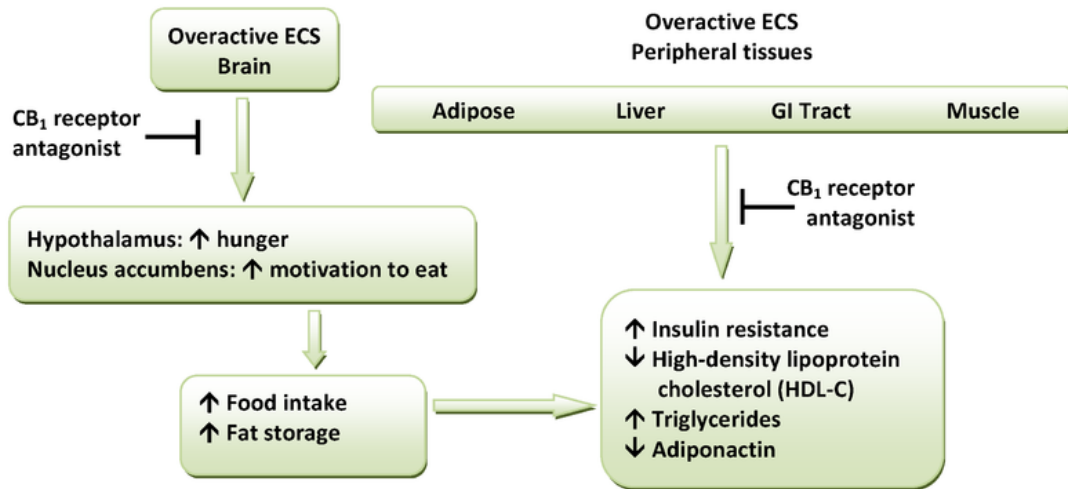


Figure 2.8, Overview of the affect of the ECS on food intake, energy storage and balance

The biological responses caused by the blocking the activation of CB receptors that implicate this process as a potential treatment for drug abuse are related to the neurotransmitter, dopamine and the dopamine dependant mesolimbic reward system [15]. As described previously, the binding of EC's has an effect on ion transport in the central nervous system which inhibits the normal release of neurotransmitters, including dopamine. The release of dopamine causes a general sense of well being and is required for an animal to function normally. By blocking the EC's from their site of action, the release of dopamine is restored.

The second facet of the rationale for inhibiting CB receptors to treat drug addiction involves the mesolimbic reward system. The release of dopamine affects the brains reward system by essentially reinforcing certain behaviors. It is accepted that this reward system participates is the biological basis of drug addiction. Though not well understood, it is suggested that blocking the EC's from binding permits a modulation of the brains reward system and thus, may have promise as a treatment for drug addiction.

The compounds which inhibit the CB receptors are often referred to as cannabinoid or endocannabinoid antagonists, or inverse agonists [16]. For clarity, several terms should be defined: agonist, a molecule which stimulates a cellular response by inducing a conformational change in the receptor; antagonist, a compound which is unable to cause the conformational change

required to stimulate a cellular response; and inverse agonist, which causes a stabilization of the receptors conformation and causes a response inverse to that of the agonist.

It is possible to further describe the different type of receptor binding using a two state model. In this model, receptors are either active or inactive. Agonists bind to receptors that are in the active state and have a stimulatory effect. Antagonists can bind to a receptor in either the active or inactive state. Inverse agonists only bind to the inactive state of a receptor, causing an inhibitory effect.

There is evidence that the CB inhibitors discussed in the next sections act as both inverse agonists, as well as antagonists. In vitro, at clinically relevant doses, these compounds act as antagonists; but at higher doses, behave as inverse agonists [16]. It is not currently known the type of inhibition that is caused in vivo. For purposes of consistency and clarity, all references to compounds which inhibit CB receptors will be referred to as antagonists.

#### *2.1.4 Rimonabant*

Rimonabant [N-(piperidin-1-yl)-5-(4-chlorophenyl)-1-(2,4-dichlorophenyl)-4-methyl-1 H-pyrazole-3-carboxamidehydrochloride)], the first selective CB1 receptor antagonist was discovered in 1994 [17]. The chemical structure of rimonabant is contained in figure 2.9. Rimonabant has been shown to be orally active. Further, administration of rimonabant is able to fully antagonize the effects of the CB receptor agonist, THC.

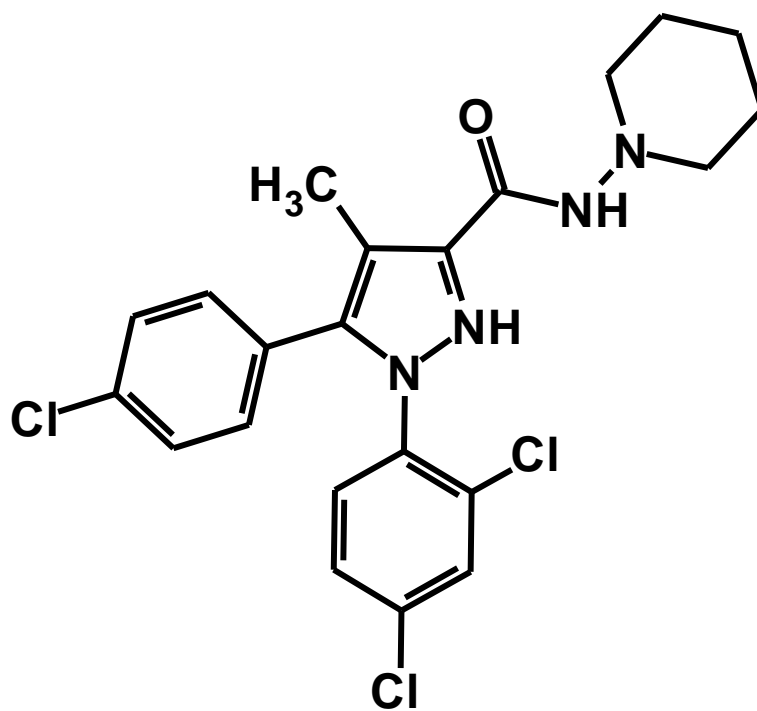


Figure 2.9, Chemical structure of rimonabant

Rimonabant has been investigated as a therapeutic agent for the treatment of both obesity and drug addiction. The administration of rimonabant to rodents has shown to reduce the rewarding/reinforcing behaviors of several drugs of abuse including heroin [18], cocaine [19], nicotine [20] and alcohol [21]. Further, there is evidence that rodents administered this drug show a marked decrease in food consumption [22].

Rimonabant has been investigated in a phase II clinical trial to be used in the treatment of alcoholism [23], a phase III clinical trial for treatment of diabetes [24] and a phase III clinical trial for treatment of obesity [25]. In 2006, rimonabant was approved under the brand name Acomplia by the European Union as an over-the-counter medication. In October of 2008, the European Medicines Agency (EMA) recommended that the use of Acomplia be suspended [26]. In November of 2008, the manufacturer of Acomplia, Sanofi Aventis, discontinued production of the drug. The reasons that Acomplia has been abandoned as a therapy relate to unwanted neurological side effects, particularly depression. It has been stated that patients taking Acomplia have twice the risk of developing depression than those taking placebo [27].

Despite rimonabant being removed from the drug pipeline, there continues to be a strong interest in its molecular modes of action and the behavioral responses which are generated. In fact, in the first half of 2009 over 50 publications have been generated further investigating this drug. Further, many publications are the result of animal behavior studies.

One of the aims of this work is to present the development of a quantitative bioanalytical method, using HPLC-MS/MS, for the determination of rimonabant in biological samples. Prior to the development of the method discussed in the next sections, no method was publicly available. This method is able to measure rimonabant in human, rat and canine plasma; as well as, in rat brain tissue. The method developed has been applied to the measurement of rimonabant in two separate animal studies. Further, the method can be applied to future clinical and toxicological studies to establish pharmacokinetic and pharmacodynamic profiles in various animal models. This work will remain a valuable resource to the research community as a better understanding of the ECS and the compounds which modulate it, emerges.

#### *2.1.5 Surinabant*

Surinabant [5-(4-bromophenyl)-1-(2,4-dichlorophenyl)-4-ethyl-*N*-(1-piperidinyl)-1*H*-pyrazole-3-carboxamide] is an CB receptor antagonist, which was developed by Sanofi Aventis [28]. The chemical structure of surinabant is contained in figure 2.10.

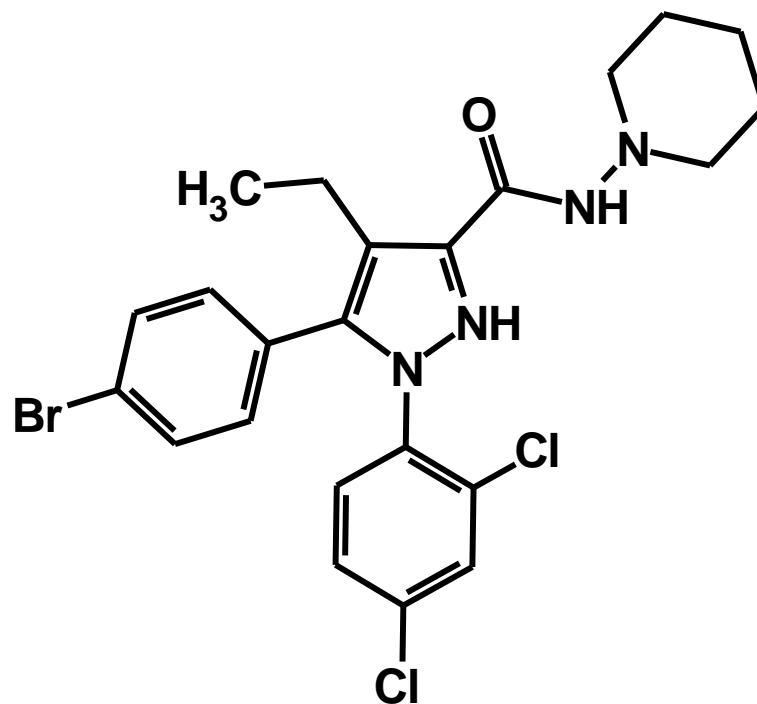


Figure 2.10, Chemical structure of surinabant

Surinabant is a second-generation CB receptor antagonist. It has a longer duration of action than the rimonabant, and enhanced oral activity [29] [30] [31]. Further, surinabant may have advantages over rimonabant in that it is reported that surinabant has both a higher affinity for CB receptors in the brain and has up to three times longer occupancy in the brain [32].

Surinabant differs structurally from rimonabant in that it has an ethyl group attached to the central nitrogen ring versus a methyl group in this position on rimonabant. It has been suggested that the enhanced biological effects of surinabant are due to its slightly larger hydrophobicity. Greater hydrophobicity has two main effects, it is able to cross the blood brain barrier more rapidly; and it may move more easily across the through the membrane of post synaptic neuronal cells.

Surinabant has been in clinical trials in Europe for treatment of both obesity [33] and nicotine addiction [34]. Current research using surinabant elucidates a relationship between nicotine, metabolism and weight gain [35]. It has further been investigated for the treatment of alcoholism and attention deficit hyperactivity disorder (ADHD). Evidence for the potential of surinabant in the treatment of alcoholism is shown in a study that describes the administration of surinabant is able to reduce both voluntary ethanol consumption as well as alcohol intake [13].

Clinical trials have been completed, and this compound has been removed from the drug pipeline of Sanofi Aventis. Despite the noticeable abandonment of this compound, there is a great deal that remains unknown about the ECS. The

method developed for the determination of rimonabant was quickly responded to with enthusiasm by the research community. It is logical that a method that can measure a compound which varies only slightly in chemical structure, yet has markedly increased biological responses; would be a valuable tool for the scientific community.

The work described here will outline the development both an HPLC-UV and an HPLC-MS/MS quantitative bioanalytical method, for the determination of surinabant in biological matrices. Prior to the publication of this work, no method was publicly available to measure the concentration of surinabant in any biological matrix.

#### *2.1.6 Conclusion*

The endocannabinoid system (ECS) is a complex signaling system that affects several biological events including; regulating energy balance and behaviors such as food intake, fear and anxiety. As previously discussed, ECs are biochemically involved in many physiological processes, including food intake and addiction. Naturally, compounds which are able to modulate, via agonism or antagonism, the ECS are of great interest.

The work presented in this chapter will describe quantitative, bioanalytical methods that can be used to measure the concentration of the CB receptor antagonists, rimonabant and surinabant. These methods have been applied to animal studies. To date, the data obtained from the use of these methods has

aided researchers in the fields of psychiatry and metabolic disorders to further understand and interpret their experimental results. The future applications of these methods cannot be predicted; however, the value to science is clearly of great value.

## **2.2 Development of a Quantitative Bioanalytical Method for the Determination of Rimonabant**

### *2.2.1 Introduction*

Prior to the development of the method presented in this section, there was no publicly available method to measure the concentration of rimonabant in biological samples. A HPLC-MS/MS method was developed and validated using a human plasma matrix. In addition to human plasma, successful measurement of rimonabant was achieved in the following matrices: rat plasma, rat brain and canine plasma. For this work validation was conducted to demonstrate the robustness and reproducibility of the method. All validation parameters followed the guidelines contained in the document, U.S. Food and Drug Administration Bioanalytical Method Development – Guidance for Industry [36]

## 2.2.2 Materials and Methods

### Reagents

Acetic acid, HPLC-grade acetonitrile, dimethyl sulfoxide (DMSO), formic acid, and 1- (2,4-dichlorophenyl)-5-(4-iodophenyl)-4-methyl-N-1-piperidinyl-1H-pyrazole-3-carboxamidetrifluoroacetate salt (AM251, the internal standard for this study), Cremophor EL, and Tween 80 were purchase from Sigma-Aldrich (St. Louis, MO, USA). Rimonabant, 5-(4-chlorophenyl)-1-(2,4-dichlorophenyl)-4-methyl-N-1-piperidinyl-1H-pyrazole-3-carboxamide was provided, at no cost, by National Institute of Mental Health (Bethesda, MD, USA) Drug Repository (NIMH code 5S-705.) Dr. Michael Kalafatis at Cleveland State University, graciously donated pooled human plasma was from Haemtech, Inc (Essex Junction, Vermont, USA).

The rimonabant ( $C_{22}H_{21}Cl_3N_4O$ ) stock solution (1.00 mg/ml) was prepared by weighing 1.12 mg of the compound into a 1.5 ml Eppendorf tube (Eppendorf, Westbury, NY, USA) and dissolving it with 1.12ml of DMSO. A stock solution (1.00 mg/ml) of AM251 trifluoroacetate salt ( $C_{22}H_{21}N_4OCl_2 \cdot C_2HF_3O_2$ ) was prepared by weighing 1.24 mg of the compound into a 1.5 mL Eppendorf tube and dissolving it with 1.24 ml of DMSO.

Once the compounds were dissolved in DMSO, both rimonabant and AM251 stock solutions were transferred to 1.5 ml amber glass autosampler vials, sealed with parafilm, and were stored at - 20 °C when not in use. A rimonabant working

solution (100 µg/ml) was prepared by a dilution (1/10) of the rimonabant stock solution with DMSO. A working solution (2.00 µg/ml) of AM251 was prepared by a three-step dilution (1/8.3, 1/10, 1/5) of the AM251 trifluoroacetate salt stock solution with DMSO. A mobile phase for liquid chromatographic separation was prepared by first adding formic acid (HCOOH) to water. The formic acid/H<sub>2</sub>O solution was mixed with acetonitrile (50:50 v/v) with the HCOOH concentration being 0.1% of the final mobile phase volume. All solutions were stored at 4°C when not in use.

### Calibrators and Controls

Pooled human, Sprague-Dawley rat and mixed breed canine plasmas which contained no detectable rimonabant were used as the blank plasmas to prepare human and rat plasma calibrators and controls for this study. Standard solutions of rimonabant (0.0100, 0.0200, 0.100, 0.150, 0.200, 1.00, 1.50, 2.00, 10.0, 15.0, 20.0 µg/ml) were prepared by a serial dilution of the working solution (100 µg/ml) with DMSO. Plasma calibrators of rimonabant (0.500, 1.00, 5.00, 10.0, 50.0, 100, 500, 1.00 x 10<sup>3</sup> ng/ml) were prepared by a 1:20 dilution of the corresponding rimonabant standard solutions with the blank plasma. A 1:20 dilution of the corresponding rimonabant standard solutions with the blank plasma was conducted to prepare the rimonabant plasma controls (7.50, 75.0, 750 ng/ml). All plasma samples were stored at – 20°C when not in use.

### Protein Precipitation

Rimonabant was extracted from plasma samples using the following protocol: First, 200 µl of plasma sample was pipetted into a 1.5 ml Eppendorf tube; thereafter, 10.0 µl of the AM251 working solution (2.00 µg/ml) and 50.0 µl of acetic acid were added to the mixture. The mixture was vortex mixed and 1.00 ml of acetonitrile was added. The ACN/plasma solution was then vortexed again subsequently centrifuged for 15 minutes at 13,000 g. The supernatant present after centrifugation was transferred to a 1.5 ml Eppendorf tube, and evaporated to dryness in a DNA 120 SpeedVac® (ThermoSavant, Hollbrook, NY, USA) at 65 °C for 90 min. The sample was reconstituted in 200 µl of the mobile phase prior to analysis.

### Rimonabant Recovery

The ability of the protein precipitation procedure to recover rimonabant by was measured using rimonabant plasma controls and rimonabant reference solutions at three different concentrations (7.50, 75.0, 750 ng/ml). The reference solutions contained the same matrix as that of plasma controls, which were prepared using blank plasma as samples by the same extraction procedure as that of plasma controls, and reconstituted in the mobile phase with corresponding rimonabant concentrations.

### Animal Samples (rat)

Sprague-Dawley rats (Taconic Farms) were bred in the vivarium of Binghamton University. On postnatal (P) day 1, litters were chosen with 7-10 subjects, whenever possible retaining six males and four females. Animals were weaned on P21, housed in same-sex pairs and maintained on a 14/10 hour light/dark cycle (lights on at 7 am) with food and water available ad libitum. All experimental procedures were approved by the Institutional Animal Care and Use Committee at Binghamton University. The animals were an average 70 days old. The average body weight of the animals was 300 grams. Rimonabant was delivered as a suspension of 2.0% Cremaphor EL, 0.1% Tween 80 and deionized water. Intraperitoneal (i.p.) injections of 10 mg/kg in a volume of 5 ml were administered. The animals were decapitated at 30 minutes and 12 hours. Trunk blood samples were obtained by allowing the blood to freely drain into centrifuge tubes. An average of 3 mL of blood was collected from each animal in tubes containing 0.1 ml of 0.1 M EDTA. High-speed centrifugation was used to separate the plasma from whole blood. Plasma was stored at - 80 °C until analysis.

### Animal Samples (canine)

Mixed breed canine plasma collected using lithium/heparin (Li-Hep) as an anticoagulant was purchased from Lampire Biological Laboratories (Pipersville,

PA, USA). Dr. Joyce Richey at the University of Southern California, Keck School of Medicine provided the canine samples to be analyzed. The plasma was collected in Li-Hep coated test tubes and EDTA was added to the plasma. No further information regarding the breeding or dosing of animals, nor the collection or storage of plasma was provided.

### Instrumental Setup

The instrumental setup used in this work consisted of an HP1100 pump by Hewlett Packard (Palo Alto, CA, USA), an HP1100 autosampler, a stainless steel in-line filter (0.5  $\mu\text{m}$  pore, 0.23  $\mu\text{l}$  dead volume) by Upchurch Scientific (Oak Harbor, WA, USA), a YMCTM Pro C4 cartridge column (3  $\mu\text{m}$ , 120  $\text{\AA}$ , 2.0 mm x 50 mm) by Waters (Milford, MA, USA), a stainless steel splitting tee (1/16" x 0.25 mm) by Valco (Houston, TX, USA), and a Quattro II triple quadrupole mass spectrometer by Micromass (Manchester, UK). All fluidic connections in the system were made using high-pressure polyether ether ketone (PEEK) tubing (0.0625 in. o.d., 0.0100 in. i.d.). The post-column split ratio was 1:2 with a smaller flow (ca. 63  $\mu\text{l}/\text{min}$ ) to the MS detector and the larger one to the waste.

### HPLC Separation

Analytical separation was performed via a Waters YMCTM Pro C4 cartridge column. Before analysis, the cartridge column was equilibrated with mobile

phase at a flow rate of 0.200 ml/min for about 15 min. During the analyses, 20 µl of sample was injected by the autosampler and carried onto the cartridge column by the mobile phase at a flow rate of 0.200 ml/min. Rimonabant and AM251 (internal standard) were separated from the sample matrix with retention times of 6.8 and 7.8 min, respectively. The total run time was 10.0 min per sample.

### MS Detector Settings

Electrospray ionization mode (ESI+) was utilized on the Micromass Quattro II triple quadrupole mass spectrometer. Tuning of the mass spectrometer was achieved by infusion of a mixture of rimonabant (1.0 µg/ml) and AM251 (1.0 µg/ml) in the mobile phase at a flow rate of 3.0 µl/min with a syringe pump (Harvard Apparatus, South Natick, MA, USA). Optimal ionization conditions were as follows: nitrogen sheath and desolvation gas at 10 and 350 l/h, capillary at 3.5 kV, HV lens at 0.5 kV, cone at 40 V, skimmer at 1.5 V, RF lens at 0.2 V, ion source temperature at 95°C, ion energy at 1.0 V, low- and high-mass resolution at 15, and multiplier at 700 V. Full-scan spectra were acquired in the continuum mode at a scan rate 400 u/s. The instrument was operated in multiple reaction monitoring (MRM) mode for quantitation, which was set as follows: m/z 463 → 363 for rimonabant, m/z 555 → 455 for AM251, argon collision gas at 2.0-2.5 µbar, cone at 40 V, collision energy at 20 V for both analytes, low- and high-mass resolution at 10 for quadrupole 1 and 15 for quadrupole 3, dwell time at 0.1 s,

and the inter-scan delay at 0.01 s. The parameters for ionization remained the same as previously discussed.

### Analysis of Data

Data acquisition and peak integration were performed using the Micromass Masslynx software (version 3.4). The peak area ratios of rimonabant plasma calibrators to the internal standard were plotted against plasma rimonabant concentrations for a regression equation. Rimonabant concentration of an unknown plasma sample was determined by the regression equation after obtaining the peak area ratio of rimonabant in the unknown to the internal standard from the mass chromatogram.

### *2.2.3 Results and Discussion*

#### Selection of Solvent for Stocks, Plasma Calibrators and Controls

Rimonabant and AM251 are caboxamide derivatives which are not water soluble. In many situations, the addition of acid to a solution will protonate the compound and, due to ionization, improve its water solubility. In this work 0.1M hydrochloric acid (HCl) was added to the solution which was not able to sufficiently aid in the solubility.

Due to the hydrophobicity of these compounds, it was not possible to dissolve them directly into plasma and a suitable stock solution solvent was required. Both compounds were easily dissolved in both acetonitrile (ACN) and methanol (MeOH). However, it has been established that when these solvents are used to prepare stock solutions, the subsequent addition to plasma can cause protein precipitation, in amounts less than 1% [37]. Protein precipitation may result in poor precision of the analytical method.

DMSO was investigated as a potential alternative to ACN and MeOH. Both rimonabant and AM251 were readily soluble in DMSO, and up to a 25% addition of DMSO to plasma did not result in appreciable protein precipitation. Therefore, DMSO was selected as the solvent for all stock and working solutions. In order to assure that no precipitation would occur, DMSO was limited to 10% v/v in all plasma controls and calibrators.

### Extraction of Analyte and Recovery

As described in section 1.2, the first step in bioanalytical method development is the extraction of the analyte from the biological matrix which it exists in. In the case of rimonabant, on-line sample extraction was first considered. On-line sample extraction is solid phase extraction (SPE) conducted “on-line”, or in the automated set-up of the instrumental procedure. SPE is discussed in detail in section 1.2.4.

The automated nature of on-line SPE provides several advantages over SPE: cost, the column used for extraction is reused, up to hundreds of times; precision, there is no pipetting involved in sample loading which reduces human error; and time, the automation of the process allows for much faster extractions than that of SPE. Unfortunately, the hydrophobic nature of rimonabant caused a significant carryover of sample between injections, and thus on-line extraction was abandoned.

Since on-line extraction was not possible, a protein precipitation protocol was developed. The protein precipitation utilized 100% ACN, as the extraction solvent. Prior to the addition of ACN, acetic acid was added to the plasma. The addition of acid protonates the plasma proteins, which can serve to reduce the binding of drug with plasma proteins. Further, protonation disrupts the hydration layer of proteins in solution as discussed in section 1.2.3. This disruption can reduce the aggregation of proteins which can lead to poor reproducibility and recovery.

The recovery of rimonabant was ascertained at three concentrations, low (7.5 ng/mL), middle (75.0 ng/mL) and high (750 ng/mL). Recovery describes the difference between the mean peak area ratio of the signal of rimonabant obtained from samples which were spiked with rimonabant prior to the protein precipitation, to the signals obtained from samples spiked with rimonabant after the protein precipitation. Both absolute recovery, the recovery of rimonabant alone; and relative recovery, the internal standard corrected recovery was calculated.

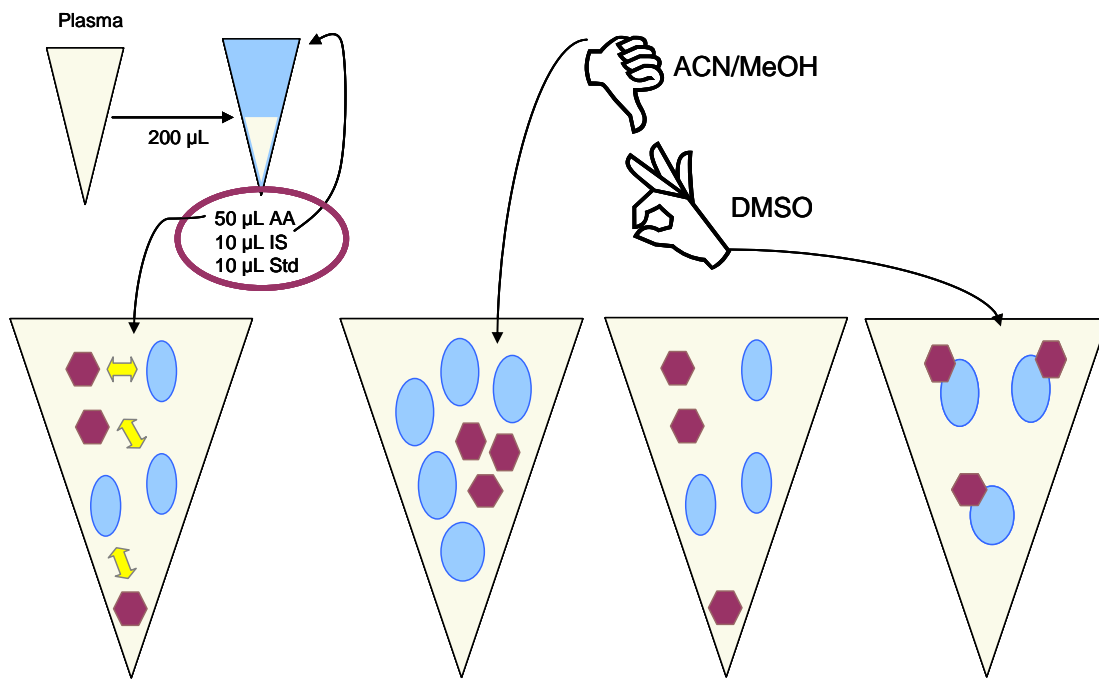


Figure 2.11, Benefit to using DMSO and acetic acid in protein precipitation

According to the FDA's guidance for the industry, there is no absolute value for recovery required. It is only necessary that the recovery be consistent and reproducible across the concentration range of interest. The absolute and relative recoveries of rimonabant from the human plasma matrix are contained in Table V.

The recovery of rimonabant in canine plasma was verified at the low, medium and high concentrations described above and were determined to be: 89.8%, 89.4% and 91.7 %, respectively. As clearly indicated by table V combined with the values obtained using canine plasma, the protein precipitation protocol is suitable for the extraction of rimonabant from these matrices.

It is worth mentioning that the use of 70% ACN as the extraction solvent was investigated. The rationale for using a lower amount of ACN was an attempt to reduce cost due to solvent consumption. The reduced ACN resulted in lower extraction efficiency. The poor recovery can be attributed to a change in the partitioning of the compounds when a lower amount of ACN was used, as discussed in section 1.2.2.

Table VI, Recovery of rimonabant in human plasma

<b>Absolute and relative recoveries of rimonabant and AM251 in human plasma</b>						
Compound	7.50 ng/ml		75.0 ng/ml		750 ng/ml	
	Recovery (%)	CV (%)	Recovery (%)	CV (%)	Recovery (%)	CV (%)
SR141716	83.0	2	83.7	4	85.1	5
AM251	87.3	3	91.0	4	85.8	4
SR141716/AM251	95.2	3	92.0	0.6	99.2	1

The number of measurements was 3 for each datum point.  
The concentration of the internal standard AM251 was 100 ng/ml.

## HPLC Separation

Although neither the MS detector, nor the application of the method, required that rimonabant and AM251 be chromatographically separated; this achievement would result in better method sensitivity. Therefore, several analytical columns and mobile phase compositions were tested to first, achieve baseline separation and secondly, assure that the retention times were not inhibitorily long.

The first conditions tested used a Waters YMC™ Pro C18 column (3 µm, 120 Å, 2.0mmx50 mm) and a mobile phase containing 90% CH<sub>3</sub>OH/0.1% HCOOH in water, rimonabant and the AM251 were co-eluted at retention times of 2.5 and 2.8 min. Next a mobile phase of 70% CH<sub>3</sub>CN/0.1% HCOOH in water, it was possible to achieve baseline separation of rimonabant and the internal standard with retention times of 4.6 and 5.6 min on the Waters YMC™ Pro C18 cartridge.

As discussed in section 1.1, a good bioanalytical method will aim to keep the cost as low as reasonable. Therefore, in an effort to reduce the amount of ACN in the mobile phase, a Waters YMC™ Pro C8 cartridge column (3 µm, 120 Å, 2.0 mm x 50 mm) was tested. With the mobile phase composition of 50% CH<sub>3</sub>CN/0.1% HCOOH in water, rimonabant and AM251 were partially separated at 13.5 and 17.0 min.

Again, it is desirable to maintain a short analysis time so, to reduce the separation time, a Waters YMC™ Pro C4 cartridge column (3 µm, 120 Å, 2.0 mm x 50 mm) and a mobile phase composition of 50% CH<sub>3</sub>CN/0.1% HCOOH in

water were used. This column and mobile phase system allowed for separation of rimonabant and AM251 with retention times of 6.8 and 7.8 min. Therefore, a Waters YMC™ Pro C4 cartridge column and a mobile phase composition of 50% CH<sub>3</sub>CN/0.1% HCOOH in water were utilized for the subsequent analytical separations. Representative mass chromatograms of rimonabant and AM251 using this chromatographic systems are contained in figure 2.12.

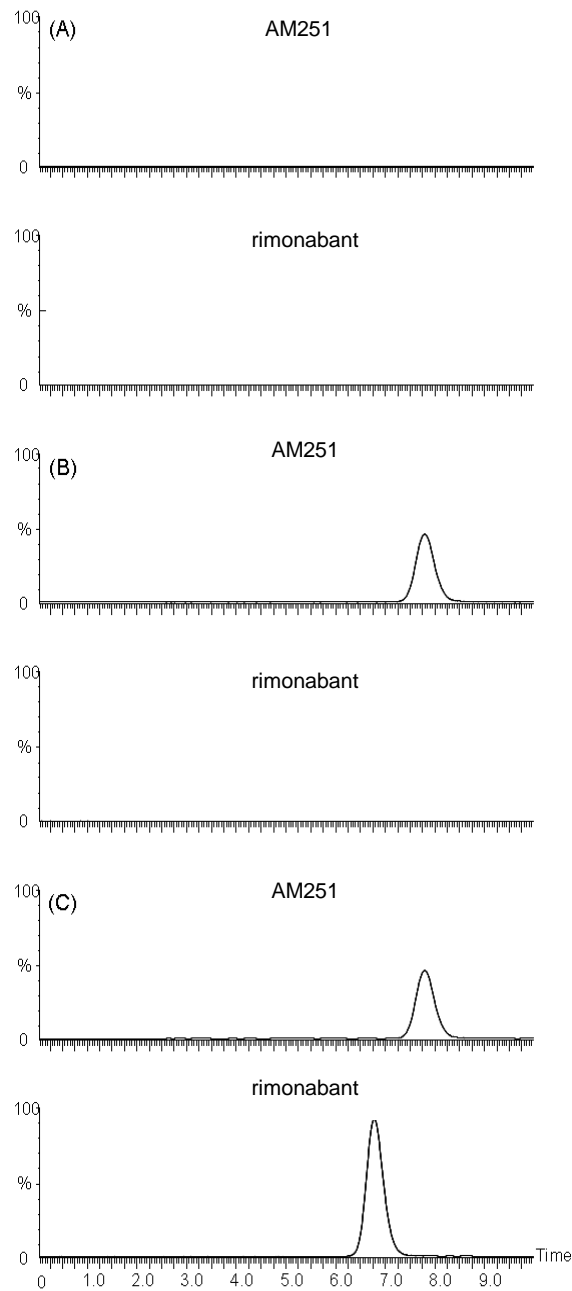


Figure 2.12, Representative mass chromatograms of rimonabant and AM251 in (A) untreated blank plasma, (B) plasma treated with rimonabant only, and (C) plasma treated with 100  $\mu$ L of both rimonabant and AM251

## MS Detection

Section 1.5 describes the theory of mass spectrometry detectors, indicating that the mass to charge or  $m/z$  ratio of ions is detected. Most modern instruments are capable of analyzing: positive ions, i.e. the molecular weight of the analyte plus a proton or  $M+H^+$ ; negative ions, i.e. the molecular weight of the analyte minus a proton or  $M-H^+$ ; or alternating between positive and negative ion detection.

This work used the MS instrument in multiple reaction monitoring mode (MRM). This is a feature of most sophisticated instruments in use today. In MRM mode, the detector is able to operate and record data for multiple analytes simultaneously. Therefore, the signal for the analyte and internal standard can be extracted from the total ion signal during the data processing step.

Based on the chemical structures of rimonabant and AM251, they will more easily undergo protonation than deprotonation, therefore positive electrospray ionization mode was employed for their detection. The full-scan spectra showed that rimonabant produced a predominant quasi-molecular ion at  $m/z$  463 and AM251 at an  $m/z$  of 555. Therefore, these ions were chosen as parent ions for fragmentation in the MRM mode.

The daughter spectra of the parent ions revealed that the predominant daughter fragments were at  $m/z$  363 for rimonabant and  $m/z$  455 for AM251. These daughter ions were chosen for analyte quantitation. The full scan and daughter fragmentation spectra are contained in figure 2.13.

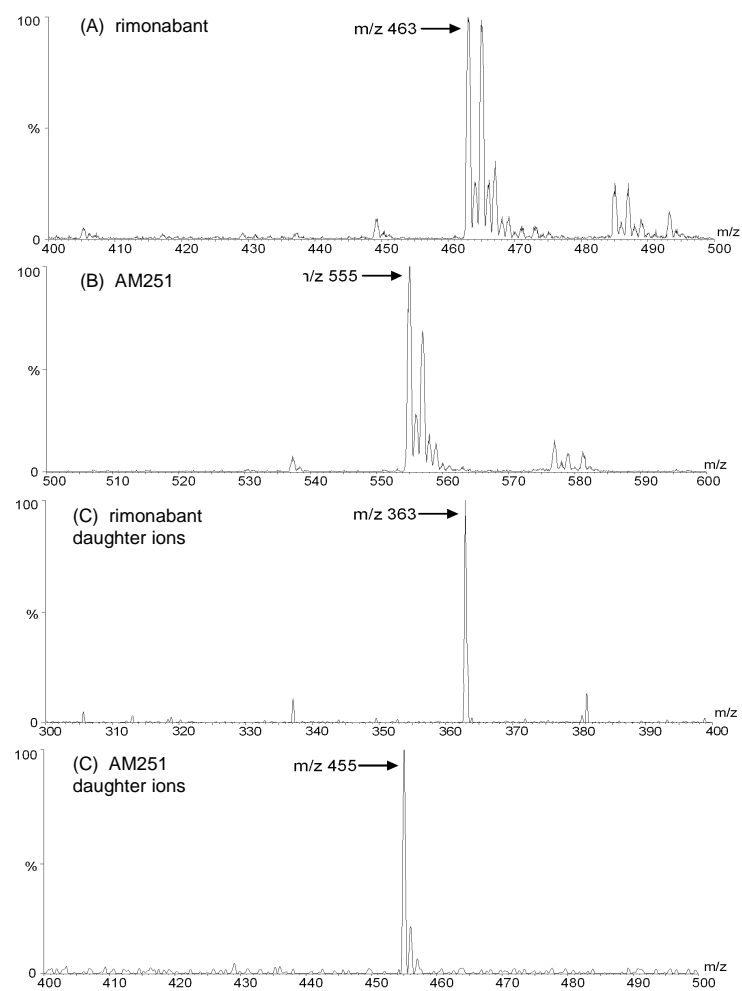


Figure 2.13, Full scan spectra of (A) rimonabant, (B) AM251; daughter spectra of (C) rimonabant and (D) AM251

The use of MRM mode for detection of rimonabant and AM251 offered suitable specificity, which is exhibited by the lack of interference from any compounds in the blank plasma, as demonstrated in figure 2.12.

The fragmentation scheme for rimonabant and AM251 can be proposed based upon the fact that the predominant daughter ions were 100 amu less than their parent ions.

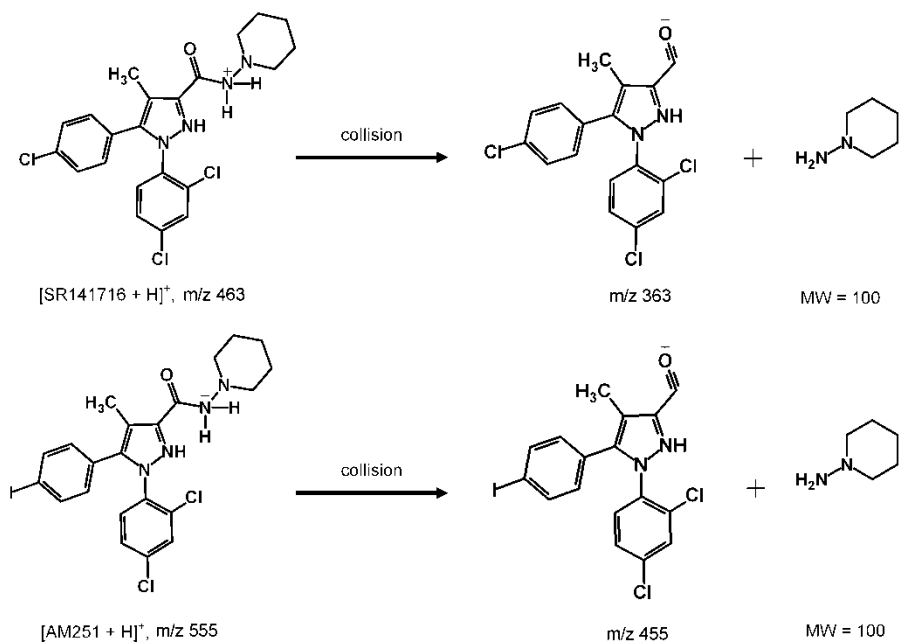


Figure 2.14, Proposed fragmentation scheme for rimonabant (SR141716) and AM251

Method Validation (Linearity, Detection Limits, Precision, Accuracy and Stability)

*Via Human Plasma for Rat Study*

As described in section 2.2.2 the volume of rat plasma obtained from each animal was limited to 3.0 mL. Several validation parameters were tested to assure that the difference in matrix had no appreciable effect on the validation. Therefore, due to the limited supply of blank rat plasma this method was validated using blank human plasma.

The linearity of the response of the detector was determined by the peak area ratios of rimonabant to the internal standard and plotted versus the concentration of plasma calibrators. This method has a linear range of 5.00 – 1000 ng/mL with a correlation coefficient of 0.999. The mean calibration equation, determined from three separate calibration curves over a 6 month period was  $y = 0.0196x$ .

The guidelines prescribed by the FDA industry guidelines sets forth several values for acceptable detection limits, precision, accuracy and stability. These values require that the limit of detection (LOD) and limit of quantitation (LOQ) must be 3 and 10 times the signal to noise, respectively. The calculated LOD and LOQ for this method (based on 5 replicates) are 1.09 and 3.62 ng/mL, respectively.

The precise detection of all samples should be accomplished with less than 15% (20% at the lowest concentration) error to ensure the reproducibility of the entire method. The intra-assay precision, or the precision afforded by the mass spectrometer was determined for this method. Additionally, the inter-assay precision from sample to sample, an indication of the human precision of the method was also determined. All precision values are reported as %CV which is calculated by dividing the standard deviation by the mean value and multiplying by 100. The precision values calculated are contained in table VI. All values reported are internal standard corrected.

The accuracy, which is determined by the relationship of the measured concentration of analyte to the real concentration, should also be within 15%.

The equation used to calculate accuracy is contained in equation 2.1.

$$[(\text{real concentration} - \text{measured concentration}) / \text{real concentration}] \times 100 \quad (2.1)$$

The accuracy of this method was ascertained at 7.5, 75.0 and 750 ng/mL and was found to be 105, 99.5 and 100% respectively. These values fall within the 15-20% error window suggested in the FDA guidelines.

Table VII, Intra- and inter-assay precision of rimonabant measurement

<b>Intra- and inter-assay precision of rimonabant in human plasma</b>		
	CV (%)	
[SR141716] (ng/ml)	<i>Intra-run</i>	<i>Inter-run</i>
7.50	0.9	6
75.0	1	0.5
750	0.4	2

The concentration of the internal standard AM251 was 100 ng/ml.  
The number of measurements was 3 for each datum point.

Finally, it is important to determine the stability of the analyte under conditions anticipated to be appropriate for the methods application. In this method, the freeze/thaw (3 cycles;  $-20^{\circ}$  → room temperature), and short term mobile phase (stock) and plasma (calibrator) stability was ascertained. Error was measured as the difference in signal obtained from the analyte after subjecting the samples to the condition to the signal of the analyte at time zero. The stability was investigated at both low and high concentrations. Under the conditions studied, the error ranged from 6.6 to 8.9%, which indicates that rimonabant is stable under these circumstances.

#### *Canine Plasma*

Before being applied to the canine plasma samples the accuracy and precision of the developed method was checked to assure the transfer of the method to this new matrix. The %CV, representing precision ranged from 1-10.3%, well within the permitted range. Further the accuracy ranged from 85.7 to 97.4%, indicating the method could accurately measure the concentration of rimonabant.

## Rat Plasma Analysis

The validated method was used to measure rimonabant in plasma samples from rats after intraperitoneal injection of rimonabant at the dose of 10 mg/kg. In the analyses, the frozen rat plasma samples and blank plasma were thawed to room temperature, 200 µl of plasma samples together with the blank plasma were prepared by the protein precipitation procedure described in Section 2.2.2 and analyzed by the LC-MS-MS method.

While there was no interference found in the untreated rat plasma (Figure 2.15A), rimonabant was detected in rat plasma after both the 30 min and 12 h injection (Figures 2.15B and 2.15C). Although the dose and the sampling times were not optimized to establish a pharmacokinetic study of this drug in the, the results demonstrate the applicability of the method for the measurement of rimonabant in plasma samples. Furthermore, the plasma concentration at 12 h after injection was higher than that at 30 min. This finding was consistent with the pharmacokinetic data in the US FDA briefing document (NDA 21-888, June 13, 2007), which showed a mean half-life of ca. 16 days for the drug in humans.

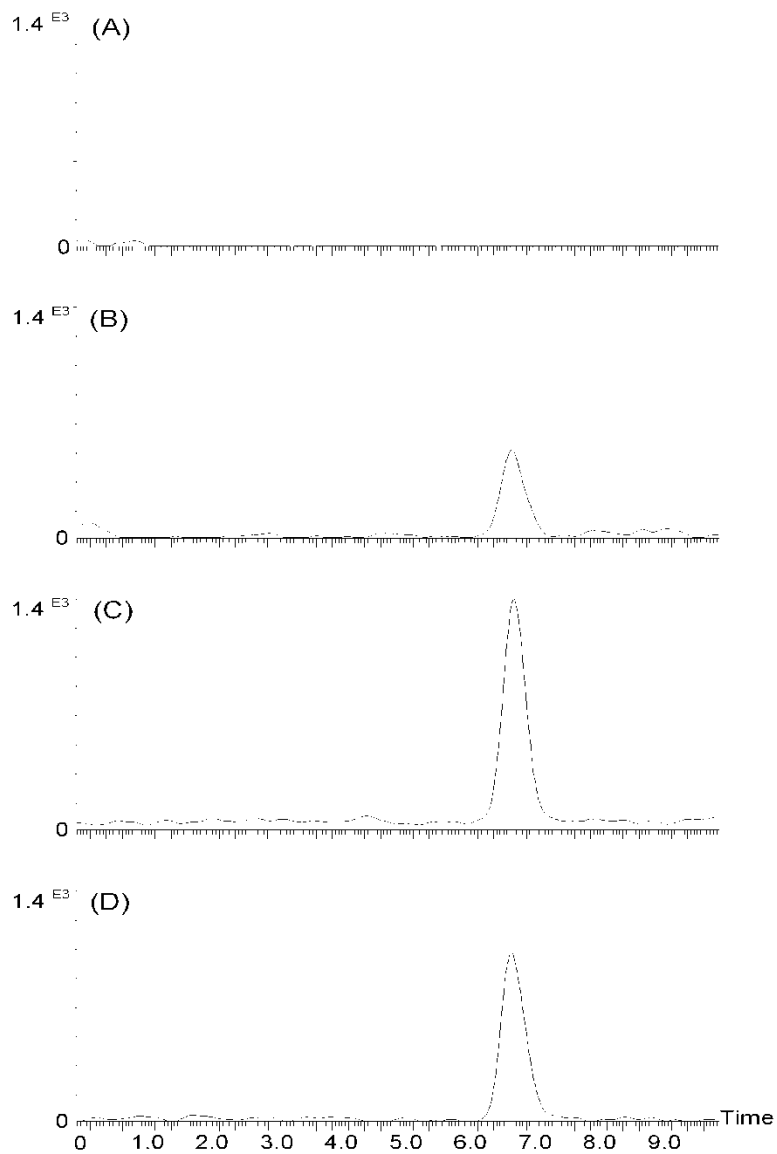


Figure 2.15, Mass chromatogram of (A) blank plasma, (B) animal treated for 30 minutes, (C) animal treated for 12 hours and (D) the low calibrator (5 ng/mL)

### Rat Brain Tissue Analysis

This method, though not validated for the brain tissue matrix, was introductorily applied to samples. In this analysis, the water in a volume of ten 5 mL/gram of brain tissue was added to the whole rat brains. The brain/water mixture was homogenized with an immersion blender. Thereafter, 200  $\mu$ L of the homogenized tissue solution was pipetted into centrifuge tubes, an amount of rimonabant calibration standard was added and the protein precipitation procedure described in section 2.2.2 was conducted. Figure 2.16 shows a representative mass chromatogram for rimonabant extracted from a brain tissue solution. As evidenced in figure 2.16, rimonabant is clearly detectable when extracted from brain tissue. No further investigation into the extraction, detection or validation of this method for the measurement of rimonabant in the brain matrix was conducted

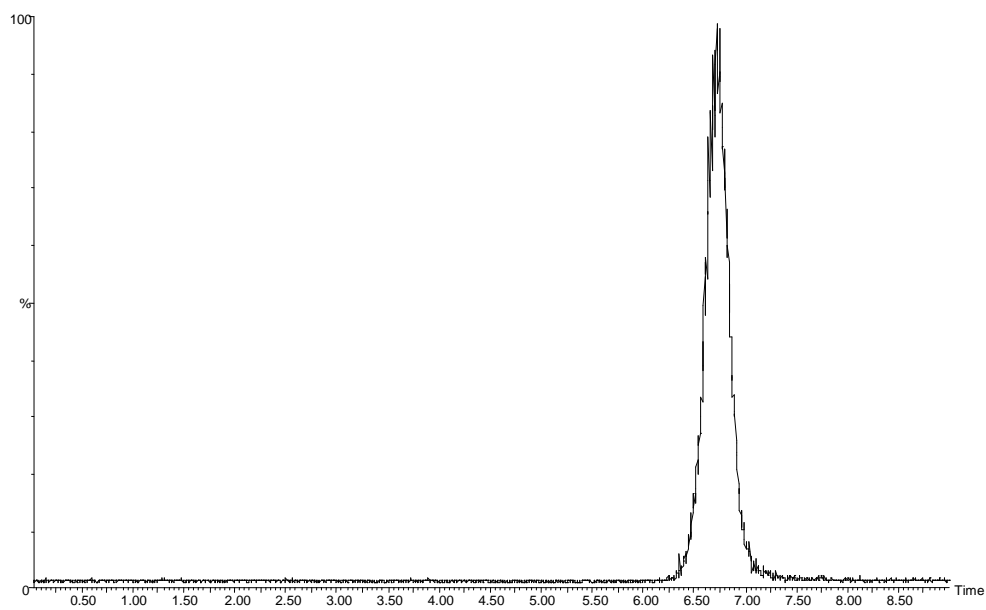


Figure 2.16, Representative mass chromatogram of rimonabant extracted from brain tissue

### Canine Plasma Analysis

The canine samples, together with calibrators and controls were prepared as described in section 2.2.2. As mentioned previously, there was no information provided regarding the dosing and time points for these samples. Based on the lack of information provided, it is not possible to discuss the measurement of rimonabant in these samples. However, the ability of the LC-MS-MS method to detect rimonabant in all samples which was expected to be found, speaks to the validity and applicability of this method in the research community. The range of rimonabant concentrations detected in this study were from 20-125 ng/mL. A representative chromatogram of the low and high end of the concentrations detected, as well as the calibrator in this range, is contained in figure 2.17.

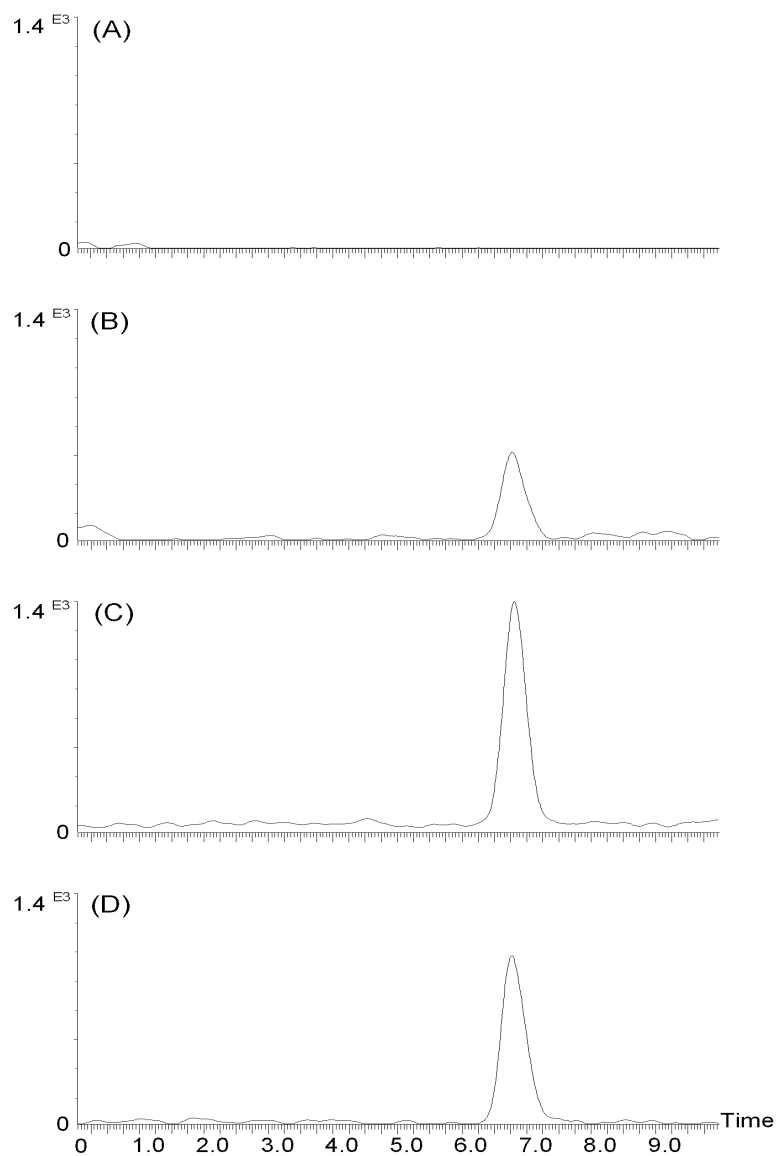


Figure 2.17, Representative mass chromatograms of rimonabant extracted from canine plasma with calculated concentrations of (A) 112 ng/mL, (B) 21 ng/mL and (C) 100 ng/mL calibrator

#### *2.2.4 Conclusion*

A rapid, sensitive HPLC-MS-MS bioanalytical method has been developed and validated for the measurement of rimonabant. This method is able to effectively extract rimonabant from the matrices with suitable precision and recovery. Further, the mass spectrometric detection of rimonabant enables an accurate measurement of analyte concentration. Finally, the method has been successfully applied to a wide range of biological matrices, including, human plasma, rat plasma, rat brain tissue and canine plasma. This method can be used in future pharmacokinetic and pharmacodynamic studies.

### **2.3 Development of a Quantitative Bioanalytical Method for the Measurement of Surinabant**

#### *2.3.1 Introduction*

The development of the bioanalytical method to measure rimonabant was met with strong enthusiasm in the research community [38]. Within months of the manuscript being published, our research group was approached to conduct the analysis of a large scale animal study. During this time, there was promising interest in the structurally similar CB antagonist, surinabant, as a therapeutic agent. Due to the structural similarities of the compounds, it was expected that

the quantitative analytical method developed for rimonabant could be applied to the measurement of surinabant.

Further, the results of the rimonabant canine study indicated that clinically relevant concentrations of the drug were in the 20-125 ng/mL range. This concentration range suggested that there are a wide range of studies which find prove useful with a method employing a UV detector. UV detectors are much less expensive, more widely available and easy to operate than a mass spectrometer. Thus, a quantitative bioanalytical method using a UV detector was development for the measurement of surinabant.

### *2.3.2 Materials and Methods*

#### Reagents

Acetic acid, HPLC-grade acetonitrile, dimethyl sulfoxide (DMSO), formic acid, and 1-(2,4-dichlorophenyl)-5-(4-iodophenyl)-4-methyl-N-1-piperidinyl-1H-pyrazole-3-carboxamide trifluoroacetate salt (AM251) were from Sigma-Aldrich (St. Louis, MO, USA). Surinabant, (5-(4-bromophenyl)-1-(2,4-dichloro-phenyl)-4-ethyl-N-1-piperidinyl-1H-pyrazole-3-carboxamide), was obtained from the drug repository (NIMH code S-908) of National Institute of Mental Health (Bethesda, MD, USA). Pooled human plasma which contained no detectable surinabant was from Haemtech, Inc (Essex Junction, Vermont, USA).

A stock solution (1.00 mg/ml) of surinabant ( $C_{23}H_{24}Cl_2N_4BrO$ ) was prepared by weighing 1.32 mg of the compound into a 1.5 ml Eppendorf tube (Eppendorf, Westbury, NY, USA) and thereafter, it was dissolved with 1.32 ml of DMSO. A stock solution (1.00 mg/ml) of AM251 trifluoroacetate salt ( $C_{22}H_{21}N_4OCl_2I \cdot C_2HF_3O_2$ ) was prepared by weighing 1.18 mg of the compound into a 1.5 ml Eppendorf tube and dissolving it with 1.18 ml of DMSO. Once the compounds had been dissolved in DMSO, both surinabant and AM251 stock solutions were transferred to 1.5 ml amber glass vials and stored at - 20 °C when not in use.

A working solution (100 µg/ml) of surinabant was prepared by a dilution (1/10) of the surinabant stock solution with DMSO. A working solution (5.00 µg/ml) of AM251 was prepared by a three-step dilution (1/8.3, 1/10, 1/2) of the AM251 trifluoroacetate salt stock solution with DMSO. A mobile phase for liquid chromatographic separation was prepared by mixing 99.9%  $CH_3OH/H_2O$  (50:50, v/v) and 0.1%  $HCOOH$ . The above solutions were stored at 4 °C when not in use.

### Calibrators and Controls

Pooled human plasma containing no detectable surinabant was used as the blank plasma to prepare human plasma calibrators and controls for this study. Surinabant standard solutions (0.100, 0.1500, 0.200, 1.00, 1.50, 2.00, 5.00, 10.0, 15.0, 20.0 and 30.0 µg/ml) were prepared by a serial dilution of the working

solution (100 µg/ml) with DMSO. Surinabant plasma calibrators (5.00, 10.0, 50.0, 100, 250, 500, 750, 1.00 x 10<sup>3</sup> and 1.50 x 10<sup>3</sup> ng/ml) were prepared by diluting the corresponding surinabant standard solutions in a 1:20 ratio with the blank plasma. Surinabant plasma controls (7.50, 75.0, 150, 600, 750 and 1.20 x 10<sup>3</sup> ng/ml) were prepared by a 1:20 dilution of the corresponding surinabant standard solutions with the blank plasma. All plasma samples were stored at – 20 °C until use.

#### Surinabant Extraction from Plasma

Plasma samples (e.g., surinabant plasma calibrators, surinabant plasma controls) were prepared using the following protocol. First, 200 µl of plasma sample was pipetted into a 1.5 ml Eppendorf tube, then followed by 10.0 µl of the AM251 working solution (5.00 µg/ml) and 50.0 µl of acetic acid. After vortex mixing, 1.00 ml of acetonitrile was added. The solution was vortexed, then centrifuged at 13,000 g for 15 min. After centrifugation, the supernatant was transferred to a 1.5 ml Eppendorf tube, and evaporated to dryness in a TurboVap LV Evaporator (Caliper Life Sciences, Hopinkton, MA, USA) at 55 °C with N<sub>2</sub> pressure of 20 psi for 2 h. Prior to analysis, 200 µl of mobile phase was added to the dried samples.

### Surinabant Recovery from Plasma

The recovery of plasma surinabant by sample preparation procedure was determined using surinabant plasma controls and surinabant reference solutions at three different concentrations, which were 7.50, 75.0, 750 ng/ml for LC-ESI-MS/MS and 150, 600 and  $1.20 \times 10^3$  ng/ml for LC-UV. The reference solutions contained the same sample matrix as that of plasma controls, which were prepared using blank plasma as samples by the same sample preparation procedure as that of plasma controls, and reconstituted in the mobile phase with appropriate surinabant concentrations.

### LC-UV Method

*Instrumentation:* A System Gold® HPLC BioEssential 126/128 from Beckman Coulter (Fullerton, CA, USA) was used in this work, which consisted of a 126-gradient pump, a 508-autosampler and cooler that was set at ambient temperature, a stainless steel in-line filter (0.5  $\mu\text{m}$  pore, 0.23  $\mu\text{L}$  dead volume) from Upchurch Scientific (Oak Harbor, WA, USA), a YMC™ Pro C4 cartridge column (3  $\mu\text{m}$ , 120 Å, 2.0 mm x 50 mm) from Waters (Milford, MA, USA), a 168-photo diode array detector that was set at 258 nm, and a 32-karat workstation. The fluidic connection of the system was made using stainless steel tubing (0.0625 in. o.d., 0.0100 in. i.d.). Data acquisition and peak integration was done by 32-karat software (version 8.0). The peak area ratios of surinabant to the

internal standard were plotted against plasma surinabant concentrations for a calibration curve.

*Chromatographic separation:* Surinabant and AM251 were separated under ambient temperatures on a Waters YMC™ Pro C4 cartridge column. Prior to the analysis, the cartridge column was first equilibrated with the mobile phase containing 99.9% CH<sub>3</sub>OH/H<sub>2</sub>O (50:50, v/v) and 0.1% HCOOH at a flow rate of 0.200 ml/min for about 30 min. In each analysis, 20 µl of sample was injected with the autosampler, and the analytes were separated on the column by isocratic elution at a flow rate of 0.200 ml/min.

#### LC-ESI-MS/MS Method

*Instrumentation:* The LC-ESI-MS/MS system used in this work consisted of an HP1100 pump by Hewlett Packard (Palo Alto, CA, USA), an HP1100 autosampler, a stainless steel in-line filter (0.5 µm pore, 0.23 µl dead volume) by Upchurch Scientific (Oak Harbor, WA, USA), a YMC™ Pro C4 cartridge column (3 µm, 120 Å, 2.0 mm x 50 mm) by Waters (Milford, MA, USA), a stainless steel splitting tee (1/16" x 0.25 mm) by Valco (Houston, TX, USA), and a Quattro II electrospray ionization triple quadrupole mass spectrometer by Micromass (Manchester, UK). All fluidic connections of the system were made using high-pressure polyether ether ketone (PEEK) tubing (0.0625 in. o.d., 0.0100 in. i.d.). The post-column split ratio was 1:2 with a smaller flow (ca. 63 µl/min) to the MS detector and the larger one to the waste. Data acquisition and peak integration

were accomplished using the Micromass Masslynx software (version 3.4). The peak area ratios of surinabant to the internal standard were plotted against plasma surinabant concentrations for a calibration curve.

*Chromatographic separation:* The separation conditions were the same as those described in the Section 2.5.

*ESI-MS/MS detection:* The Micromass Quattro II triple quadrupole mass spectrometer was operated under the positive electrospray ionization mode (ESI<sup>+</sup>). Tuning of the mass spectrometer was accomplished by infusion of a mixture of surinabant (2.0 µg/ml) and AM251 (2.0 µg/ml) in the mobile phase at a flow rate of 3 µl/min with a syringe pump (Harvard Apparatus, South Natick, MA, USA). Ionization conditions were optimized as follows: nitrogen sheath and desolvation gas at 10 and 350 l/h, capillary at 3.5 kV, HV lens at 0.5 kV, cone at 45 V, skimmer at 1.5 V, RF lens at 0.2 V, ion source temperature at 95 °C, ion energy at 0.1 V, low- and high-mass resolution at 15, and multiplier at 700 V. Full-scan spectra were acquired in the continuum mode at a scan rate 400 u/s. Multiple reaction monitoring (MRM) mode was used for quantitation, which was set at the following conditions: m/z 523 → 423 for surinabant, m/z 555 → 455 for AM251, argon collision gas at 2.0-2.5 µbar, cone at 45 V, collision energy at 20 V for both analytes, low- and high-mass resolution at 10 for quadrupole 1 and 15 for quadrupole 3, dwell time at 0.4 s, and the inter-scan delay at 0.01 s. The ionization parameters were the same as those described previously.

### *2.3.3 Results and Discussion*

#### Calibrator and Control and Plasma Sample Preparation

When choosing a solvent for dissolution of analytes into a solution, there are two key considerations; first, the solvent chosen must dissolve the compound completely to produce a homogenous solution; secondly, the solvent should not cause matrix precipitation upon its addition to biological samples. The chemical structures of both surinabant and AM251 indicates that they are hydrophobic compounds and are expected to have low solubilities in aqueous solution. Therefore, it will not be possible to dissolve either compound directly in biological samples.

Our previous experiments with rimonabant showed that protonation of amine groups 0.1 M HCl had little effect on the water solubility of the compound. Since surinabant has a similar structure with rimonabant which is completely soluble in DMSO and the addition of DMSO at 25% or lower does not cause protein precipitation in plasma [38], DMSO has been chosen as the solvent for the preparations of surinabant and AM251 stock and working solutions, as well as surinabant standard solutions. The percent composition of DMSO in surinabant plasma calibrators and controls in this work was 10% (v/v) in which there was no protein precipitation observed.

Plasma samples were prepared by the protein precipitation procedure described in section 2.2.2. The supernatant containing surinabant and AM251 was evaporated to dryness in a TurboVap LV Evaporator. The drying time may be shortened by increasing either the temperature of the water bath or the pressure of nitrogen flow. The sample preparation procedure used has been proven by the recovery data (Table 1) to be adequate for the analysis of surinabant by LC-UV and LC-ESI-MS/MS methods.

#### HPLC Method Using UV Detection

In this work, a Waters YMC<sup>TM</sup> Pro C4 column was used based on the success of this column in the method developed for rimonabant. Although surinabant has a smaller molecular weight than AM251, the presence of an ethyl group at the 4-position of its pyrazole ring causes surinabant to be more hydrophobic than AM251. The elution sequence from a C4 column was AM251 (7.4 min) first, then surinabant (9.4 min), and the total run time for each sample was about 11.0 min. Both surinabant and AM251 showed maximum absorptivity at 258 nm and no detectable interference from the blank human plasma was present in this range. Therefore, the signal at 258 nm was used for quantitation.

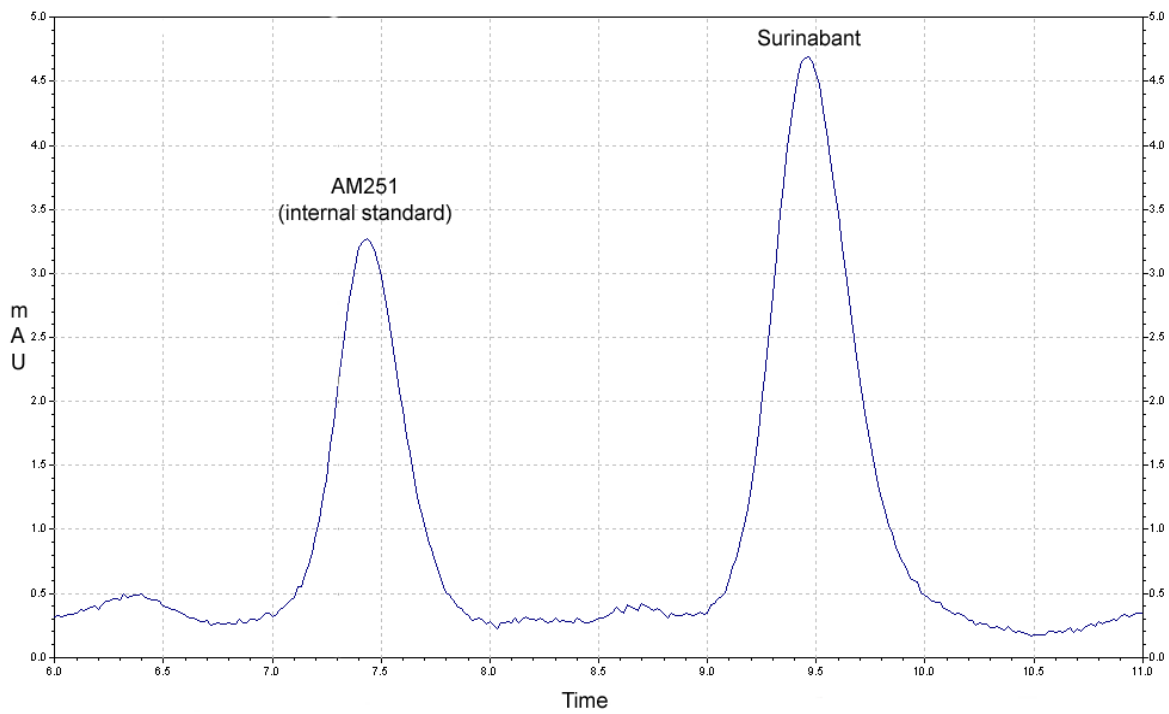


Figure 2.18, Chromatogram of surinabant (500 ng/mL) and AM251 (250 ng/mL)

The recovery of surinabant was ascertained using the protein precipitation procedure and LC-UV method with surinabant plasma controls and surinabant reference solutions at three different concentrations (150, 600 and  $1.2 \times 10^3$  ng/mL). The relative recoveries of surinabant were determined by comparing the mean-peak-area ratios of surinabant to the internal standard in the plasma controls to those of surinabant to the internal standard in the reference solutions. As discussed in section 2.2.3, the recovery should be consistent across the concentration range of interest.

The precision of the LC-UV method was established by analyzing surinabant plasma controls at three different concentrations (150, 600 and  $1.2 \times 10^3$  ng/mL) and was determined by the duplicate measurements of the peak-area ratio of surinabant to the internal standard from five separate samples at each concentration. The ability of the LC-UV method to accurately measure the concentration of surinabant was also established using the low, middle and high concentrations used to determine precision. The recovery, precision and accuracy of the LC-UV method is contained in table VII. The data provided in this table indicates exceptional analytical performance of the LC-UV method to measure surinabant in human plasma.

Table VIII, Analytical performance of the HPLC-UV method

<b>[Surinabant] (ng/mL)</b>	<b>Recovery (%)</b>	<b>Standard Deviation</b>	<b>CV (%)</b>	<b>Accuracy (%)</b>
150	103%	0.0099	3.0%	87%
600	95.0%	0.0535	3.9%	97%
1.20 x 10 <sup>3</sup>	97.0%	0.0857	3.1%	93%
All determinations were based on the mean value obtained from five (5) separate samples at each concentration. The concentration of internal standard was fixed (250 ng/mL)				

The linear response of the LC-UV method was determined by plotting the internal standard corrected surinabant peak-area versus the concentration of surinabant calibrator. A linear calibration range of 100-1500 ng/ml with a correlation coefficient of 0.999 was achieved. A calibration equation,  $y = 0.00232x - 0.0619$ , was derived from the average peak area ratio of two separate injections from a single sample at each of the six concentrations (100, 250, 500, 750, 1000 and 1500 ng/ml) over the calibration range. A second condition which was not discussed in section 2.2.3 for the identification of the lower limit of quantification (LLOQ) suggested by the FDA guidelines is that the precision and accuracy of this measurement fall within a 20% error range. The LLOQ of the LC-UV method was determined by the lowest plasma surinabant calibrator on the calibration curve to be 100 ng/ml with a CV and an accuracy of 8.0 and 95.0%, respectively.

#### HPLC Method with Mass Spectrometric Detection

In the LC-ESI-MS/MS method, the chromatographic separation conditions were the same as those described in the LC-UV method. However, because the fluidic connection of this system included a post column splitter, the elution times of AM251 and surinabant were slightly longer than (ca. 0.9 min) those of the LC-UV method. A post-column splitter is required to divert a portion of the sample flow to waste; thereby assuring that the flow rate entering the MS is under the

100  $\mu\text{L}/\text{min}$  discussed in section 1.5.2. The total run time for each sample was approximately 12.0 min.

The full-scan mass spectra by positive electrospray ionization revealed that surinabant and AM251 produced predominant protonated molecular ions at  $m/z$  523 and 555, respectively. These parent ions were fragmented to produce daughter mass spectra which resulted in predominant product ions at  $m/z$  423 for surinabant and  $m/z$  455 for AM251.

As with the method for rimonabant, these product ions were measured by the multiple-reaction-monitoring (MRM) mode for internal calibration and quantitation of surinabant. The selectivity and specificity of the LC-ESI-MS/MS method by MRM mode for the measurement of surinabant and AM251 is illustrated by the mass chromatograms contained in figure 2.20 which show no interference from the plasma matrices.

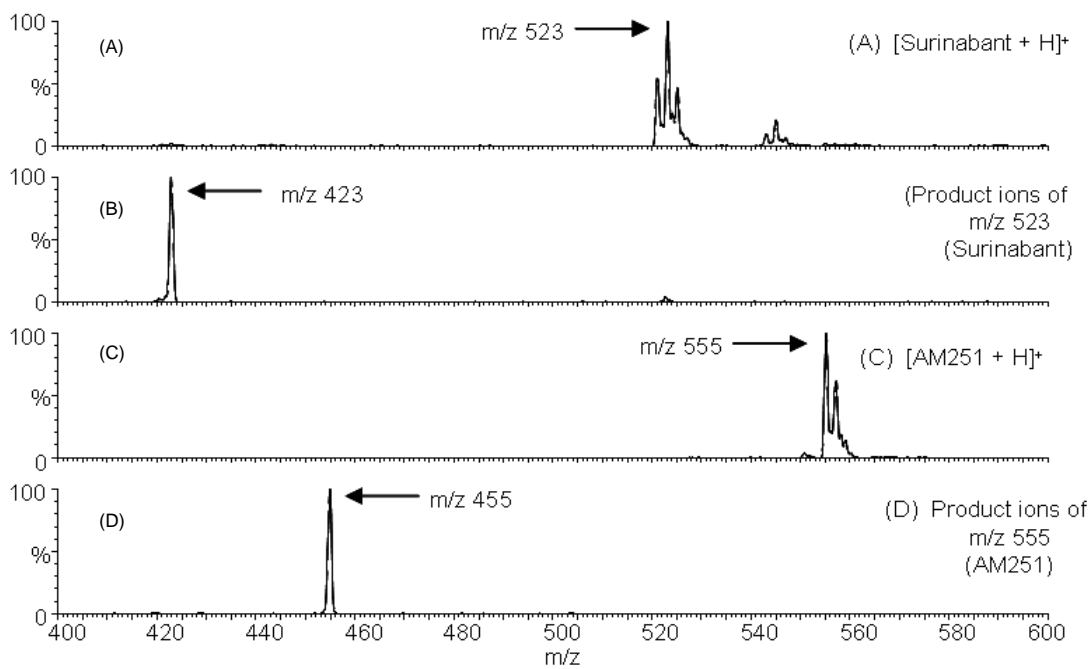


Figure 2.19. (A) Full scan of surinabant, (B) daughter ions of surinabant, (C) full scan of AM251 and (D) daughter ions of AM251

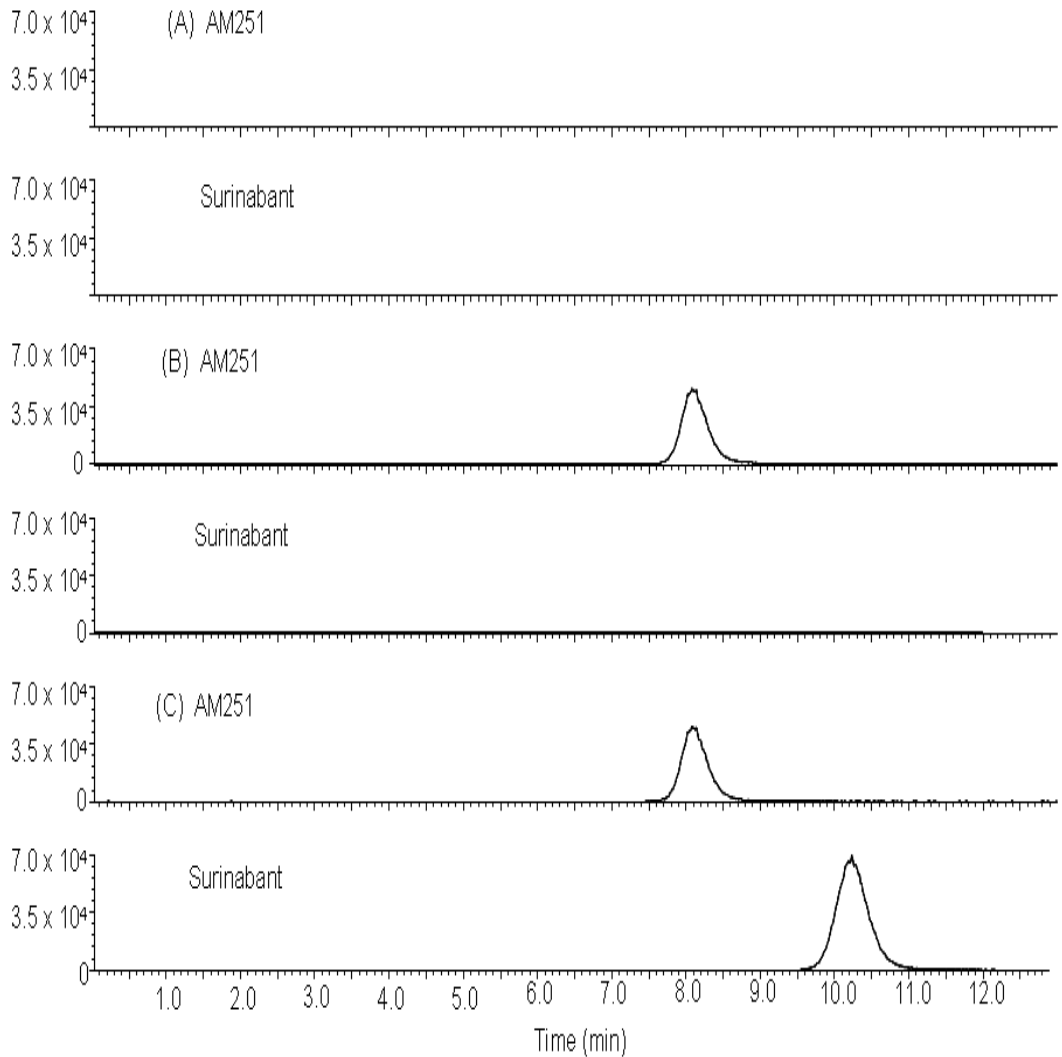


Figure 2.20, Representative mass chromatograms of surinabant and AM251 in (A) blank plasma, (B) plasma treated with AM251 (250 ng/mL) only and (C) plasma treated with both surinabant (500 ng/mL) and AM251 (250 ng/mL)

The fragmentation of surinabant produced a predominant product ion of 100 amu less than its parent ion, a pattern identical to that rimonabant and AM251 described in our previous work. Therefore, the fragmentation reaction of surinabant could be proposed and is contained in figure 2.21.

The recovery of surinabant was established using the protein precipitation procedure and LC-ESI-MS/MS method previously described with surinabant plasma controls and surinabant reference solutions at three different concentrations (7.50, 75.0 and 750 ng/ml). The precision (%CV) and accuracy was determined by the triplicate measurements of the peak area ratio of surinabant to the internal standard from five separate samples at each of the three concentrations listed above. The method for calculating for these parameters has been previously discussed. The recovery, precision and accuracy values are reported in Table VIII.

The linear calibration range of the LC-ESI-MS/MS method was 5.00 to 1000 ng/ml with a correlation coefficient of 0.999. A calibration equation,  $y = 0.00373x - 0.00941$ , was derived from the average peak area ratio of three separate injections from a single sample at each of the six concentrations (5.00, 10.0, 50.0, 100, 500 and 1000 ng/ml) over the calibration range. The LLOQ for the LC-ESI-MS/MS method was determined to be 5.00 ng/ml with a CV and an accuracy of 6.0 and 90.9%, respectively.

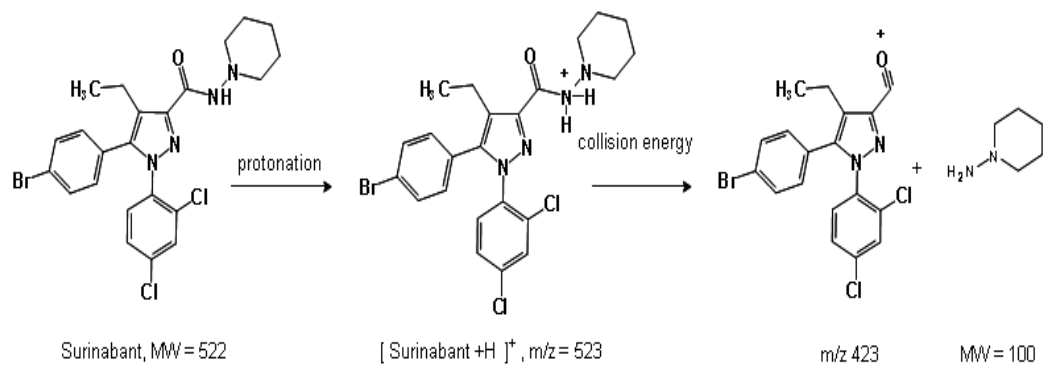


Figure 2.21, Proposed fragmentation scheme of surinabant

Table IX, Analytical performance of HPLC-MS method

<b>[Surinabant] (ng/mL)</b>	<b>Recovery (%)</b>	<b>Standard Deviation</b>	<b>CV (%)</b>	<b>Accuracy (%)</b>
7.50	101%	$2.60 \times 10^{-3}$	7.7%	92%
75.0	96.0%	0.009	2.9%	87%
750	100%	0.145	5.7%	93%
All determinations were based on the mean value obtained from five (5) separate samples t each concentration. The concentration of internal standard was fixed (250 ng/mL)				

### Surinabant Stability

The stability of surinabant in plasma was established by three aliquots at each low and high controls. As with rimonabant, all error reported refers to the difference between the condition the sample was exposed to and time zero. After three freeze (-20 °C) and thaw (room temperature) cycles, a maximum relative error of 6% was observed. The short-term temperature stability of surinabant in plasma was established by storing the surinabant plasma controls at room temperature for 24 h with the maximum relative error observed being 4%. A study was conducted to determine the necessity of storing surinabant samples in amber vials to protect the compound from light degradation. Surinabant plasma controls stored in amber versus clear vials for six weeks at -20 °C gave a maximum relative error of 7% which showed that surinabant could be stored safely under these conditions without protection from light. Overall, in all situations investigated, surinabant exhibits sufficient stability.

#### *2.3.4 Conclusion*

Two methods, an LC-UV and an LC-ESI<sup>+</sup>-MS/MS method have been developed and validated for the quantitative measurement of surinabant in human plasma using AM251 as the internal standard. A protein precipitation procedure using acetonitrile was established, which resulted in consistent

recovery of surinabant. A LLOQ of 100 ng/ml and a calibration range of 100-1500 ng/ml was obtained for surinabant. LC-ESI-MS/MS detection had a LLOQ of 5.00 ng/ml and a calibration curve of 5.00-1000 ng/ml for surinabant. Both methods developed exhibited strong analytical performance which is validated by the recovery, precision and accuracy of the methods to measure surinabant. The low limits of detection achieved with these methods permits their application to a variety of studies involving the pharmacology, toxicology and biochemical mechanisms of surinabant.

## Chapter II References

- [1] Gaoni, Y., Mechoulam, R., Journal of the American Chemical Society, 86 (1964) 1646
- [2] Lupica, C.R., Reigel, A.C., Hoffman, A.F., British Journal of Pharmacology, 143 (2004) 227
- [3] Pertwee, R.G., et al., The Handbook of Experimental Pharmacology, 168 (2005) 657
- [4] Wilson, R.I., Nicoll, R.A., Nature, 410 (2001) 588
- [5] DiMarzo, V., Matias, I., Nature Neuroscience, 8 (2005) 585
- [6] DiMarzo, V., Melck, D., Bisogno, T., De Petrocellis, L., Trends in Neuroscience, 21 (1998) 521
- [7] DiMarzo, V., Bifulco, M., DePetrocellis, L., Nature Reviews in Drug Discovery, 3 (2004) 771
- [8] Wilson, R.I., Nicoll, N.A., Science, 96 (2002) 678

- [9] Joy, J.E., Marijuana as Medicine: The Science Behind the Controversy, National Academic Press (2001)
- [10] Osei-Hyiaman, D., et al., Journal of Clinical Investigation, 115 (2005) 1298
- [11] Miller, A.M., Stella, N., British Journal of Pharmacology, 153 (2008) 299
- [12] McAllister, M.D., Glass, M., Prostaglandins Leukotrienes and Essential Fatty Acids , 66 (2002) 161
- [13] Pertwee, R.J., Pharmacology and Therapeutics, 74 (1997) 129
- [14] Demuth, D.G., Molleman, A., Life Science, 78 (2006) 549
- [15] S. Xie, M.A., Furjancia, M.A., Ferrara, J.J., McAndrew, N.R., Ardino, E.L., Ngondara, A., Bernstin, Y., Thomas, K.J., Kim, E., Walker, J.M., Nagar, S., Ward, S.J., Raffa, R.B., Journal of Clinical Pharmacy and Therapeutics 32 (2007) 209
- [16] Pertwee, R.J., Life Science, 76 (2005) 1307
- [17] Carmona, M.R., Barth, F., H'eaulme, M., FEBS Letters, 350 (1994) 24

[18] Navarro, M., Carrera, R.A., Fratta, W., Valverde, O., Cossu, G., Fattore, L., Chowen, A., Gomex, R., De Arco, I., Villanua, M.A., Journal of Neuroscience, 21 (2001) 5344

[19] De Vries, T., Shaham, Y., Homberg, J., Crombag, H., Schuurman, K., Dieben, J., Vanderschuren, L., Schoffelmeer, A., Nature Medicine 7 (2001) 1151

[20] Cohen, C., Perrault, G., Voltz, C., Steinberg, R., Soubrie, P., Behavioral Pharmacology 13 (2002) 451

[21] Colombo, G., Vacca, G., Serra, S., European Journal of Pharmacology, 498 (2004) 119

[22] Carai, M., Colombo, G., Gessa, G., Gian, L., Life Science, 77 (2005) 2339

[23] ClinicalTrials.gov Identifier: NCT00075205

[24] ClinicalTrials.gov Identifier: NCT00449605

[25] ClinicalTrials.gov Identifier: NCT00386061

[26] The European Medicines Agency recommends suspension of the marketing authorization of Acomplia, available at,

<http://www.emea.europa.eu/humandocs/PDFs/EPAR/acompia/53777708en.pdf>,  
retrieved July 18, 2009

[27] Sanofi-aventis to Discontinue all Clinical Trials with rimonabant, available at  
[http://en.sanofi-aventis.com/binaries/20081105\\_rimonabant\\_en\\_tcm28-22682.pdf](http://en.sanofi-aventis.com/binaries/20081105_rimonabant_en_tcm28-22682.pdf), retrieved July 18, 2009

[28] Carmona, M.R., et al., Journal of Pharmacology and Experimental Therapeutics, 310 (2004) 905

[29] Lallemand, P.D., DeWitte, P., Alcohol 39 (2006) 125

[30] Lange, J.H.M., Kruse, C.G., Drug Discovery Today, 10 (2005) 693

[31] Vemuri, D.R., Janero, D.R., Makriyannis, A., Physiology and Behavior, 93 (2008) 671

[32] Bouaboula, M., Poinot-Chzel, C., Boiurrie, B., Canat, X., Journal of Biochemistry, 312 (1995) 637

[33] ClinicalTrials.gov Identifier: NCT00239174

[34] ClinicalTrials.gov Identifier: NCT00432575

[35] Svíženská, I., Dubový, P., Šulcová, A., Pharmacology, Biochemistry and Behavior , 90 (2008) 501

[36] Guidance for Industry Bioanalytical Method Validation, available at:

<http://www.fda.gov/downloads/Drugs/GuidanceComplianceRegulatoryInformation/Guidances/UCM070107.pdf>, retrieved July 18, 2009

[37] Grozav, A., Hutson, T., Zhou, X., Bukowski, R., Ganapathi, R., Xu, Y., Journal of Pharmaceutical and Biomedical Analysis, 36 (2004) 125

[38] McCulloch, M., Zhou, X., Xu, Y., Journal of Chromatography B, 863 (2008) 258

## CHAPTER III

### PRELIMINARY WORK CONDUCTED TO DEVELOP BIOANALYTICAL METHODS FOR THE MEASUREMENT OF ANTI-CANCER AGENTS, QUINACRINE AND TRIAPINE

#### 3.1 Quinacrine

##### 3.1.1 *Introduction*

Quinacrine is a drug with a long history and broad, interesting therapeutic applications. The chemical structure of quinacrine is contained in figure 3.1. It was first used in the 1930's as an antimalarial compound [1]. Over the years it has also been used to treat infections of the parasite *Giardia* [2].

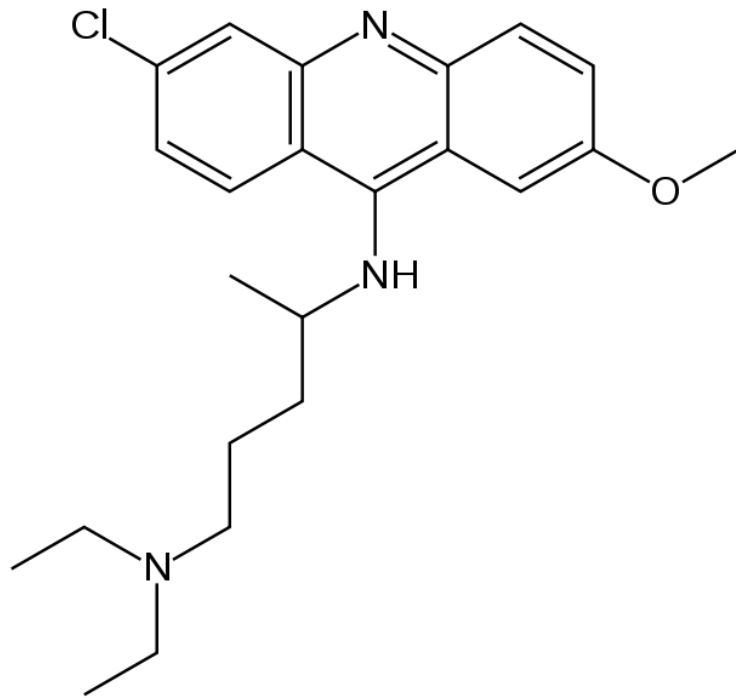


Figure 3.1, Chemical structure of quinacrine

A controversial, but common use of quinacrine is to cause female sterilization; primarily in poor, underdeveloped and overpopulated areas [3]. Quinacrine has also offered hope for the currently, untreatable, condition of prion disease [4]. Finally, quinacrine has shown promise as an anti-cancer agent [5]. The recent interest in the use of quinacrine for the treatment of both prion disease and cancer resulted in an anticipated need for a bioanalytical method to measure this compound, which led to the preliminary steps presented in this work.

The role of quinacrine in the treatment of cancer revolves around its ability to inhibit tumor protein 53 (p53) [6]. P53 is transcription factor which is present on both tumor and non-tumor cells. In tumor cells, p53 is generally inactivated. Therefore, typical cancer therapy's cause tumor cells die via non-apoptotic processes. On the contrary, normal tissues undergo a high rate of apoptosis during cancer treatment which is responsible for the deteriorative, adverse side effects. Research has shown that quinacrine can serve as a p53 activator, thereby re-establishing the ability of tumor cells to undergo apoptosis [6] [7]. In this sense, quinacrine is able to sensitize the tumor cells to an increased death rate of these cells.

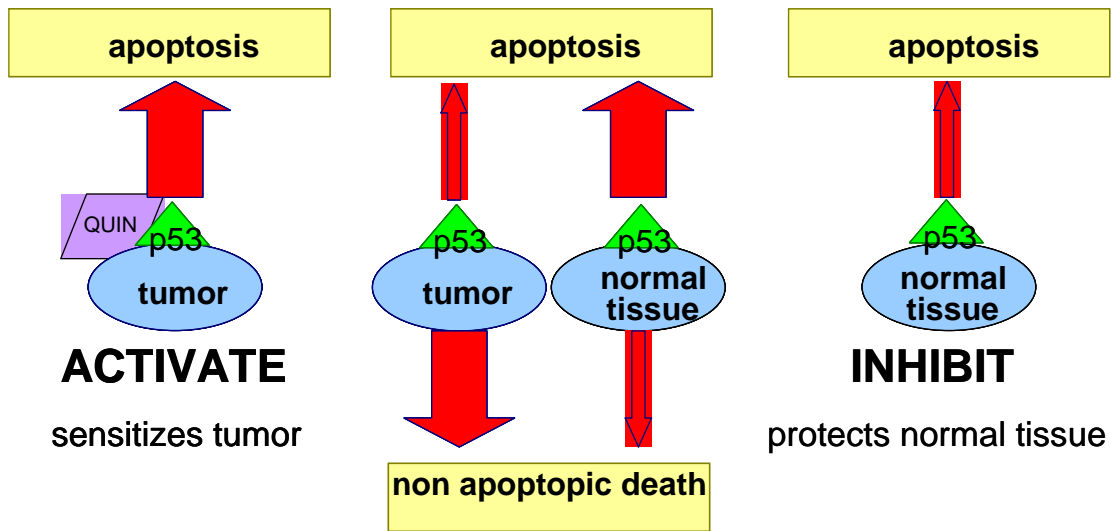


Figure 3.2, Block diagram describing the role of quinacrine in cancer treatment

There is no current pharmacological treatment for prion disease; a severe, progressive, neurological disorder. Prion disease is caused by the propagation of a misfolded prion protein, PrP. PrP<sup>SC</sup> is the isoform of PrP which is indicated in prion disease. PrP<sup>SC</sup> converts the structure PrP to the infectious PrP<sup>SC</sup> form. Quinacrine is able to block the conversion of PrP to PrP<sup>SC</sup> in vitro [8]. It should be mentioned that neither the mechanism involved in the structural change from PrP to PrP<sup>SC</sup>, nor quinacrine's ability to inhibit it; is well understood.

In 2004 research was published which established an HPLC-MS/MS method for the measurement of quinacrine [9]. The research described paints an initial pharmacokinetic profile of quinacrine as it relates to the treatment of prion disease. The study published in this article provides a strong stepping stone for the measurement of this compound. However, the work was lacking many features which are critical to demonstrating the performance of a quantitative bioanalytical method. Notably, there lacked a discussion regarding the sample extraction methods and validation of the ability of the method to measure quinacrine.

### 3.1.2 *Materials and Methods*

#### Reagents

Acetic acid, HPLC-grade acetonitrile and methanol, dimethyl sulfoxide (DMSO), and formic acid, ammonium acetate and quinacrine were purchased from Sigma-Aldrich (St. Louis, MO, USA). The internal standard, NCI number 10593-V/2 was provided, at no cost, by National Cancer Institute Drug Depository

The quinacrine stock solution (1.00 mg/ml) was prepared by weighing 0.85 mg of the compound into a 1.5 ml Eppendorf tube (Eppendorf, Westbury, NY, USA) and dissolving it with 0.85 ml of MeOH:H<sub>2</sub>O (50:50 v/v). A stock solution (1.00 mg/ml) of 10593-V/2 was prepared by weighing 1.20 mg of the compound into a 1.5 mL Eppendorf tube and dissolving it with 1.20 ml of MeOH:H<sub>2</sub>O (50:50 v/v).

Once the compounds were dissolved, both quinacrine and the internal standard stock solutions were transferred to 1.5 ml amber glass autosampler vials, sealed with parafilm, and were stored at - 20 °C when not in use. Quinacrine and internal standard working solutions (100 µg/ml) was prepared by a dilution (1/10) of the stock solution with MeOH:H<sub>2</sub>O (50:50 v/v). A mobile phase for liquid chromatographic separation was prepared by first adding ammonium acetate to water. The ammonium acetate/H<sub>2</sub>O solution was mixed with methanol

(50% v/v) with the ammonium acetate concentration being 5mM of the final mobile phase volume. All solutions were stored at 4°C when not in use.

### Instrumental Setup

The instrumental setup used in this work consisted of an HP1100 pump by Hewlett Packard (Palo Alto, CA, USA), an HP1100 autosampler, a stainless steel in-line filter (0.5 µm pore, 0.23 µl dead volume) by Upchurch Scientific (Oak Harbor, WA, USA), a Oasis HLB cartridge column (2.1 mm x 20 mm) by Waters (Milford, MA, USA), and a HCT ion trap mass spectrometer by Bruker Daltronics (Billerica, MA, USA). All fluidic connections in the system were made using high-pressure polyether ether ketone (PEEK) tubing (0.0625 in. o.d., 0.0100 in. i.d.).

### HPLC Separation

Analytical separation was performed via a Oasis HLB cartridge column (3 µm, 120 Å, 2.0 mm x 50 mm) by Waters (Milford, MA, USA). Before analysis, the cartridge column was equilibrated with mobile phase at a flow rate of 0.100 ml/min for about 20 min. During the analyses, 20 µl of sample was injected by the autosampler and carried onto the cartridge column by the mobile phase at a flow rate of 0.100 ml/min. Under the conditions described above, quinacrine and the internal standard had a retention times of 3.5 and 3.8 minutes, respectively.

### MS Detector Settings

A Bruker HCT ion trap mass spectrometer was used for the detection of quinacrine and the internal standard, 10953-V/2. The IT-MS parameters used were as follows: positive polarity, a capillary voltage of -4500 V, nebulizer gas pressure of 35 psi, drying gas flow of 9.0 L/min, a drying gas temperature of 340°C, and a fragmentation amplitude of 0.6V. The IT-MS was operated in ultra scan mode to provide optimum resolution and sensitivity.

#### *3.1.3 Discussion*

The focus of the work here was primarily to determine whether an on-line sample extraction would be possible for the measurement of quinacrine in biological matrices. As discussed in Chapters I and II, on-line sample extraction has many advantages over traditional, LLE, protein precipitation and SPE procedures.

The development of an HPLC separation method was investigated using a Waters Oasis HLB column. An IT-MS was used for the detection of quinacrine and the internal standard. The internal standard, identified as 10593-V/2, was provided by the National Cancer Institute Drug Repository Program, the chemical structure is contained in figure 3.3.

## Mass Spectrometric Detection

As evidenced by the chemical structure of quinacrine, there are several nitrogen groups which may be protonated. When a compound exists in several ionic forms, the mass spectrometric sensitivity can be compromised. As discussed in Chapter I, the MS detector reports a signal based on the  $m/z$  ratio of the analyte. Multiple charged species result in several  $m/z$  ratios being attributed to a single analyte mass. When conducting quantitation using MRM mode, only one  $m/z$  ratio is selected to undergo isolation and fragmentation. As predicted by the chemical structure, a full scan of quinacrine revealed the presence of two molecular ions; the singly protonated ion at  $m/z$  400 and the doubly protonated species at  $m/z$  200.6 (figure 3.4).

The solvent used to dissolve quinacrine which resulted in the spectra contained in figure 3.4 was a 50:50 mixture of MeOH:H<sub>2</sub>O, 0.3% formic acid, pH 4.0. In order to preferentially select for the singly protonated form of quinacrine, several mobile phase compositions were tested. The solvent chosen to dissolve quinacrine was 50:50 mixture of MeOH:H<sub>2</sub>O, 5mM ammonium acetate, pH 5.8. Figure 3.5 contains the full scan spectra of the predominantly singly protonated ions of quinacrine and the internal standard

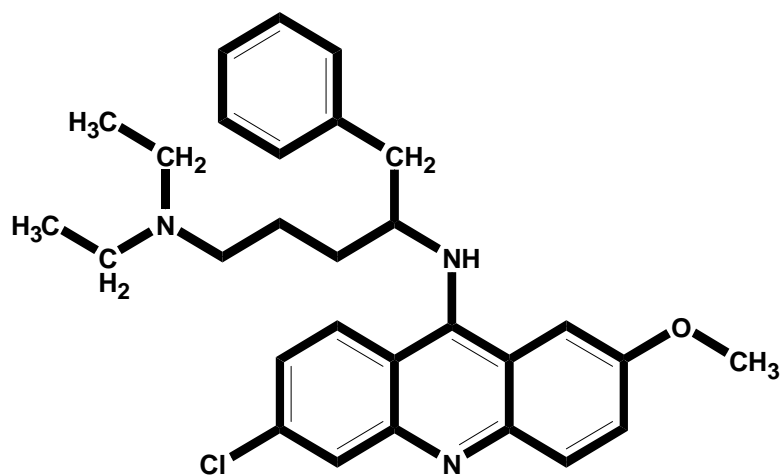


Figure 3.3, Chemical structure of 10593-V/2

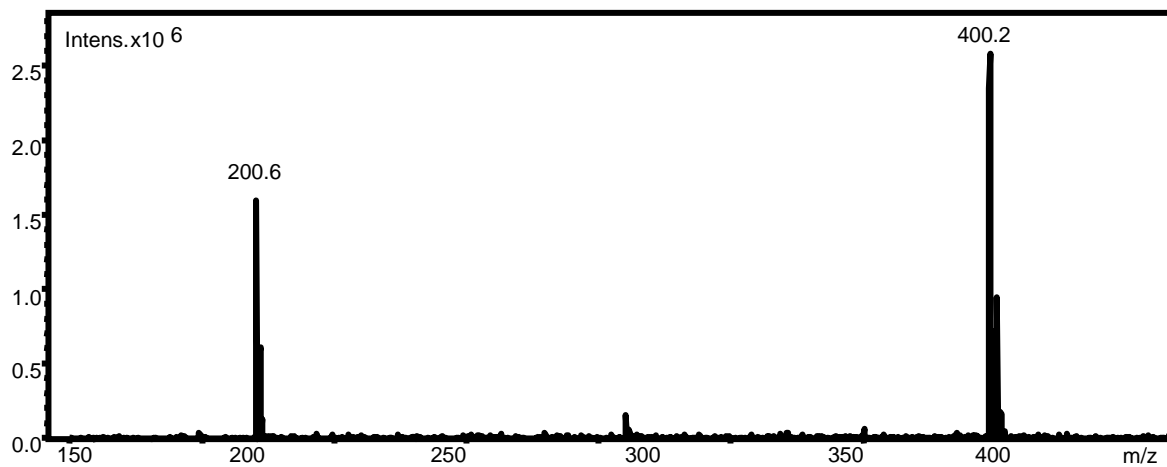


Figure 3.4, Full scan spectra of quinacrine

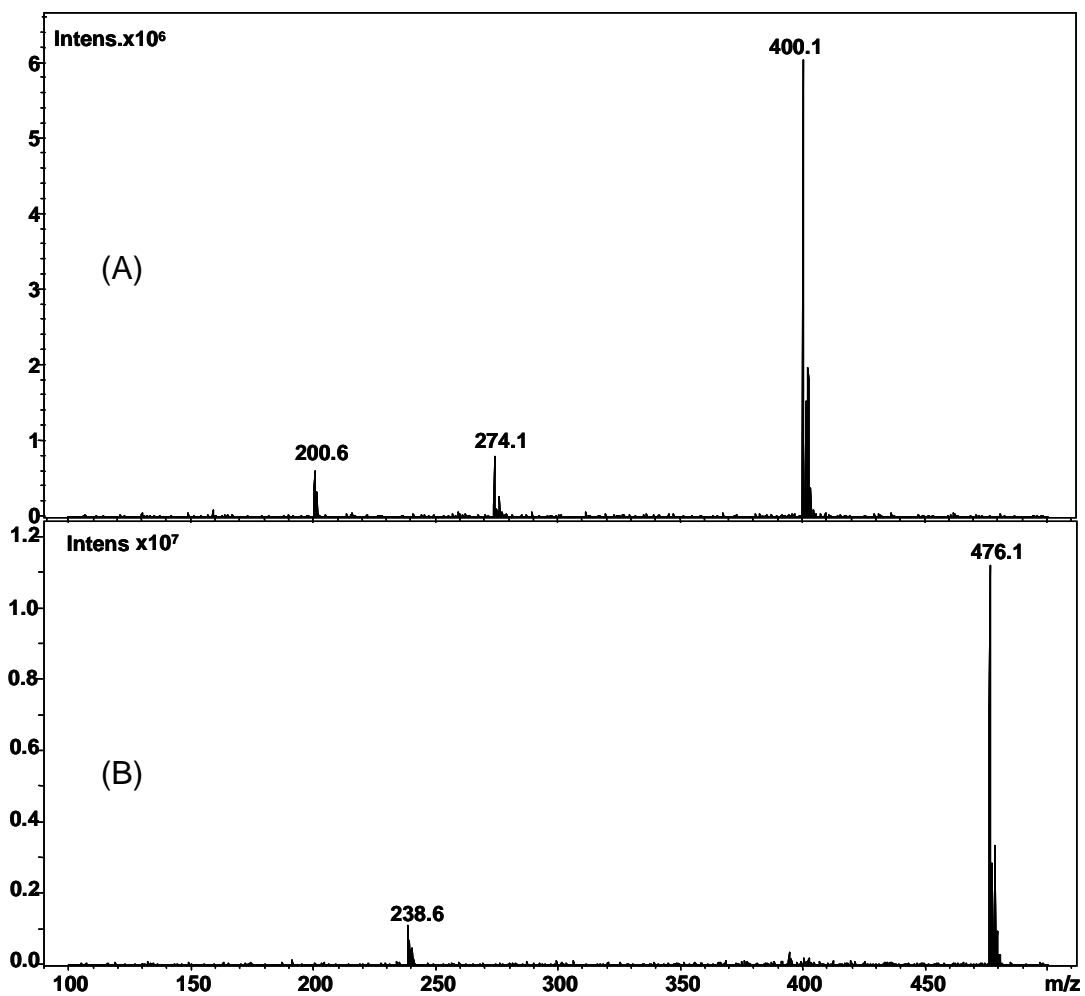


Figure 3.5, Full scan spectra of (A) quinacrine and (B) 10593-V/2, the internal standard

Daughter ion spectra of quinacrine and the internal standard are contained in figure 3.6. The fragments selected for the detection of quinacrine and the internal standard in subsequent analysis were  $m/z$  244 for quinacrine and  $m/z$  403 for 10593-V/2, the internal standard.

Mass chromatograms for quinacrine and the internal standard are exhibited in figure 3.7. Using the HPLC-MS parameters discussed, a calibration curve was obtained for quinacrine standards with the linear range of 50 – 2000 ng/mL and a correlation coefficient of 0.999.

#### Analyte Extraction via On-line Sample Extraction

The Waters Oasis HLB is marketed for its ability to work well in the design an on-line extraction procedure. In this case, the idea is that plasma containing quinacrine can be directly injected onto the column; quinacrine would be retained by the column, while the plasma proteins and other matrix components would travel to waste. This is accomplished by using a column switch to alternate between the column eluent flowing to waste or to the mass spectrometer. A flow diagram of the set up of one example of a fluidic profile tested is contained in figure 3.8.

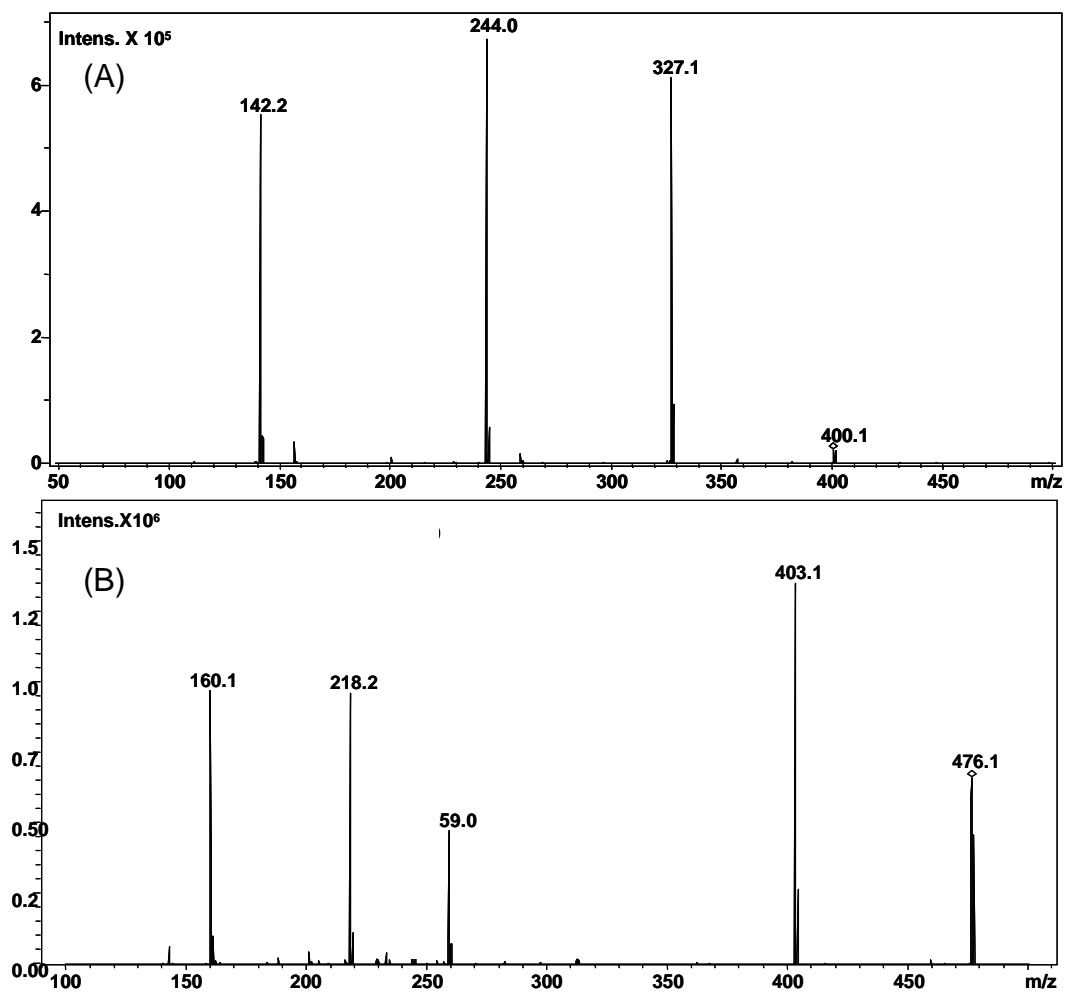


Figure 3.6 Daughter ion spectra of (A) quinacrine and (B) 10593-V/2, the internal standard

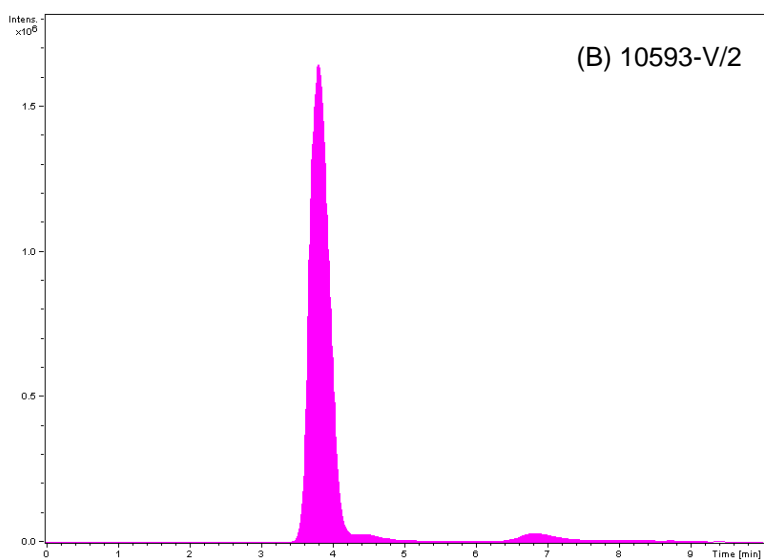
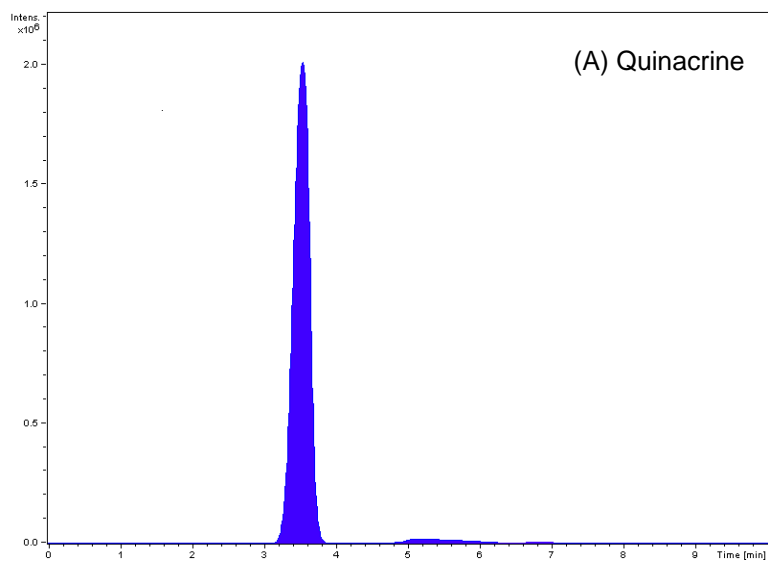


Figure 3.7, Mass chromatograms of (A) quinacrine and (B) 10593-V/2

As evidenced in figure 3.8, initially the aqueous mobile phase flows at 200  $\mu\text{L}/\text{min}$  for 1.0 minutes to load the sample onto the column. Next, the flow is kept constant and a mobile phase with a 50% organic composition is introduced to the column. During this step, quinacrine is retained by the column while the matrix components are diverted to waste. Thirdly, the column switch changes the flow so that the column eluent is able to travel to the MS detector. It is during this time that the analyte is eluted from the column and subsequently detected. The next two steps involve regenerating the aqueous solvent through the column at a high flow rate and finally, reducing the flow of the aqueous solvent to allow for pressure equilibration.

Quinacrine is a hydrophobic compound which resulted in it being retained so strongly by the HLB column that a high degree of carryover occurred between analyses. The carryover dilemma resulted in the feasibility of on-line extraction being abandoned. Without the development of an on-line extraction procedure, the further investigation into developing a quantitative bioanalytical method for quinacrine was not warranted.

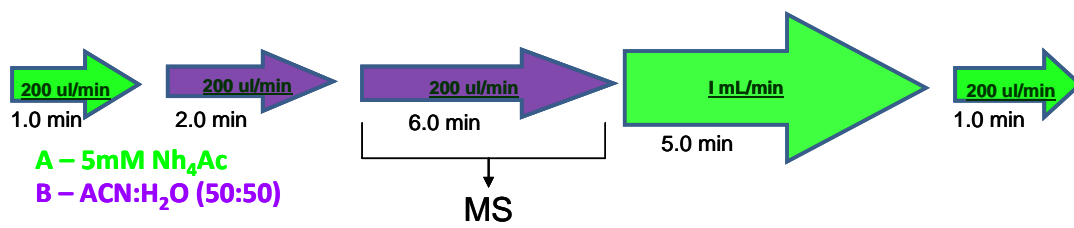


Figure 3.8, Fluidic profile for on-line sample extraction of quinacrine

## 3.2 Triapine

### 3.2.1 *Introduction*

Triapine (3-AP) is a relatively new compound being investigated for use as an anti-cancer therapy [10]. The chemical structure of 3-AP is contained in figure 3.9. Vion Pharmaceuticals is developing 3-AP which is currently in both Phase I [11] [12] [13] and II [14] clinical trials.

Cancer is caused by the uncontrolled proliferation of tumor cells.

Ribonucleotide reductase (RNR) is an enzyme which affects cellular proliferation both by catalyzing the transformation of ribonucleotides (NTP's) to deoxyribonucleotides (dNTP's), the building blocks of DNA; as well as by involvement in the DNA repair process [15]. 3-AP belongs to a class of compounds referred to as RNR inhibitors [16].

The ability of 3-AP to inhibit the conversion of NTP's to dNTP's effectively halts cellular proliferation and thus, the development of tumors. It has been reported that the ability of 3-AP to inhibit RNR lies in the metal chelating properties of 3-AP [15]. Chelation involves the ability to a ligand such as 3-AP to form complexes with metal ions.

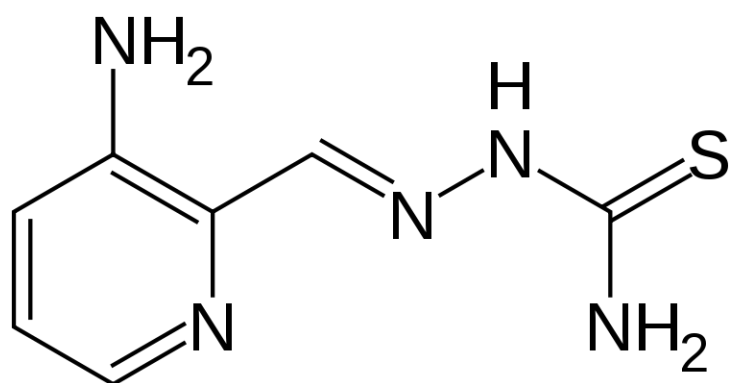


Figure 3.9, Chemical structure of 3-AP

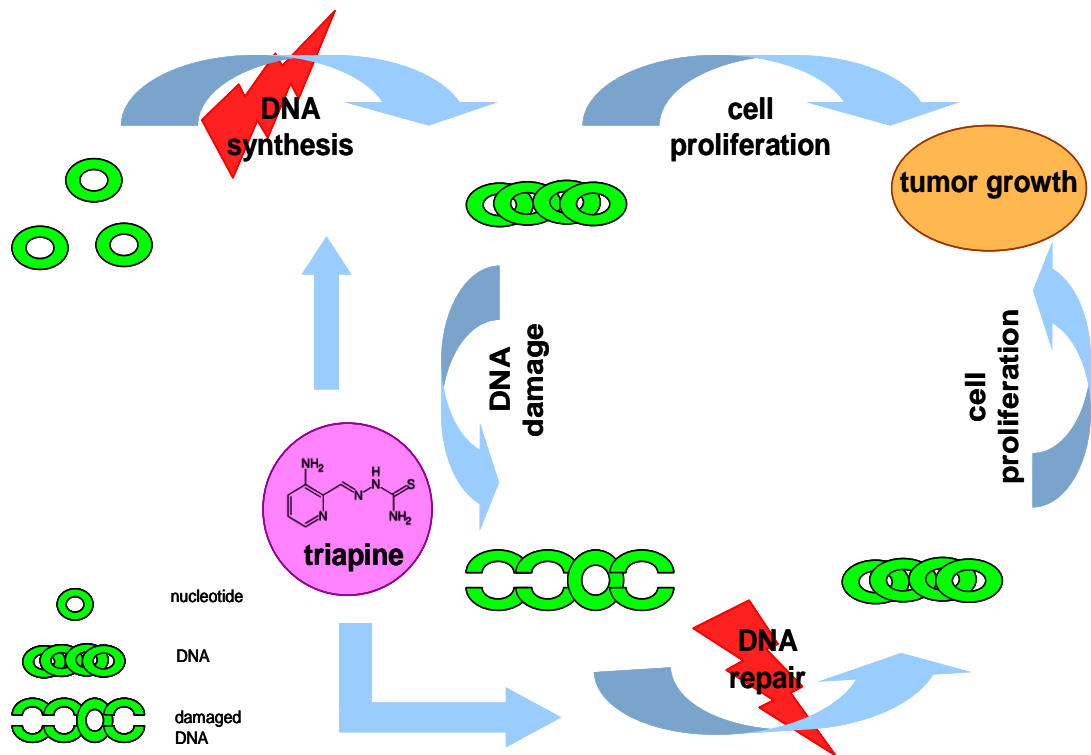


Figure 3.10, Role of triapine in cellular proliferation

RNR is an iron dependant enzyme which catalyzes the reaction of NTP's to dNTP's via a free radical reaction. This reaction occurs at the active site of the protein molecule which contains an iron, essential to the enzyme function. It has been suggested that the ability of triapine to inhibit this process is related to 3-APs involvement with the iron in the active site of RNR.

As mentioned, 3-AP is a new cancer treatment which is the subject of heavy clinical investigation. Currently there are no publicly available bioanalytical methods for the measurement of 3-AP. Thus, the development of such method is of strong importance. The scope of this work encompasses: the preliminary data obtained for the detection of triapine using HPLC-MS methods; the challenges faced; and suggestions for the future development of this method.

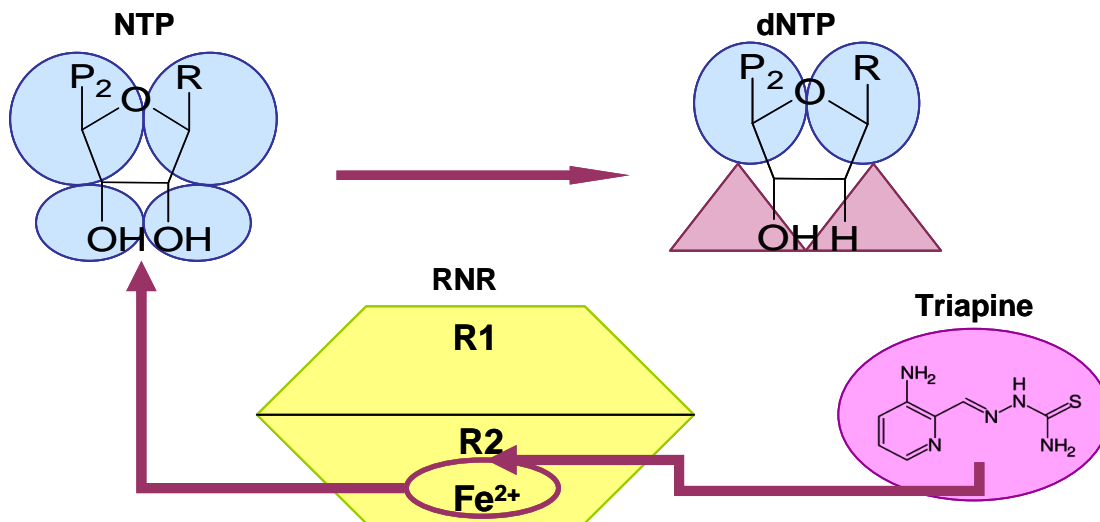


Figure 3.11, 3-AP as it relates to the conversion of NTP's to dNTP's

### 3.2.2 *Materials and Methods*

#### Reagents

Acetic acid, HPLC-grade acetonitrile, dimethyl sulfoxide (DMSO), and formic acid, were purchased from Sigma-Aldrich (St. Louis, MO, USA). 3-aminopyridine-2-carboxaldehyde thiosemicarbazone (Triapine or 3-AP) was provided, at no cost, by Vion Pharmaceuticals (New Haven, CT, USA). Thioacetazone, the internal standard, was provided at no cost from the National Cancer Institute Drug Depository (NCI reference #3550).

The 3-AP stock solution (1.00 mg/ml) was prepared by weighing 1.28 mg of the compound into a 1.5 ml Eppendorf tube (Eppendorf, Westbury, NY, USA) and dissolving it with 1.28ml of solvent (either DMSO or a MeOH:H<sub>2</sub>O mixture). A stock solution (1.00 mg/ml) of thioacetazone was prepared by weighing 1.45 mg of the compound into a 1.5 mL Eppendorf tube and dissolving it with 1.45 ml of solvent.

Once the compounds were dissolved, both 3-AP and internal standard stock solutions were transferred to 1.5 ml amber glass autosampler vials, sealed with parafilm, and were stored at - 20 °C when not in use. 3-AP working solutions (100 µg/ml) was prepared by a dilution (1/10) of the 3-AP stock solution with solvent. A mobile phase for liquid chromatographic separation was prepared by first adding formic acid (HCOOH) to water. The formic acid/H<sub>2</sub>O solution was

mixed with methanol (35% v/v) with the HCOOH concentration being 0.1% of the final mobile phase volume. All solutions were stored at 4°C when not in use.

### Instrumental Setup

The instrumental setup used in this work consisted of an HP1100 pump by Hewlett Packard (Palo Alto, CA, USA), an HP1100 autosampler, a stainless steel in-line filter (0.5 µm pore, 0.23 µl dead volume) by Upchurch Scientific (Oak Harbor, WA, USA), a YMC™Pro C18 cartridge column (3 µm, 120 Å, 2.0 mm x 50 mm) and YMC™Pro C18AQ cartridge column (3 µm, 120 Å, 2.0 mm x 50 mm) by Waters (Milford, MA, USA), a stainless steel splitting tee (1/16" x 0.25 mm) by Valco (Houston, TX, USA), and a Quattro II triple quadrupole mass spectrometer by Micromass (Manchester, UK). All fluidic connections in the system were made using high-pressure polyether ether ketone (PEEK) tubing (0.0625 in. o.d., 0.0100 in. i.d.). The post-column split ratio was 1:2 with a smaller flow (ca. 63 µl/min) to the MS detector and the larger one to the waste.

### HPLC Separation

Analytical separation was performed via a Waters YMC™Pro C18 or YMC™Pro C18AQ cartridge column. Before analysis, the cartridge column was equilibrated with mobile phase at a flow rate of 0.100 ml/min for about 20 min. During the analyses, 20 µl of sample was injected by the autosampler and

carried onto the cartridge column by the mobile phase at a flow rate of 0.200 ml/min. Under the conditions described above, 3-AP had a retention time of 2.75 minutes.

### MS Detector Settings

Electrospray ionization mode (ESI+) was utilized on the Micromass Quattro II triple quadrupole mass spectrometer. Tuning of the mass spectrometer was achieved by infusion of a 3-AP (10.0 µg/ml) in the mobile phase at a flow rate of 3.0 µl/min with a syringe pump (Harvard Apparatus, South Natick, MA, USA). Optimal ionization conditions were as follows: nitrogen sheath and desolvation gas at 10 and 350 l/h, capillary at 3.5 kV, HV lens at 0.5 kV, cone at 30 V, skimmer at 1.5 V, RF lens at 0.2 V, ion source temperature at 80°C, ion energy at 1.0 V, low- and high-mass resolution at 10, and multiplier at 700 V. Full-scan spectra were acquired in the continuum mode at a scan rate 400 u/s. The instrument was operated in multiple reaction monitoring (MRM) mode for quantitation, which was set as follows: m/z 196 → 94 and 196 → 120 for 3-AP, argon collision gas at 2.0-2.5 µbar, cone at 30 V, collision energy at 30 V, low- and high-mass resolution at 10 for quadrupole 1 and 10 for quadrupole 3, dwell time at 0.4 s, and the inter-scan delay at 0.01 s. The parameters for ionization remained the same as previously discussed.

### 3.2.3 Discussion

#### Sample Preparation

As discussed 3-AP is a metal chelator, therefore precautions should be taken to avoid the introduction of metals to the analyte when preparing stock solutions. A wooden or plastic was employed for the removal and weighing of 3-AP, but the challenge remains to reduce the contact of 3-AP with metal ions throughout sample preparation and analysis.

A common approach to avoid unwanted interactions of an analyte that is a metal chelator is the use of a stronger chelator, such as ethylenediaminetetraacetic acid (EDTA). EDTA can be added to stock solutions and mobile phases in order to preferentially bind with any metals, thus leaving 3-AP unreacted and detectable. In the case of HPLC-UV methods, EDTA is a common additive and has little effect of the sensitivity of the method. However, in HPLC-MS, the detection of analyte is depending on ionization, as discussed in Chapter 1.

The use of any additive in mass spectrometry, including EDTA; can negatively impact the sensitivity of the method based on the ion suppression theory. Ion suppression is a type of matrix effect caused when there is an excess of ionizable molecules eluted from the HPLC system concurrently with the analyte molecules. A graphical representation of ion suppression is contained in figure 3.12.

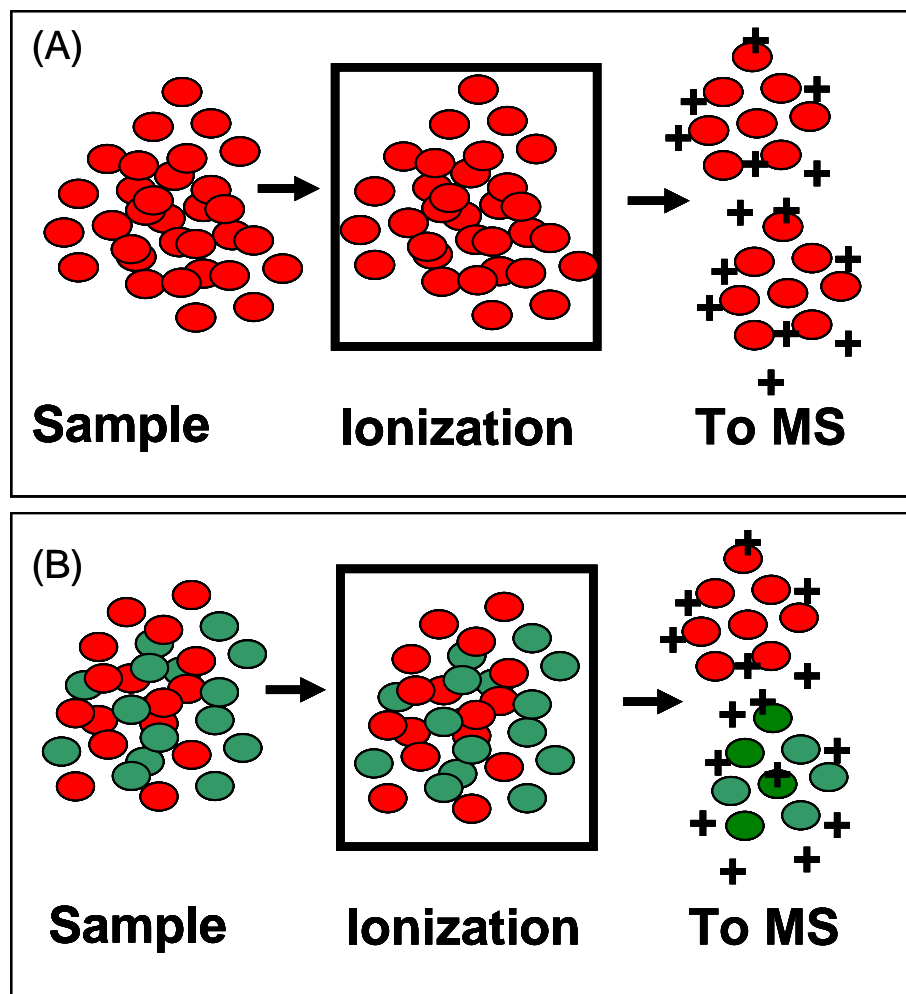


Figure 3.12, (A) ideal ionization versus (B) ion suppression

To understand ion suppression, it is helpful to consider that at during any given timeframe, there only exists enough electrical current to ionize a fixed amount of molecules. In figure 3.12(A) which represents ideal ionization, the entire electrical field is able to be applied to the analyte, depicted in red. However, if elution from the HPLC results in matrix components present during the ionization of the analyte, only a fraction of the molecules ionized and thereafter detected, will be analyte molecules. In this sense, ion suppression diminishes the sensitivity of the method being developed.

The suppression is exasperated in any matrix component which is more easily ionized than the analyte molecules, which is often the case when EDTA is used. Therefore, if EDTA is employed as an additive, consideration must be taken to determine the ratio between the amounts which are beneficial versus the amount which causes detriment to the detection of the analyte.

A final aspect of 3-AP sample preparation is the ability of the compound to dissolve. As expected from the chemical structure, 3-AP is not water soluble. Further 3-AP has a pKa of 4.2 which indicates that it will exist in a protonated form at a pH less than 4.2. Several solvent compositions were tested for their ability to dissolve 3-AP. DMSO readily dissolves the compound; however, in order to achieve control of the pH, the solvent composition should have an aqueous component. Both 50% DMSO and 50% MeOH in H<sub>2</sub>O, adjusted to pH 4.0 with formic acid are able to dissolve 3-AP. It is important to note that the addition of an acidic component to the solvent causes a dramatic increase (10 fold) in the bright yellow color observed.

## Mass Spectrometric Detection

The first step in the development of an HPLC-MS method is to optimize the ionization, fragmentation and detection parameters of the MS instrument. This process was undertaken by infusion of 10 µg/mL of the analyte dissolved in a solution of 50% MeOH in H<sub>2</sub>O, adjusted to a pH of 4.0. Figure 3.13 contains the full scan and daughter ion spectra for 3-AP. The instrument used for the detection of 3-AP was a Quattro II triple quadrupole mass spectrometer by Micromass.

As evident in figure 3.13(A), the predominant analyte ion is present at the m/z of 196, which represents the singly protonated 3-AP molecule. Fragmentation of the ion at m/z of 196 results in two predominant daughter peaks; m/z 94 and m/z of 120. The ratio of daughter peaks is variable depending primarily upon the collision gas pressure.

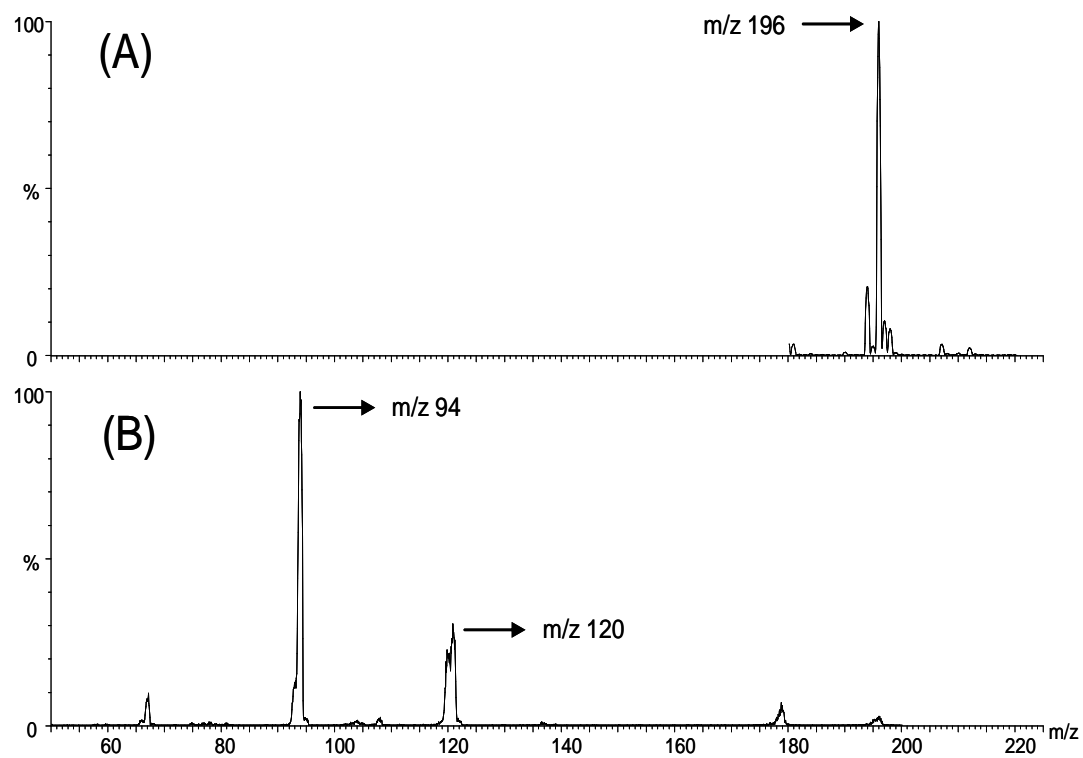


Figure 3.13, (A) full scan, and (B) daughter spectra of 3-AP

Figure 3.14 contains mass chromatograms of the total ion signal due to the ion with the m/z ratio of 196, and the extracted signal of the daughter ions at both m/z 94 and 120. It is evident in this figure that a significant portion of the total signal is due to the signal of both daughter ions. These mass chromatograms were obtained using the following HPLC parameters: a Waters YMC Pro C18 column; a mobile phase composition of 35% MeOH in H<sub>2</sub>O adjusted to a pH of 4.0 with formic acid; a flow rate of 100 µL/min with a post column splitter diverting 2/3rds of the flow to waste.

Figure 3.15 contains mass chromatograms of stock solutions of 3-AP ranging from 1.00 ng/mL to 100 ng/mL. For the purpose of the current clinical investigations, it is expected that a detection limit in the range of 1 ng/mL will be required to precisely and accurately measure 3-AP in human plasma. As evidenced by this figure, the sensitivity achieved with efforts to date, are not sufficient to continue forward with steps to develop a procedure for extraction of 3-AP from a plasma matrix.

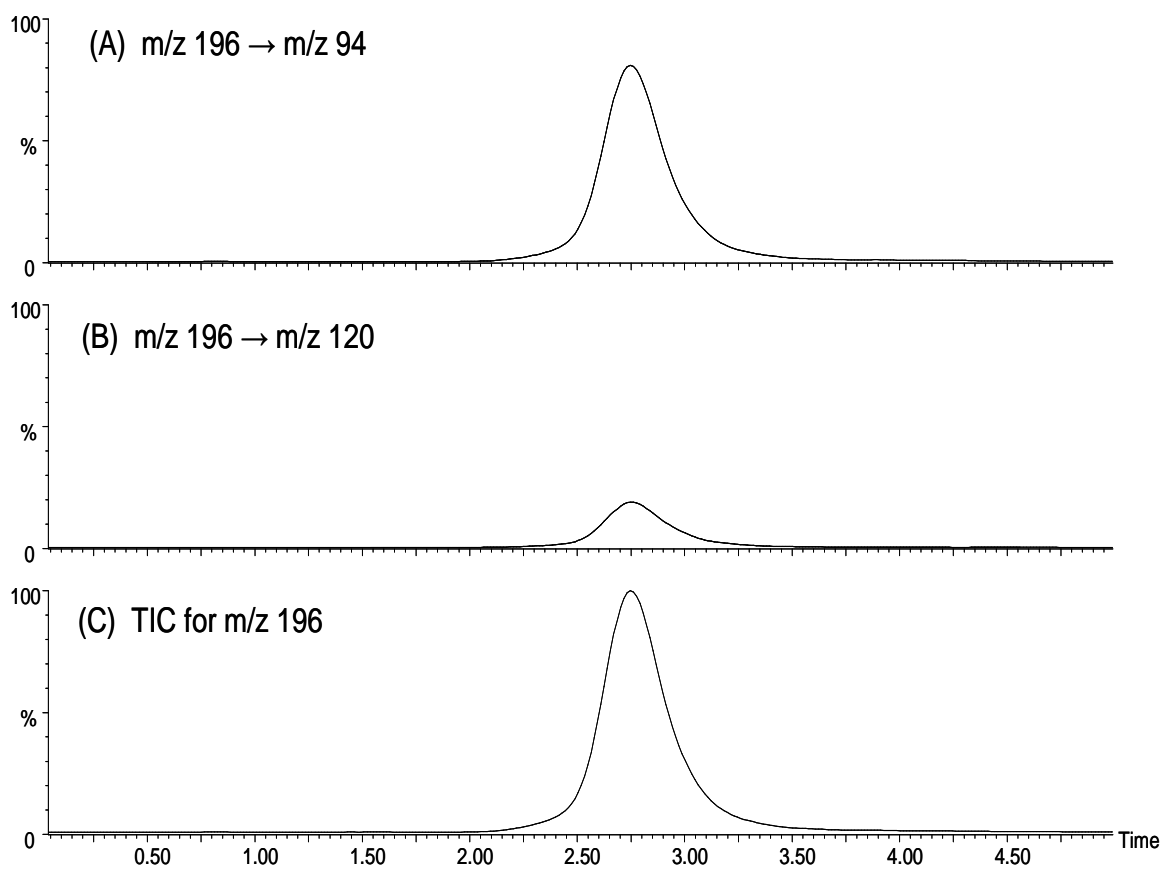


Figure 3.14, Extracted ion chromatogram for 3-AP of (A) daughter ion m/z 94, (B) daughter ion m/z 120 and (C) the total ion chromatogram of 3-AP which (A) and (B) were extracted from

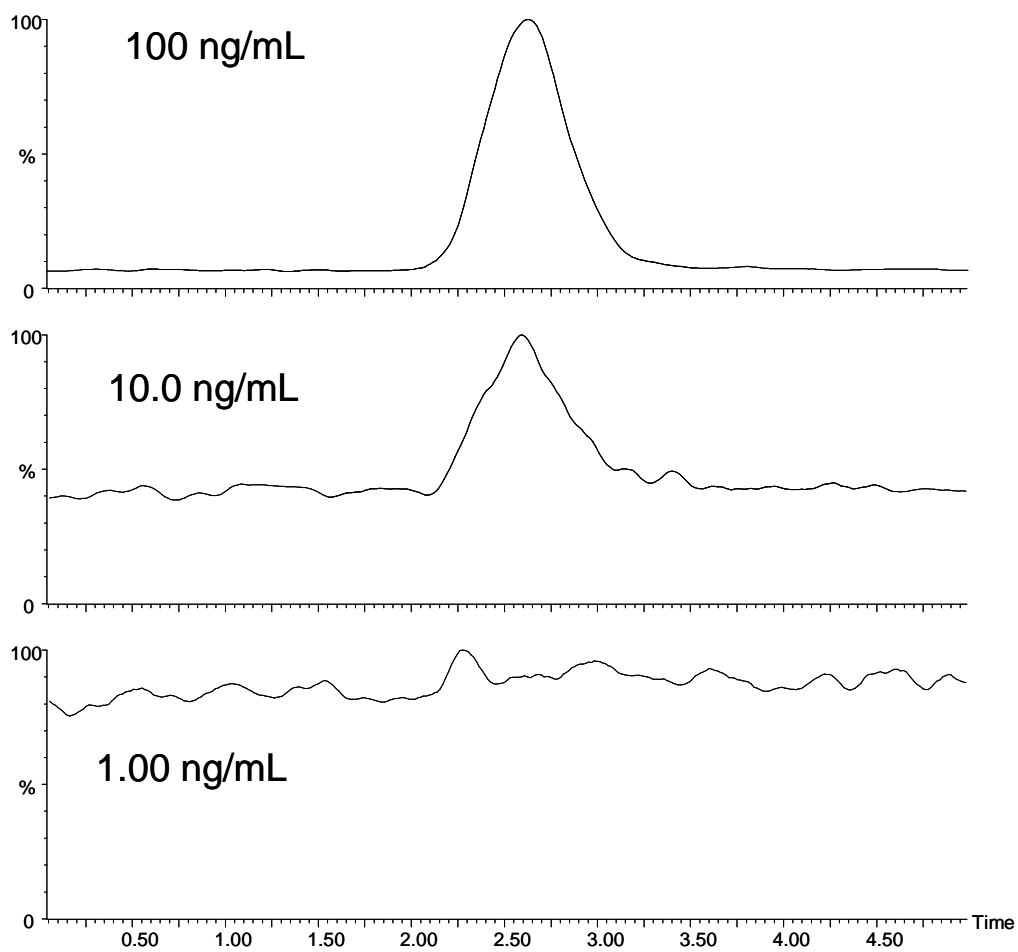


Figure 3.15, Mass chromatograms at 3-AP from 1.00 to 100 ng/mL

### *3.2.4 Challenges and Future Direction for The Development of a Quantitative Bioanalytical Method to Measure 3-AP*

The challenges faced during the preliminary development of a bioanalytical method for the measurement of 3-AP were centered on two major hurdles: first, the nature of 3-AP as a metal chelator; and secondly, the apparent resistance of 3-AP to electrospray ionization.

#### Metal Chelation

As discussed, 3-AP is a metal chelator and the current approach to analysis of this compound requires that it remain in a non-chelated, free form. While the introduction of metal ions can be avoided in many respects, the design of modern instruments involves a substantial amount of metal components. The interaction with the analyte cannot be avoided in these instances.

One solution to the metal chelation challenge is to employ the use of stronger chelating compounds in the preparation of stock solutions and mobile phases. EDTA is one such compound, but its use is a “double-edged sword”; the benefits afforded by its chelating power may be outweighed by the ion suppression it causes.

The first step in overcoming any challenge that metal chelation poses in the development of this method would be to conduct a systematic study using EDTA as an additive at varying ratios to 3-AP. Further, alternative chelating

agents such as nitriloacetic acid (NTA) may be investigated as superior substitutes to EDTA.

### Ionization

It is not possible to develop a successful quantitative bioanalytical method using HPLC-MS without ionizing the compound to be analyzed. Great detail was provided in Chapter I regarding the importance of ionization and the various ion sources commercially available. Often the chemistry of a compound leaves it resistant to the acceptance (or loss of) a proton. Additionally, it is not uncommon for a compound to undergo substantial fragmentation during the ionization process.

In the case of 3-AP, the resistance of the compound to protonation should be investigated. As previously discussed, 3-AP has a pKa of 4.2, and the dissolution of the compound in acidic solutions generates a strong color change. It is possible that once triapine undergoes the initial protonation in the dissolution process, that the resulting chemical structure is stabilized in a neutral form and that the normal ESI process is unable to protonate the analyte further. In this case, it should be investigated whether the acidic conditions during sample preparation are required for 3-AP to dissolve.

In some instances; it is not a chemical resistance to protonation which causes a lack of ions for analysis, but a disintegration of the analyte material during ionization. As described in Chapter I, the ESI process can be enhanced

through the introduction of a nebulizing gas such as nitrogen. The pressure of this nebulizing gas is a parameter which should be optimized to achieve maximum ionization.

However, it is not only the gas pressure which can prematurely fragment and render an analyte undetectable. In some situations, the chemical structure of a compound is such that the desolvation process itself creates instability and results in unwanted fragmentation. Typically, ESI is the ionization process of choice due to the balance between its gentle yet powerful mechanism. For 3-AP, it would be useful to investigate the benefit of an alternate, even softer ionization source such as APCI.

### Conclusion

Mass spectrometry is one of the most sensitive detection methods available to the analytical chemist. It is impossible to establish the underlying cause for the inability of this technique to perform in the detection ranges expected with the experiments' conducted with 3-AP to date. Two directions have been proposed to increase the detection ability of the mass spectrometer for this compound. Overall success may not come from taking just one route and may involve a modulation of both.

### Chapter III References

[1] **Maier, J., Bang, F.B., Hairston, N.G., American Journal of Tropical Medicine, 3 (1948) 401**

[2] Canete, R., Escobedo, A.A., Gonzalez, M.E., Almirall, P. World Journal of Gastroenterology 39 (2006) 6366

[3] Suhadi, A., Soejoenes, A., Family and Sterility, 5 (1997) 966

[4] Doh-Ura, K., Iwaki, T., Caughey, B., Journal of Virology, 74 (2000) 4894

[5] Gurova, K.V., Hill, J.E., Guo C., Prokvolit, A., Burdelya, L.G., Samoylova, E., Khodyakova, A.V., Ganapathi, R., Ganapathi, M., Tararova, N.D., Bosykh, D., Lvovskiy, D., Webb, T.R., Stark, G.R., Gudkov, A.V., Proceedings of the National Academy of Science, 48 (2005) 17448

[6] Gudkov, A.V., Komarova, E.A., Human Molecular Genetics, 16 (2007) R67

[7] Gorbachev, A.V., Gasparian, A.V., Gurova, K.V., Gudkov, A.V., Fairchild, R.L., European Journal of Immunology, 8 (2007) 2257

[8] Barret, A., Tagliavini, F., Forloni, G., Bate, C., Salmona, M., Colombo, L., De Luigi, A., Limido, L., Suardi, S., Rossi, G., Auvré, F., Adjou, K., Salès, N, Journal of Virology, 77 (2003) 8462

[9]Yung, L., Yong, H., Lessard, P., Legname, G., Lin, E.T., Baldwin, M., Prusiner, S.B., Ryou, C., Guglielmo, J., BMC Infections Diseases, 4 (2004). 53

**[10] Nutting, C.M., Van Herpen, C. M. L., Miah, A. B., Bhide, S. A., Machiels, J.-P. Buter, J., Annals of Oncology, 7 (2009) 1275**

[11] ClinicalTrials.gov Identifier: NCT00293345

[12] ClinicalTrials.gov Identifier: NCT00288093

[13] ClinicalTrials.gov Identifier: NCT00390052

[14] ClinicalTrials.gov Identifier: NCT00335998

[15] Eklund, H., Uhlin, U., Farnegardh, M., Logan, D.T., Nordlund, P., Progress in Biophysics and Molecular Biology, 77 (2001) 177

[16] Finch, R. A., Liu, M., Grill, S.P., Rose, W.C., Loomis, R., Vasquez, K.M., Cheng, Y., Sartorelli, A.C., Biochemical Pharmacology 59 (2000) 983

